



University of Kentucky
UKnowledge

Theses and Dissertations--Electrical and
Computer Engineering

Electrical and Computer Engineering

2013

VISION BASED REAL-TIME MONITORING AND CONTROL OF METAL TRANSFER IN LASER ENHANCED GAS METAL

Yan Shao

University of Kentucky, yanshao9@gmail.com

[Right click to open a feedback form in a new tab to let us know how this document benefits you.](#)

Recommended Citation

Shao, Yan, "VISION BASED REAL-TIME MONITORING AND CONTROL OF METAL TRANSFER IN LASER ENHANCED GAS METAL" (2013). *Theses and Dissertations--Electrical and Computer Engineering*. 20. https://uknowledge.uky.edu/ece_etds/20

This Doctoral Dissertation is brought to you for free and open access by the Electrical and Computer Engineering at UKnowledge. It has been accepted for inclusion in Theses and Dissertations--Electrical and Computer Engineering by an authorized administrator of UKnowledge. For more information, please contact UKnowledge@lsv.uky.edu.

STUDENT AGREEMENT:

I represent that my thesis or dissertation and abstract are my original work. Proper attribution has been given to all outside sources. I understand that I am solely responsible for obtaining any needed copyright permissions. I have obtained and attached hereto needed written permission statements(s) from the owner(s) of each third-party copyrighted matter to be included in my work, allowing electronic distribution (if such use is not permitted by the fair use doctrine).

I hereby grant to The University of Kentucky and its agents the non-exclusive license to archive and make accessible my work in whole or in part in all forms of media, now or hereafter known. I agree that the document mentioned above may be made available immediately for worldwide access unless a preapproved embargo applies.

I retain all other ownership rights to the copyright of my work. I also retain the right to use in future works (such as articles or books) all or part of my work. I understand that I am free to register the copyright to my work.

REVIEW, APPROVAL AND ACCEPTANCE

The document mentioned above has been reviewed and accepted by the student's advisor, on behalf of the advisory committee, and by the Director of Graduate Studies (DGS), on behalf of the program; we verify that this is the final, approved version of the student's dissertation including all changes required by the advisory committee. The undersigned agree to abide by the statements above.

Yan Shao, Student

Dr. YuMing Zhang, Major Professor

Dr. Zhi Chen, Director of Graduate Studies

VISION BASED REAL-TIME MONITORING AND CONTROL
OF METAL TRANSFER IN LASER ENHANCED GAS METAL
ARC WELDING

DISSERTATION

A dissertation submitted in partial fulfillment of the requirements
for the degree of doctor of Philosophy in the College of
Engineering
at the University of Kentucky

By
Yan Shao
Lexington, Kentucky
Director: Dr. YuMing Zhang, Professor of Electrical Engineering
Lexington, Kentucky
2012
Copyright © Yan Shao 2012

ABSTRACT OF DISSERTATION

VISION BASED REAL-TIME MONITORING AND CONTROL OF METAL TRANSFER IN LASER ENHANCED GAS METAL ARC WELDING

Laser enhanced gas metal arc welding (GMAW) is a novel welding process where a laser is applied to provide an auxiliary detaching force to help detach the droplet such that welds may be made in gas tungsten arc welding high quality at GMAW high speeds. The current needed to generate the electromagnetic (detaching) force is thus reduced. The reduction in the current helps reduce the impact on the weld pool and over-heat fumes/smokes. However, in the previous studies, a continuous laser is applied. Since the auxiliary is only needed each time the droplet needs to be detached and the detachment time is relatively short in the transfer cycle, the laser energy is greatly wasted in the rest of the transfer cycle. In addition, the unnecessary application of the laser on the droplet causes additional over-heat fumes. Hence, this study proposes to use a pulsed laser such that the peak pulse is applied only when the droplet is ready to detach. To this end, the state of the droplet development needs to be closely monitored in real-time. Since the metal transfer is an ultra-high speed process and the most reliable method to monitor should be based on visual feedback, a high imaging system has been proposed to monitor the real-time development of the droplet. A high-speed image processing system has been developed to real-time extract the developing droplet. A closed-loop control system has been established to use the real-time imaging processing result on the monitoring of the developing droplet to determine if the laser peak pulse needs to be applied. Experiments verified the effectiveness of the proposed methods and established system. A controlled novel process – pulsed laser-enhanced GMAW - is thus established for possible applications in producing high-quality welds at GMAW speeds.

KEYWORDS: GMAW, Laser, Metal Transfer, Machine Vision, Real-Time

Yan Shao

Student's Signature

03/25/2013

Date

VISION BASED REAL-TIME MONITORING AND CONTROL
OF METAL TRANSFER IN LASER ENHANCED GAS METAL
ARC WELDING

By

Yan shao

YuMing Zhang

Director of Dissertation

Zhi Chen

Director of Graduate Studies

12/15/2012

ACKNOWLEDGEMENTS

This work is funded by the National Science Foundation under grand CMMI-0825956 entitled “Control of metal Transfer at Given Arc Variables”.

I would like to give my sincere thanks and appreciations to my advisor Dr. YuMing Zhang for his profound knowledge, patient guidance, continuous encouragement and support during my study at University of Kentucky. I am also thankful to Dr. Larry Holloway, Dr. Yuan Liao, Dr. Alan T. Male and Dr. Fuqian Yang for their helpful instructions and advices for my research and dissertation preparation. I would like to express my appreciation to Dr. Yu Shi from Lanzhou University of Technology, China, and Dr. Yusheng Liu from Sichuan University, China who shared experiences and knowledge with me. Moreover, I would like to thank my colleagues in the Welding Research Laboratory: Dr. Hongsheng Song, Dr. Xiaopei Liu, Dr. Kehai Li, Dr. Kun Qian, Dr. Xiaodong Na, Dr. Zhijiang Wang, Mr. Jinsong Chen, Dr. Yi Huang, Dr. Xiaoji Ma, Mr. Xiang Zhang, Mr. Weijie Zhang and Mr. Jun Xiao.

I would like to thank my family for their love, support and faith in me. I want to give my special thanks to my wife Xiao He for her love, trust and continuously support.

TABLE OF CONTENTS

Acknowledgements.....	iii
List of Tables	vii
List of Figures.....	viii
CHAPTER 1 INTRODUCTION.....	1
1.1 Background	1
1.2 Objective and Focus	6
1.3 Dissertation structure.....	6
CHAPTER 2 Metal Transfer	8
2.1 Basic variables in GMAW	11
2.2 Metal Transfer in GMAW.....	14
2.2.1 Short-circuit metal transfer.....	16
2.2.2 Globular transfer.....	18
2.2.3 Spray transfer.....	19
2.2.4 Factors affecting metal transfer types.....	19
2.3 Previous research on novel welding process and metal transfer.....	21
2.3.1 Laser-MIG hybrid welding.....	21
2.3.2 Surface tension transfer	23
2.3.3 Double electrodes GMAW	26
2.3.4 Double bypass GMAW	28
2.3.5 Other metal transfer control methods of GMAW.....	29
2.4 Existing efforts on laser-enhanced GMAW	31
CHAPTER 3 Pulsed Laser Enhanced GMAW.....	41
3.1 Metal Transfer Control.....	41
3.2 Metal Transfer Waveform Control.....	44

3.3 Requirements from Proposed Controls	47
CHAPTER 4 EXPERIMENTAL SYSTEM.....	48
4.1 Hardware	50
4.2 System Set-Up.....	55
4.2.1 Experimental system.....	55
4.2.2 Installation parameters.....	58
CHAPTER 5 Image Processing.....	61
5.1 Basic Algorithm	62
5.1.1 Measurement of the growth of the droplet	63
5.1.2 Droplet Tracking and Measurement Algorithm	71
5.1.3 Summary.....	78
5.2 Algorithm without Visible Laser.....	79
5.3 Simplified Algorithm for Real-time Implementation.....	86
5.4 Summary	89
CHAPTER 6 Control System	91
6.1 Background.....	91
6.2 Control System	92
6.3 Control Algorithm	95
6.4 Summary.....	102
CHAPTER 7 Experimental Verification	103
7.1 Experimental Conditions.....	103
7.2 Experimental Methods	105
7.3 150 A Peak Current without Laser.....	106
7.4 150 A Peak Current with Laser.....	109
7.5 145 A Peak Current without Laser.....	112

7.6 145 A Peak Current with Laser	115
7.7 Summary	117
CHAPTER 8 Peak Current Reduction.....	118
8.1 Experiments.....	119
8.2 Discussion	129
CHAPTER 9 Conclusions and future work.....	131
9.1 Conclusions	131
9.2 Future work	133
References.....	134
VITA.....	140

List of Tables

Table 2-1 Classification of Metal Transfer in GMAW.....	15
Table 5-1 Experimental condition and welding current	62
Table 7-1 Major Parameters in Verification Experiments	105
Table 8-1 Parameters for Successful Detachment Experiments	120

List of Figures

Fig. 1-1 Illustration of GTAW and GMAW processes and weld penetration	2
Fig. 1-2 Transfer mode for continuous waveform current [4]	4
Fig. 1-3 The integrated torch proposed	5
Fig. 2-1 Illustration of GTAW	8
Fig. 2-2 Illustration of GMAW process	11
Fig. 2-3 Electrode extension	13
Fig. 2-4 Short-circuiting transfer	17
Fig. 2-5 Bead contour and penetration patterns for various shielding gases	20
Fig. 2-6 Laser-MIG/MAG welding process.....	22
Fig. 2-7 Torch installation of laser-MIG.....	23
Fig. 2-8 Surface tension transfer (STT) process	24
Fig. 2-9 Non-consumable DE-GMAW system diagram.....	26
Fig. 2-10 System diagram of consumable DE-GMAW	27
Fig. 2-11 Arc forces act on the droplet in DB-GMAW	28
Fig. 2-12 Illustration of DB-GMAW	29
Fig. 2-13 Principle and major forces acting on the droplet in Laser Enhance GMAW....	31
Fig. 2-14 System installation	33
Fig. 2-15 Installation of GMAW and Laser (the shielding board is not shown in the picture)	34
Fig. 2-16 Illustration of metal transfer image.	35
Fig. 2-17 Typical metal transfer in comparative experiments with and without laser under (300 in./min, 30 volts, 0) and (300 in./min, 30 volts, 62 watts/mm ²)	36
Fig. 2-18 Typical metal transfer in comparative experiments with and without laser under (250 in./min, 30 volts, 0) and (250 in./min, 30 volts, 62 watts/mm ²)	37
Fig. 2-19 Typical metal transfer in comparative experiments with and without laser under (350 in./min, 30 volts, 0) and (350 in./min, 30 volts, 62 watts/mm ²)	38
Fig. 2-20 Typical metal transfer in comparative experiments with and without laser under (400 in./min, 30 volts, 0) and (400 in./min, 30 volts, 62 watts/mm ²)	38
Fig. 3-1 GMAW Enhanced with a Laser Spot.....	42
Fig. 3-2 Current and Laser Waveforms in Pulsed Laser Enhanced GMAW	42

Fig. 3-3 Metal Transfer Frequency Control System	46
Fig. 3-4 Double-loop control for metal transfer waveform	47
Fig. 4-1 Experimental system diagram	48
Fig. 4-2 Laser and its installation in relation to the welding torch	51
Fig. 4-3 High speed camera and installation fixture	52
Fig. 4-4 Response Characteristic of the GZL-CL-22C5M Camera Image Sensor	53
Fig. 4-5 Second high speed camera for image recording and off-line analysis	54
Fig. 4-6 Experimental system	56
Fig. 4-7(b) Laser installation in relation with the torch: view 2	58
Fig. 4-8(b) Installation of the Proposed System: View 2	60
Fig. 5-1 Original images	64
Fig. 5-2 ROI of an original image.....	64
Fig. 5-3 Interpolated image.....	65
Fig. 5-4 Filtered image.....	66
Fig. 5-5 Droplet edges detected by the Sobel operator	67
Fig. 5-6 Droplet edges detected by the Canny operator.....	68
Fig. 5-7 Edge detection in four sub-regions.....	68
Fig. 5-8 Edge detection result with two operators combined	69
Fig. 5-9 Result of clustering after center approximation	70
Fig. 5-10 Result of clustering after second pass center estimation.....	70
Fig. 5-11 Comparison of the detected edge with the original droplet	71
Fig. 5-12 ROIs of a series of consecutive images.....	72
Fig. 5-13 Binarized images	72
Fig. 5-14 Edges detected based on estimated droplet center	73
Fig. 5-15 First calculation results after second pass center estimation.....	74
Fig. 5-16 Second pass clustering results with the new center (p, q)	74
Fig. 5-17 The fitted second order curve as the estimated boundary of the droplet.....	76
Fig. 5-18 Revised fitted second order curve	77
Fig. 5-19 Compare the revised fitting result with the droplet boundary.....	78
Fig. 5-20 Droplet growth period during the base current time.	80
Fig. 5-21 Selected regions of interest for images in Fig. 5-20.....	81

Fig. 5-22 Edges detected for images in Fig. 5-21 using the Sobel operator	82
Fig. 5-23 Noise reduction results for edges detected for images in Fig. 5-21 using the Sobel operator	84
Fig. 5-24 Fitted edges	84
Fig. 5-25 Comparison of the fitted edges with the original images	85
Fig. 5-26 Captured image for simplified real-time processing algorithm	87
Fig. 5-27 Processing result of the simplified image processing algorithm.....	89
Fig. 6-1 Optical System	92
Fig. 6-2 captured frame of the consumable electrode.....	93
Fig. 6-3 Recorded metal transfer process	94
Fig. 6-4 Block diagram of proposed control algorithm.	97
Fig. 6-5 Captured image of the electrode in calibration mode	98
Fig. 6-6 Laser on the electrode	99
Fig. 6-7 Droplet transfer in laser enhanced GMAW.....	101
Fig. 7-1 Typical first pulsing cycle to detach a droplet without laser using 150 A current for 6 ms	107
Fig. 7-2 A typical second pulsing cycle to detach a droplet without laser using 150 A current for 6 ms.....	108
Fig. 7-3 A typical pulsing cycle to detach a droplet with laser using 150 A current for 6 ms.....	110
Fig. 7-4 A typical pulsing cycle to detach a droplet with laser using 150 A current for 6 ms after a successful detachment.....	111
Fig. 7-5 A typical first pulsing cycle to detach a droplet without laser using 150 A current for 8 ms	113
Fig. 7-6 A typical second pulsing cycle to detach a droplet without laser using 150 A current for 8 ms.....	114
Fig. 7-7 A typical pulsing cycle to detach a droplet with laser using 145 A current for 8 ms.....	115
Fig. 7-8 A typical pulsing cycle to detach a droplet with laser using 145 A current for 8 ms after a successful detachment.....	116

Fig. 8-1 Typical two consecutive cycles in experiment 1 with 150 amp peak current. (a) Cycle one; (b) Cycle two. 122

Fig. 8-2 Typical two consecutive cycles in experiment 2 with 145 amp peak current. (a) Cycle one; (b) Cycle two. 124

Fig. 8-3 Typical two consecutive cycles in experiment 3 with 140 amp peak current. (a) Cycle one; (b) Cycle two. 126

Fig. 8-4 Typical two consecutive cycles in experiment 4 with 135 amp peak current. (a) Cycle one; (b) Cycle two. 128

CHAPTER 1 INTRODUCTION

1.1 Background

This dissertation research is part of a project that aims at providing an innovative gas metal arc welding process. This project is to (1) test the hypothesis that low but adaptively adjusted power laser spots can be used to fully control the gas metal arc welding (GMAW) process so that the droplet of melted wire metal can be detached to achieve the desired droplet mass/diameter, impact speed, trajectory with whatever the current/arc pressure used; (2) test the hypothesis through a selected case that a fully controlled GMAW process has the potential to produce GTA (gas tungsten arc) class welds; (3) establish the knowledge base needed to build next generation GMAW machines for the fully controlled GMAW process so that GTA class welds can be produced at much higher GMAW class productivity. To demonstrate the urgent demand on this fully controlled GMAW process, conventional GMAW process needs to be analyzed first in comparison with GTA welding (GTAW).

In GMAW as illustrated in Fig. 1-1(a), a mandatory wire is fed to the contact tube which is typically connected to the positive terminal of the power supply. The shielding gas is supplied to surround the wire and is restricted by the nozzle to deliver to the local area which surrounds the wire. When the wire touches the negatively charged work piece (connected to the negative terminal of the power supply), the tip of the wire is rapidly burnt forming a gap between the wire and the work piece and an arc is ignited across this gap. The arc melts the wire and melted metal forms a droplet at the tip of the wire; after the droplet is detached, a new droplet starts to form and a new cycle starts. This metal melting and droplet forming, growing, detaching, and traveling process is referred to as the metal transfer process. The metal transfer process plays the most critical role in

determining/controlling the weld quality because the stability of the arc, the amount of spatters, and the heat, force and mass inputs are all related to metal transfer process.

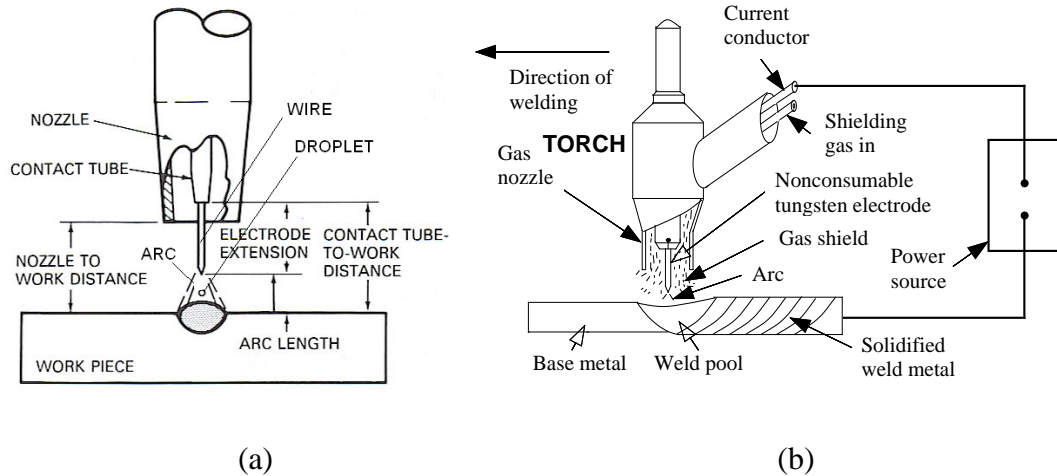


Fig. 1-1 Illustration of GTAW and GMAW processes and weld penetration

(a) GMAW and partial penetration (b) GTAW and full penetration

However, in GTAW as shown in Fig. 1-1(b), an arc is established between the non-consumable tungsten electrode and work piece (also referred to as base metal depending on the content and author's preference). The base metal is melted by the arc and forms a liquid weld pool which joins the two pieces of base metal together after solidification. An optional filler metal (not shown in Fig. 1-1(b)) can be added if necessary but is melted by the arc column rather than one of the two arc spots. The optional filler is not one of the arc terminals and there is no metal transfer process as in GMAW which affects the arc stability and production of quality welds in a significant way. The GTAW process is thus simple and stable and can produce high quality welds. However, its productivity in filling a joint/groove as required in many welding applications is low because the efficiency of arc column in melting filler metal is very low.

A controlled GMAW process may produce GTA class weld quality in much higher productivity. We see that the control of future GMAW process must have three levels.

The basic level of control is provided by the power supply itself so that the melting speed is balanced with the feeding speed [1-3]. At the second level, the welding parameters are selected to deliver the desired process characteristic outputs (process variables hereafter) which directly determine/control the weld quality such as the weld joint penetration. At the third level of control, the weld quality related variables which specify the weld quality are directly controlled by adjusting the process variables. Current GMAW machines can deliver the desired electrical variables but these electrical variables are not the process variables which can directly control/determine the ultimate weld quality. Basically, as can be seen in Fig. 1-2, its metal transfer mode that determines the arc stability and weld quality depends on the current used. Based on careful analysis of the GMAW process, we propose the following major process variables: arc heat q , arc force f , and droplet mass m , denoted as $\vec{u} = (q, f, m)^T$. Here \vec{u} (typically used to represent inputs in literature) is used to denote the process variables because these variables are the control variables or inputs in the third level of control. The goal of our project is to provide a fully controlled GMAW process which can assure that the desired $\vec{u} = (q, f, m)^T$ can be achieved so that they can be freely adjusted to produce the desired weld quality in the third level of control.

Now the controllability issue of GMAW process becomes clear: (1) the process variables include metal transfer related variables $\vec{u}_{MT} = m$ and arc related variables $\vec{u}_{arc} = (q, f)^T$; (2) while \vec{u}_{arc} is directly determined by the welding parameters (electrical variables), these welding parameters also determine \vec{u}_{MT} ; (3) the coupling of \vec{u}_{MT} with \vec{u}_{arc} restricts the free control of both them. That is, unless an innovative, acceptable modification is proposed, at its present form the GMAW process is not fully controllable so that it can deliver whatever needed values for all variables in $\vec{u} = (q, f, m)^T$ to control the weld quality.

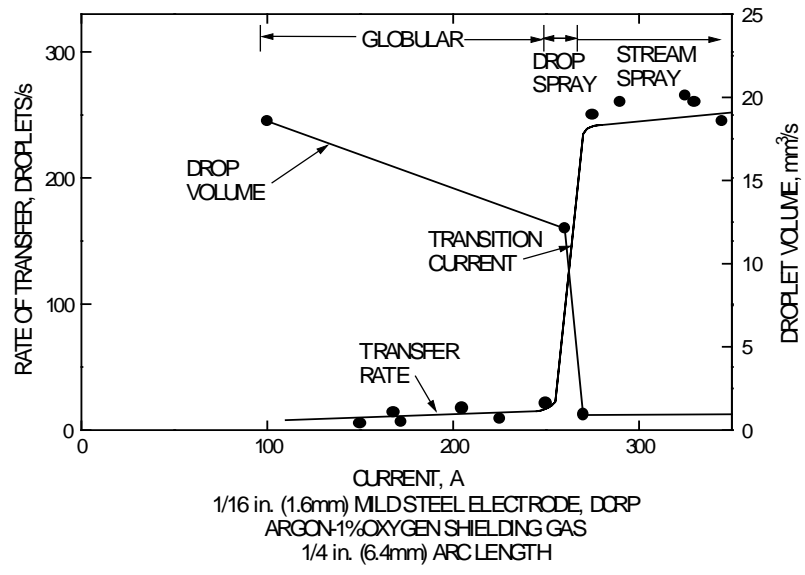


Fig. 1-2 Transfer mode for continuous waveform current [4]

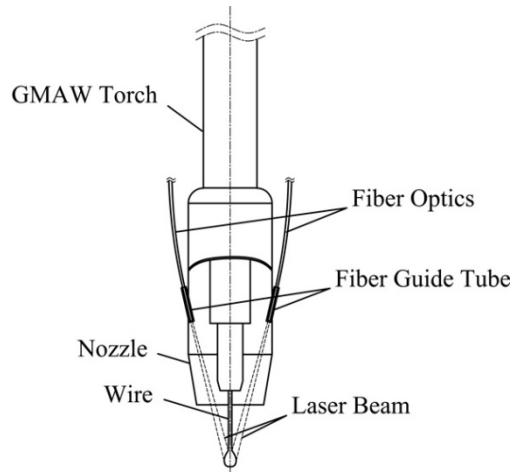


Fig. 1-3 The integrated torch proposed

The method proposed as the end product of this project is to use two symmetrically installed pulsed laser spots as shown in Fig. 1-3 to generate the needed detaching force in time to detach the droplet at whatever, possibly low, current. Using this method, whenever a droplet needs to be detached, two pulsed laser spots with adaptively adjusted powers can be applied onto the droplet so that the droplet is detached with the desired \vec{u}_{MT} from the wire at whatever the actual \vec{u}_{arc} used. In particular, the power of each laser spot can be separately adjusted to control the amplitude and direction of the detaching force added through the laser spots. The amplitude and direction of the added detaching force can be determined based on the needed droplet impact speed and trajectory, and the electromagnetic force which is determined by the current level and droplet mass. As a result, the welding current can be determined based on the needed \vec{u}_{arc} and the needed \vec{u}_{MT} are then controlled by adjusting the laser spots' powers and their firing timing. The GMAW process can thus become fully controlled.

At the University of Kentucky, the first part of the project has been recently done by projecting a 1 kW laser stripe of 14 mm x 1mm onto the droplet [5-7]. The feasibility of the method proposed for this project is experimentally verified. The length of the laser stripe is aligned with the wire and droplet. While this alignment provides an easy way to apply the force from the laser on the right location where the detaching force can be effectively utilized, out of this 1 kW laser energy, only a small fraction is effectively

utilized. The rest is wasted and is adversely applied on the work-piece. Further, to assure the laser is applied when it is needed, the laser is continuously applied. The laser energy is further wasted and adversely applied onto the work-piece. More critically, because of the presence of the continuous force due to the laser, the detachment occurs anytime when the surface tension is balanced out by the combined detaching force due to the laser, droplet mass (gravitational force) and electromagnetic force. The detachment time and mass are not controlled although smaller droplets can be detached with relatively small currents.

1.2 Objective and Focus

The objective of the present dissertation research is to move one step toward the goal of the entire project, i.e., to apply a pulsed laser spot onto the droplet at the right location where the detaching force from the laser is needed and at the right time when the detaching force from the laser is needed. This can eliminate the waste of the laser energy and the effect of the unintentional laser application on the work-piece and provide accurate control on the droplet mass and detaching time.

To realize the objective, a pulsed laser-enhanced GMAW process is developed as the second part of the project. In this process, the metal transfer process is monitored in real-time. When the droplet enters the location the laser aims at, a laser pulse is applied. To reduce the need for laser energy to a level achievable using our existing spot laser, the current is pulsed simultaneously with the laser. To make sure the pulses of the laser and current are correctly synchronized, the monitoring of the metal transfer process is done using high speed imaging system and real-time image processing algorithm. The accurate monitoring of the droplet using the image method can eliminate the effect of the variations in the wire feed speed, melting speed, and contact-tube-to-work distance such that the synchronization can be accurately assured.

1.3 Dissertation structure

This dissertation has an organizational structure which is listed below.

Chapter 1 gives an introduction about the background and motivation of the project.

Chapter 2 reviews the metal transfer in the GMAW process and existing control technologies.

Chapter 3 introduces the control methods proposed for the pulsed laser-enhanced GMAW.

Chapter 4 presents the construction and the hardware of the developed laser-enhanced GMAW system.

Chapter 5 introduces the high speed image processing algorithms used to analyze the images and extract the important information about the droplet.

Chapter 6 introduces the machine vision based control system which controls the metal transfer in the pulsed laser-enhanced GMAW.

Chapter 7 presents the experiments that verify the effectiveness of the metal transfer control system and the laser in the laser-enhanced GMAW.

Chapter 8 illustrates that the laser can help transfer the droplets with reduced peak current that is lower than the transition current.

Chapter 9 concludes the dissertation with future work.

References are listed at the end of the dissertation.

CHAPTER 2 Metal Transfer

GTAW

Gas Tungsten Arc Welding (GTAW), also known as tungsten inert gas (TIG) welding, is an arc welding process that uses an arc between a tungsten electrode and the weld pool to heat and melt the work-piece. The weld pool and solidified area are protected with shielding gas. The process may be used with or without filler metal. Figure 2-1 shows its principle.

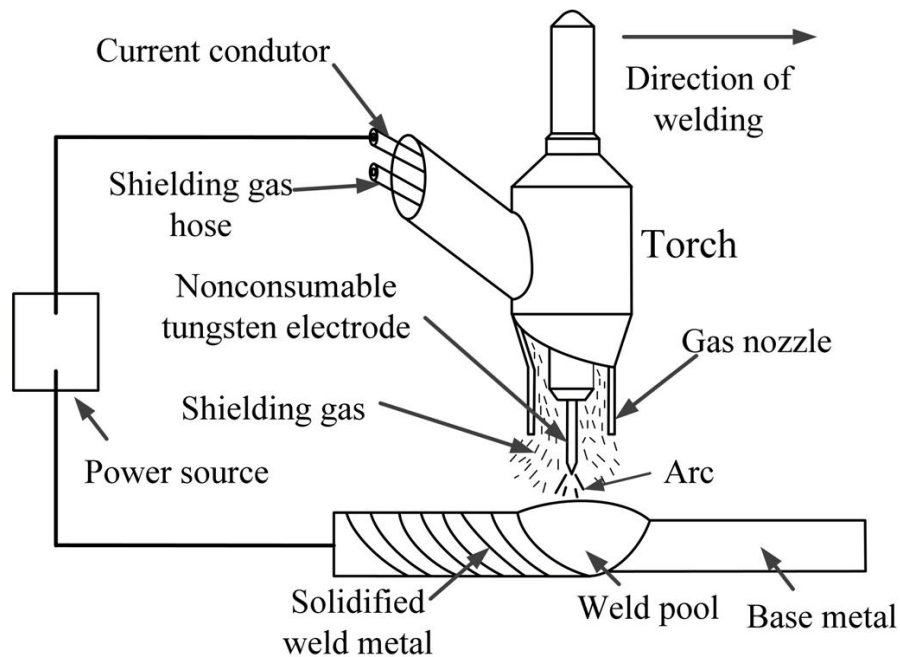


Fig. 2-1 Illustration of GTAW

The GTAW process uses a non-consumable tungsten electrode that is fixed in a torch. Shielding Gas is fed through the torch when the arc is established. Inert gas is used as the shielding gas in order to protect the electrode and the weld pool from contamination. The current passes through the electrode, the ionized conductive shielding gas and finally reach the base metal, thus an arc is established. The arc generates enough heat and melts the base metal. The torch will then move along the weld seam.

The advantages of the GTAW include:

1. Producing superior quality welds, generally free of defects.
2. Free of spatters which typically occur in other arc welding processes.
3. Allowing for excellent control of root pass weld penetration.
4. Allowing precise control on welding variables.

The limitations of the GTAW:

1. Deposition rates are lower than those possible with consumable electrode arc welding processes such as gas metal arc welding (GMAW) and its variants.
2. There is a need for slightly more dexterity and welder skill than with Gas Metal Arc Welding and shielded metal arc welding for manual welding.
3. It is less economical than the consumable electrode arc welding processes for thicker sections greater than 3/8 in.
4. There is a difficulty in shielding the weld zone properly in drafty environments.

GMAW

Gas metal arc welding (GMAW), also known as MIG (metal inert gas) welding, is a semi-automatic or automatic arc welding process in which a continuous and consumable wire electrode and a shielding gas are fed through a welding gun. The principles of gas metal arc welding began to be understood in the early 1800s, after Humphry Davy's discovery of the electric arc in 1800. Initially, carbon electrodes were used, but by the late 1800s, metal electrodes had been invented by N.G. Slavianoff and C. L. Coffin. In 1920, an early predecessor of GMAW was invented by P. O. Nobel of General Electric. It used a bare electrode wire and direct current, and used arc voltage to regulate the feed rate. It did not use a shielding gas to protect the weld, as developments in welding atmospheres did not take place until later that decade. In 1926 another forerunner of GMAW was released, but it was not suitable for practical use [8-9, 14].

It was not until 1948 that GMAW was finally developed by the Battelle Memorial Institute. It used a smaller diameter electrode and a constant voltage power source, which

had been developed by H. E. Kennedy. It offered a high deposition rate, but the high cost of inert gases limited its use to non-ferrous materials and cost savings were not obtained. In 1953, the use of carbon dioxide as the shielding gas was developed, and it quickly gained popularity in GMAW, since it made welding steel more economical. In 1958 and 1959, the short-arc variation of GMAW was released, which increased welding versatility and made the welding of thin materials possible while relying on smaller electrode wires and more advanced power supplies. It quickly became the most popular GMAW variation. The spray-arc transfer variation was developed in the early 1960s, when experimenters added small amounts of oxygen to inert gases. More recently, pulsed current has been applied, giving rise to a new method called the pulsed spray-arc variation [9, 13-15].

GMAW is currently one of the most popular welding methods, especially in industrial environments. It is adopted extensively by the sheet metal industry and, by extension, the automobile industry where it is often used to do arc spot welding, thereby replacing riveting or resistance spot welding. It is also popular in robotic welding, in which robots carry the welding torch to quicken the manufacturing process [8, 10, 13-15].

Generally, it is unsuitable for welding outdoors, because the movement of the surrounding atmosphere can dissipate the shielding gas and thus make welding more difficult, while also decreasing the quality of the weld [8, 10, 13-15]. This problem can be alleviated to some extent by increasing the shielding gas output, but this can be expensive and may also affect the quality of the weld. In general, processes such as shielded metal arc welding and flux cored arc welding are preferred for welding outdoors, making the use of GMAW in the construction industry rather limited. Furthermore, the use of a shielding gas makes GMAW an unpopular underwater welding process, and for the same reason it is rarely adopted in space applications.

In GMAW process as illustrated in Fig. 2-2 [8], a mandatory wire is fed to the contact tube which is typically connected to the positive terminal of the power supply. When the wire touches the negatively charged work piece, the tip of the wire is rapidly burnt forming a gap between the wire and the work piece and an arc is ignited across this gap. The arc melts the wire and melted metal forms a droplet at the tip of the wire; after the

droplet is detached, a new droplet starts to form and a new cycle starts. This metal transfer process is subject to periodic change in the arcing conditions and plays the most critical role in determining/controlling the weld quality in GMAW. To produce high quality welds similarly as the gas tungsten arc welding (GTAW) where the arcing conditions are stationary, the metal transfer needs to be appropriately controlled.

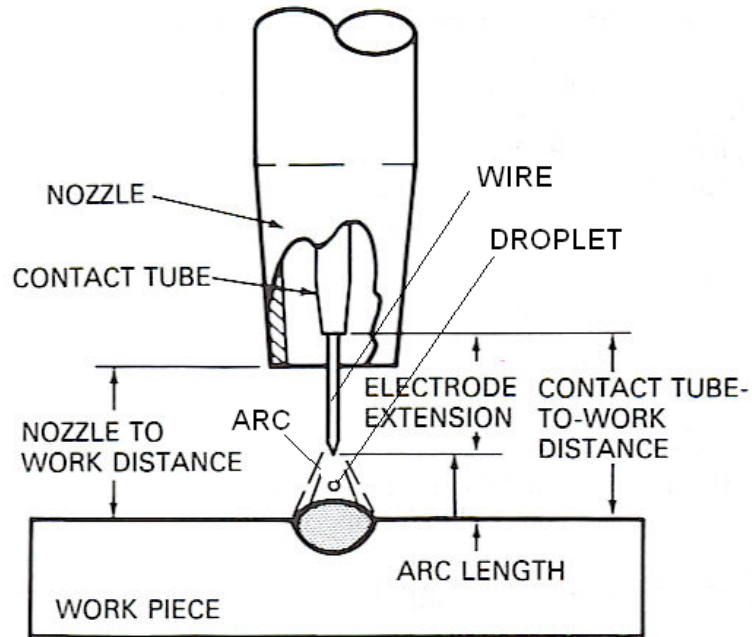


Fig. 2-2 Illustration of GMAW process

As GMAW is a focus topic in welding research and application, there are many aspects which need special work. Hereby, basic variables will be introduced for the later analysis.

2.1 Basic variables in GMAW

There are a number of basic variables of GMAW which affect metal transfer, weld penetration, bead geometry and overall weld quality. They usually have strong coupling relationship implying that they influence each other significantly [8-10, 13-15].

Current Density: Current density is defined as the current employed with a particular electrode diameter divided by its current carrying cross-sectional area. If the wire feed

speed is low with other parameter the same, then the current density will be low, and vice versa. Lower current density applied to a given electrode is associated with the short-circuit mode of metal transfer. At the same time, higher current density is associated with the higher energy modes of metal transfer: globular, axial spray transfer or the more advanced pulsed spray metal transfer.

Welding Current: When all other variables are held constant, the welding current varies with the electrode feeding speed or melting rate in a nonlinear relation. Generally speaking, for a chosen filler wire, welding current increases itself along with the increment of wire feeding speed. The upper limit of the welding current permitted is often regulated by the material and geometry of base metal in order to prevent burn through.

Electrode Efficiencies: Electrode efficiency refers to the percentage of electrode that actually ends up in the weld deposit. Spatter levels, smoke, and slag formers affect the electrode efficiency in GMAW. The electrode efficiency is a numeric value that is assigned to the particular mode of metal transfer.

Polarity: Polarity is used to describe the electrical connection of the welding torch with relation to the terminals of a direct current power source. When the torch power lead is connected to the positive terminal, the polarity is designated as direct current electrode positive (DCEP), also called reverse polarity. When the torch is connected to the negative terminal, the polarity is designated as direct current electrode negative (DCEN), originally called straight polarity [15].

Arc Voltage: Arc voltage and arc length are terms that are often used interchangeably because of their linear relationship. With GMAW, arc length is a critical variable that must be fully controlled [8].

Travel speed: Travel speed is the linear rate at which the arc is moved along the weld joint. With all other conditions held constant, weld penetration is maximum at an intermediate travel speed. [8-10, 13-16].

Deposition Rate: The melt-off rate for a particular electrode does not include consideration for the efficiency of the mode of metal transfer or the process. Its interest is in how much electrode is being melted. Deposition rate is applied to the amount of electrode, measured in wire fed per unit of time, that is fed into the molten puddle. Importantly, its value reflects the use of the factor for electrode efficiency.

Electrode Extension: The electrode extended from the end of the contact tip to the arc is properly known as electrode extension. The popular non-standard term is electrical stick-out (ESO). In GMAW, this is the amount of electrode that is visible to the welder. The electrode extension includes only the length of the electrode, not the extension plus the length of the arc. The use of the term electrode extension is more commonly applied for semiautomatic welding than it is for robotic or mechanized welding operations. Fig. 2-3 shows the scheme image of electrode extension in GMAW.

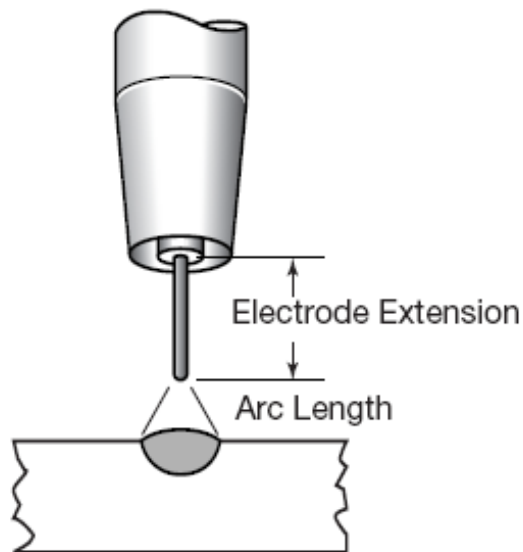


Fig. 2-3 Electrode extension

Besides, other parameters such as electrode orientation and shielding gas are also important which influence the process significantly.

2.2 Metal Transfer in GMAW

In GMAW, the electrode wire melts forming a droplet at its end and the droplet eventually transfers into the base metal. This periodical metal melting and droplet forming, growing, detaching, and traveling process is traditionally referred to as the metal transfer process.

The American Welding Society classifies the metal transfer into three major types/modes: short-circuiting, globular, and spray [8]. Metal transfer modes are affected by several operational factors, such as welding current, composition of shielding gas, wire extension, the ambient pressure, active elements in the electrode, polarity, and welding material [16-19]. Of all of these, welding current is the most important factor to determine the metal transfer mode. When a continuous waveform current is used and the current is small, the droplet may not be detached until the droplet contacts the weld pool. This transfer mode is referred as short-circuiting transfer. If the welding current increases or the arc length increases, the droplet will gradually grow until the gravitational force could not balance the surface tension, and then the droplet will detach. This transfer mode is globular transfer. When the current further increases, the electromagnetic force may become a sufficiently large enough detaching force to detach the droplets whose diameter is similar (drop spray) to or much smaller (streaming spray) than that of the electrode wire. The metal transfer modes were widely studied in the literatures [19-21]. Metal transfer control was also a focus in the research community [22-25]. The International Institute of Welding (IIW) further classifies globular transfer into Drop Globular and Spelled Globular [21, 26]. The IIW classification of metal transfer is shown in Table 2-1 [21, 37].

– Given this table below

Table 2-1 Classification of Metal Transfer in GMAW



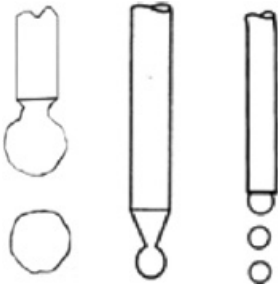

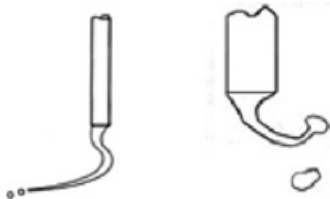
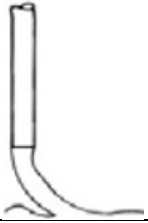
Metal Transfer Mode	Sketch	ExAles	
1. Free Flight Transfer	1.1 Globular 1.1.1 Drop		Low Current GMAW
	1.1.2 Repelled		CO ₂ Shield GMAW
	1.2 Spray 1.2.1 Projected		Intermediate Current GMAW
	1.2.2 Streaming		Medium-Current GMAW
	1.2.3 Rotating		High-Current GMAW
	1.3 Explosive		SMA (Coated Electrode)

Table 2-1 Classification of Metal Transfer in GMAW (Continued)

2 Bridging Transfer	2.1 Short-Circuiting		Short-Arc GMAW
	2.2 Bridging without interruptions		Welding with Filler Wire Addition
3 Slag Protected Transfer	3.1 Flux Wall Guided		SAW
	3.2 Other Modes		SMA, Cored Wire, Electroslag

2.2.1 Short-circuit metal transfer

Different modes of metal transfer are generated by different levels of current when the wire diameter and material, the shielding gas, and the polarity are given. When the current is small, the droplet may not be detached until the droplet contacts the weld pool. In this case, the transfer mode is short-circuiting [8-10 13-15, 28-31].

The transfer of a single molten droplet of electrode occurs during the shorting phase of the transfer cycle (See Fig. 2-4). Physical contact of the electrode occurs with the molten weld pool, and the number of short-circuiting events can occur up to 200 times per second. The current delivered by the welding power supply rises, and the rise in current accompanies an increase in the magnetic force applied to the end of the electrode. The electromagnetic field, which surrounds the electrode, provides the force, which squeezes (more commonly known as pinch) the molten droplet from the end of the electrode.

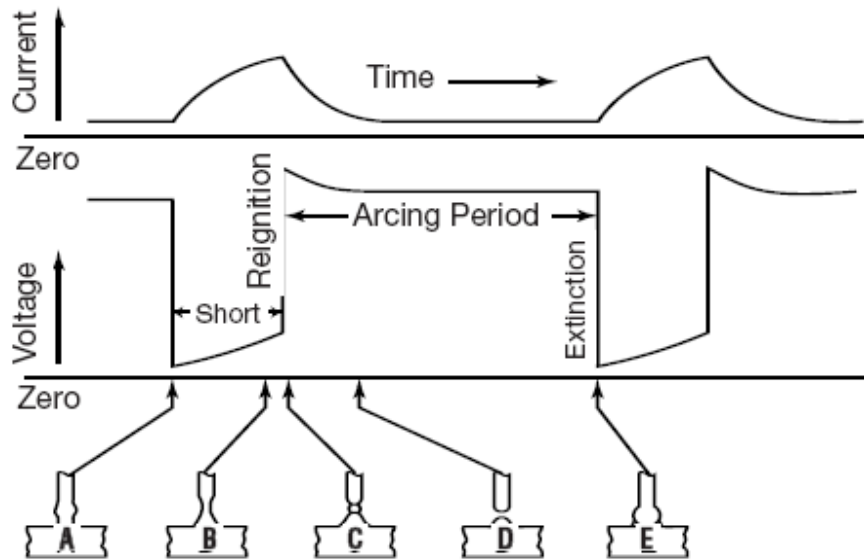


Fig. 2-4 Short-circuiting transfer

A The solid or metal-cored electrode makes physical contact with the molten puddle. The arc voltage approaches zero, and the current level increases. The rate of rise to the peak current is affected by the amount of applied inductance.

B This point demonstrates the effect of electromagnetic forces that are applied uniformly around the electrode. The application of this force necks or pinches the electrode. The voltage very slowly begins to climb through the period before detachment, and the current continues to climb to a peak value.

C This is the point where the molten droplet is forced from the tip of the electrode. The current reaches its maximum peak at this point. Jet forces are applied to the molten puddle and their action prevents the molten puddle from rebounding and reattaching itself to the electrode.

D This is the tail-out region of the short-circuit waveform, and it is during this downward excursion toward the background current when the molten droplet reforms.

E The electrode at this point is, once again, making contact with the molten puddle, preparing for the transfer of another droplet. The frequency of this varies between 20 and 200 times per second. The frequency of the short-circuit events is influenced by the

amount of inductance and the type of shielding gas. Additions of argon increase the frequency of short-circuit and it reduces the size of the molten droplet.

Because of the low-heat input associated with short-circuiting transfer, it is more commonly applied to sheet metal thickness material. However, it has frequently found use for welding the root pass in thicker sections of material in open groove joints. The short-circuiting mode lends itself to root pass applications on heavier plate groove welds or pipe.

2.2.2 Globular transfer

If the current increases, but not large enough to generate a sufficiently large electromagnetic force [8] to detach the formed droplet, then the droplet may surpass the diameter of the electrode wire and be detached mainly by gravity. This transfer mode is globular [8-10 13-15, 28-31].

Globular metal transfer is one of GMAW major metal transfer modes, whereby a continuously fed solid or metal-cored wire electrode is deposited in a combination of short-circuits and gravity-assisted large drops. The larger droplets are irregularly shaped.

During the use of all metal-cored or solid wire electrodes for GMAW, there is a transition where short-circuiting transfer ends and globular transfer begins. Globular transfer characteristically gives the appearance of large irregularly shaped molten droplets that are larger than the diameter of the electrode. The irregularly shaped molten droplets do not follow an axial detachment from the electrode, instead they can fall out of the path of the weld or move towards the contact tip. Cathode jet forces, which move upwards from the work-piece, are responsible for the irregular shape and the upward spinning motion of the molten droplets.

The process at this current level is difficult to control, and spatter is severe. Gravity is instrumental in the transfer of the large molten droplets, with occasional short-circuits.

2.2.3 Spray transfer

If the current further increases, then the transfer mode may become the projected spray if the detaching electromagnetic force becomes sufficiently large. In this case, the streaming or rotating spray transfer may occur [8-10 13-15, 21, 28-31].

Spray metal transfer is the highest energy mode of metal transfer, whereby a continuously fed solid or metal-cored wire electrode is deposited at a higher energy level, resulting in a stream of small molten droplets. The droplets are propelled axially across the arc. It is the highest energy form of GMAW metal transfer.

There are many advantages of spray metal transfer.

- High deposition rates.
- High electrode efficiency of 98% or more.
- Employing a wide range of filler metal types in an equally wide range of electrode diameters.
- Excellent weld bead appearance.
- High operator appeal and ease of use.
- Little post weld cleanup required.
- Absence of weld spatter.
- Excellent weld fusion.
- Widely applications in semiautomatic, robotic, and hard automation fields.

However, there are still some limitations of axial spray transfer. For example, welding fume generation is higher. The higher-radiated heat and the generation of a very bright arc require extra welder and bystander protection. The higher heat input may cause welder distortion.

2.2.4 Factors affecting metal transfer types

Metal transfer modes are affected by several operational factors, such as welding current, composition of shielding gas, wire extension, the ambient pressure, active elements in the

electrode, polarity, and welding material [8-10, 16-21, 28-31]. Of all of them, welding current is the most important factor to determine the metal transfer mode.

Different shielding gases can produce totally different metal transfer types. Argon and helium are the two inert shielding gases often used for protecting the molten weld pool in GMAW. These two inert shielding gases do not react with the molten metal so that they will not influence the components of welds. In the GMAW process, the shielding gas will be ionized to become a conductive gas. The thermal conductivity is the most important consideration for selecting a shielding gas. High thermal conductivity levels result in more conduction of the thermal energy into the work-piece. The thermal conductivity also affects the shape of the arc and the temperature distribution within the region. As argon has a lower thermal conductivity rate which is about 10% of level for helium, it is suitable for the full penetration research. CO₂ is a reactive shielding gas used in GMAW. When CO₂ is adopted, it is very difficult to obtain free flight metal transfer as the electromagnetic force will become retaining force. Fig. 2-5 shows the different bead contour and penetration patterns for various shielding gas [10].

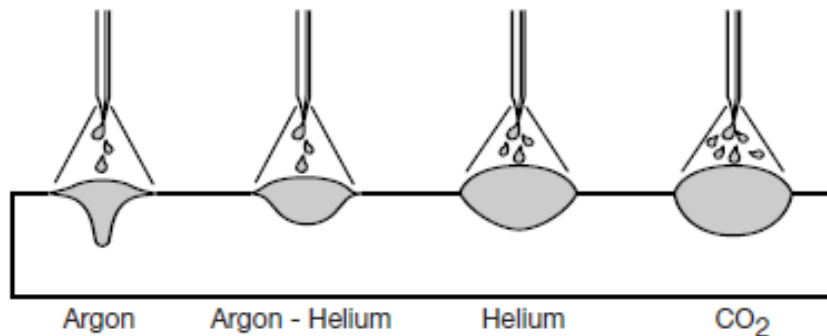


Fig. 2-5 Bead contour and penetration patterns for various shielding gases

Wire extension is also important to influence the metal transfer types. With a longer electrode extension, the transition current from globular to spray will decrease. Other influence factors play important roles in affecting the metal transfer but will be not discussed in this dissertation as they are not as important as the ones that have been discussed.

2.3 Previous research on novel welding process and metal transfer

As the distortion and internal stress in the welds are related to the square of welding through work-pieces, the best way to reduce them is to reduce the welding current. However, when the welding current is lower than the transition current, short-circuiting or globular transfer will be generated. As such, researchers did much work to propose and develop novel modified GMAW to lower welding current and eliminate the spatters.

2.3.1 Laser-MIG hybrid welding

The laser-MIG hybrid welding process is a coupling of a traditional MIG welding, that is, GMAW, process and a laser welding process [32-36, 59-65]. In laser-MIG hybrid welding process, the laser beam aims at the welding pool to increase the welding penetration and coupling with the arc. The laser preheats the work piece to make the droplet transfer easier which also results in a deeper penetration. The MIG torch provides the molten metal for the joining process. The metal transfer type is mainly determined by the GMAW process. To ensure a stable metal transfer process, the welding current is usually higher than the transition current. Fig. 2-6 shows the working process of laser-MIG hybrid welding [36]. Laser –MIG hybrid welding leads to significant improvements in welding speed and weld quality [65]. Figure 2-7 shows torch installation of laser-MIG [35].

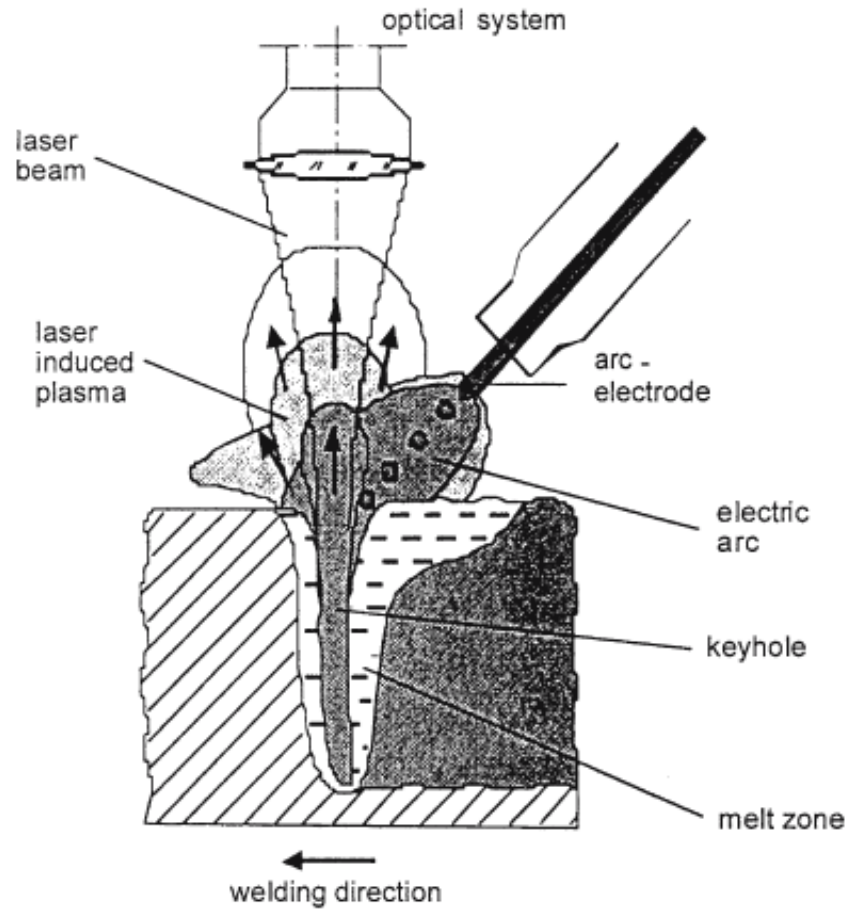
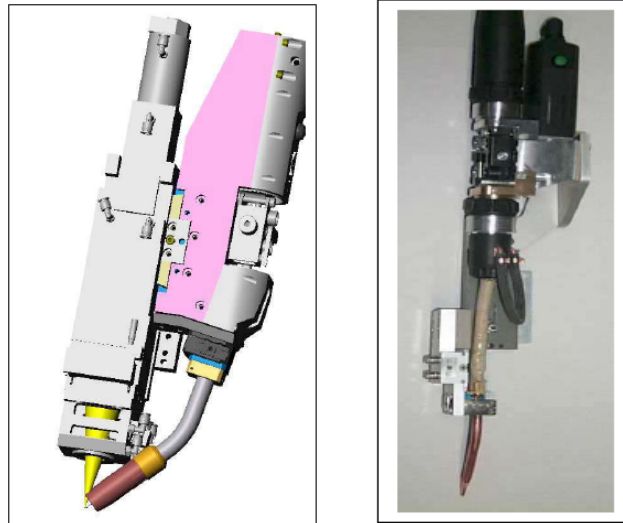


Fig. 2-6 Laser-MIG/MAG welding process

The hybrid welding process is involved in a growing number of industrial applications due to its technical advantages. It will increase the welding speed thus high productivity. In hybrid process, the cost of power source will be reduced and the electrical efficiency will increase. A good weld quality is obtained with low and predictable distortion, which implies a reduction in the need for rework.



(a) Instruction diagram (b) Real Torch

Fig. 2-7 Torch installation of laser-MIG

There are certain disadvantages that limit laser-MIG welding application. First it is expensive to employ a high power laser in the industry process. Second the laser-MIG hybrid welding process has large numbers of parameters to be set up. The set up of the processing parameters requires a high degree of skill and accuracy, and these imperatives added to an incomplete knowledge of the process are limiting factors for the industrial application. Moreover, laser-MIG hybrid welding can't reduce base metal heat input because laser is a great heat source and metal transfer was determined by the GMAW itself.

2.3.2 Surface tension transfer

Surface Tension Transfer (STT) welding is a GMAW, controlled short circuit transfer process developed and patented by The Lincoln Electric Company [37-38]. Unlike standard CV GMAW machines, the STT machine has no voltage control knob. STT uses current controls to adjust the heat independent of wire feed speed, so changes in electrode extension do not affect heat.

A Background Current between 50 and 100 A maintains the arc and contributes to base metal heating. After the electrode initially shorts to the weld pool, the current is quickly

reduced to ensure a solid short transfer. Pinch Current is then applied to squeeze molten metal down into the pool while monitoring the necking of the liquid bridge from electrical signals. When the liquid bridge is about to break, the power source reacts by reducing the current to about 45-50 A. Immediately following the arc re-establishment, a Peak Current is applied to produce plasma force pushing down the weld pool to prevent accidental short-circuiting and to heat the puddle and the joint. Finally, exponential Tail-out is adjusted to regulate overall heat input. Background Current serves as a fine heat control [48-49 43-44].

The basic principle of STT control technology can be explained below with reference to Fig. 2-8in [39-45].

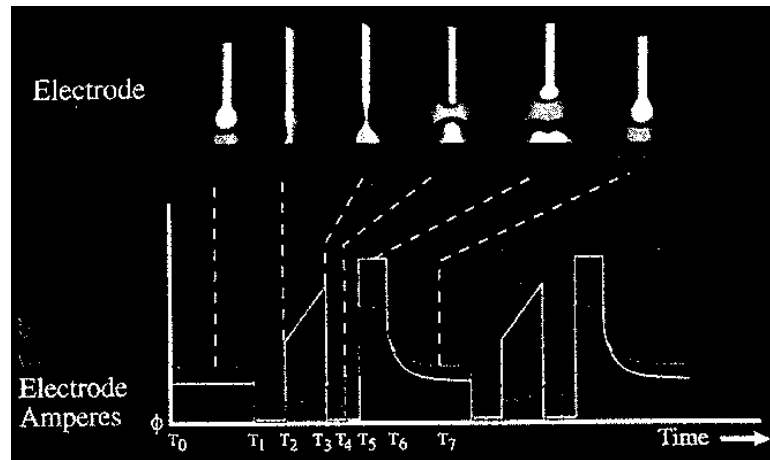


Fig. 2-8 Surface tension transfer (STT) process

(1) Background current period $T_0 - T_1$: In this period, the current is at the level of the arc prior to shorting to the weld pool. It is a steady-state current level, between 50 and 100 A.

(2) Ball time $T_1 - T_2$: When the electrode initially shorts (at the background current), the “arc voltage” detector provides a signal that the “arc” is shorted. The background current is further reduced from the background level to 10 A for approximately 0.75 ms. This time interval is referred to as the ball time.

(3) Pinch mode $T_2 - T_3$: Following the ball time, a high current is applied to the shorted electrode in the form of an increasing, dual-slope rA. This accelerates the transfer of the molten metal from the electrode to the weld pool by applying electric pinching forces. (Note that the electrode-to-work voltage is non zero during this period due to the high resistivity of iron at its melting point of 1550 °C)

(4) The dv/dt calculation $T_3 - T_4$: This calculation is included within the pinch mode. It is the calculation of the rate of change of the shorted electrode voltage vs. time. When this calculation indicates that a specific dv/dt value has been attained, indicating that fuse separation is about to occur, the current is reduced to 50 A in milliseconds. (Note, this event occurs before the shorted electrode separates. T_4 indicates the separation has occurred, but at a low current.)

(5) Plasma boost $T_5 - T_6$: This mode follows immediately the separation of the electrode from the weld pool. It is the period of high arc current where the electrode is quickly “melted back.”

(6) Plasma $T_6 - T_7$: During this period, the arc is reduced from plasma boost to the background current level.

STT welding has many advantages. First, good penetration and low heat input control could be obtained, so that it is ideal for welding on joints with open root, gaps, or on thin material with no burn-through. The ability to concentrate the arc also aids in the elimination of cold lapping on open root joints for pipe and pressure vessels. The lower heat input provides the advantage of less material distortion and burn-through by providing only the required amount of heat to produce the weld, even in sensitive material like stainless steel. This precise control of heat means that even thin gauge galvanized sheet metal can be welded without burning off the galvanized plating on the back side of the metal. Second, as current is controlled to achieve optimum metal transfer, spatters and fumes will be reduced. As STT has the ability to use 100% CO₂ or argon shielding gas blends with larger diameter wires, costs will be reduced. Good bead control and faster travel speeds will be achieved [37-45].

2.3.3 Double electrodes GMAW

Double-Electrode GMAW (DE-GMAW) was proposed and developed in the Center for Manufacturing at the University of Kentucky [46-52]. The aims are to seek for a method to double the welding productivity meanwhile reducing heat input to the work-piece. It also provides an effective method to produce spray transfer at very low base metal current. . It is proposed because high welding productivity requires fast wire melting speed requiring a larger melting current. In conventional GMAW, all melting current flows through base metal which means that melting current equals base metal current. Thus, it is impossible to increase the melting current freely without increasing the base metal current. However, the base metal current is typically restricted by the application and material. Excessive heat input to work-piece will produce distortion and internal stress resulting in increased costs of post-weld treatment.

DE-GMAW is oriented to solve this dilemma by adding a bypass torch to conventional GMAW such that the melting current does not have to all pass through the base metal, as shown in Fig. 2-9 [46]. In the system shown in Fig. 2-9, a GTAW torch was added to bypass the total current through the GMAT torch.

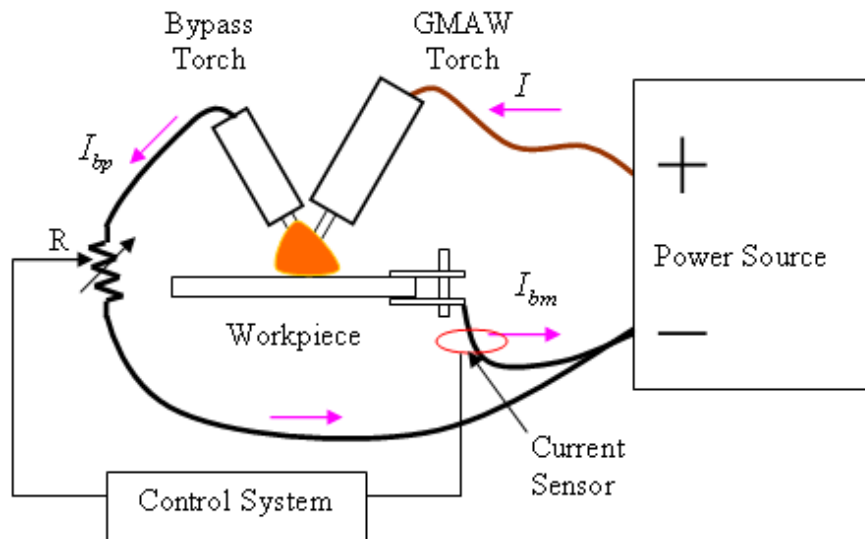


Fig. 2-9 Non-consumable DE-GMAW system diagram

In DE-GMAW, the current relationship is represented by

$$I_{total} = I_{melting} = I_{base\ metal} + I_{Bypass} \quad (2-1)$$

From Eq. (2-1), the total welding current is divided into base metal current and bypass current. The total current of DE-GMAW is determined by the wire feed speed in order to balance the melting with the feeding. The base current could be adjusted by changing the bypass current. The melting current could be significantly increased without changing the base current. The metal transfer type could be also controlled by controlling the bypass current such that free flight metal transfer could be obtained with welding current below the transition current.

To better utilize the bypass current, DE-GMAW is further developed such that the bypass GTAW torch is replaced by another GMAW torch. In this case, the bypass current will be used to melt welding wire and productivity will be further increased. Its system schematic figure is shown in Fig. 2-10 [49].

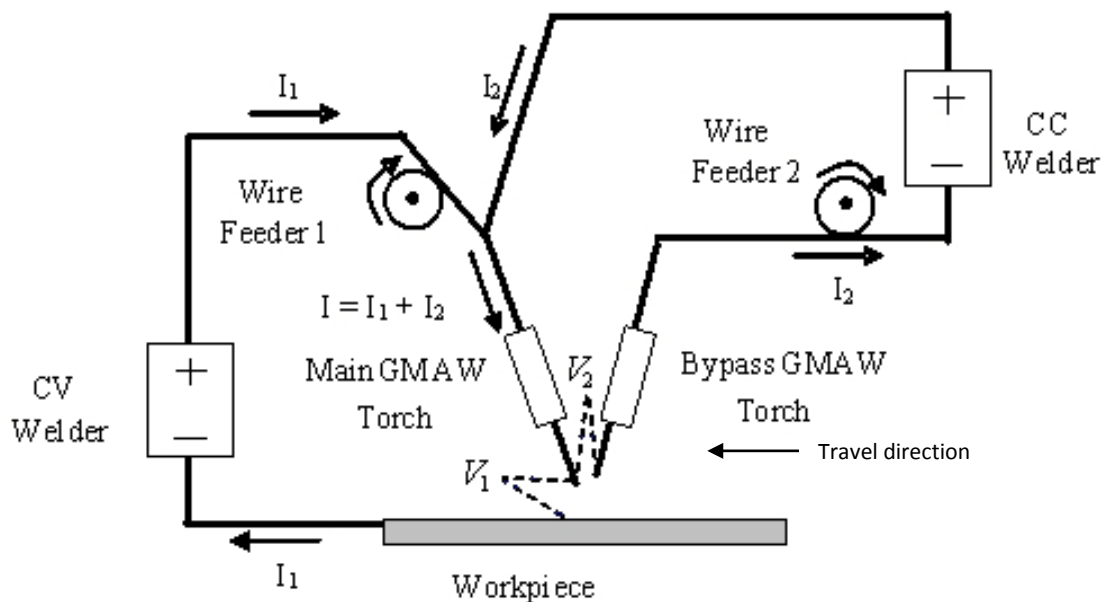


Fig. 2-10 System diagram of consumable DE-GMAW

The DE-GMAW provides an effective way to increase welding productivity and minimize the heat input into work-piece. However, the use of a bypass torch reduces the compactness of the torch and affects its accessibility.

2.3.4 Double bypass GMAW

To further increase the productivity and reduce heat input, Double Bypass GMAW (DB-GMAW) is developed in the Center for Manufacturing at the University of Kentucky [53-55]. Two GTAW torches are adopted to bypass the melting current. As shown in Fig. 2-11, the force acting on the droplet will be balanced by the bypass forces themselves. The left bypass current will be the same as the right one, and they could be monitored and controlled.

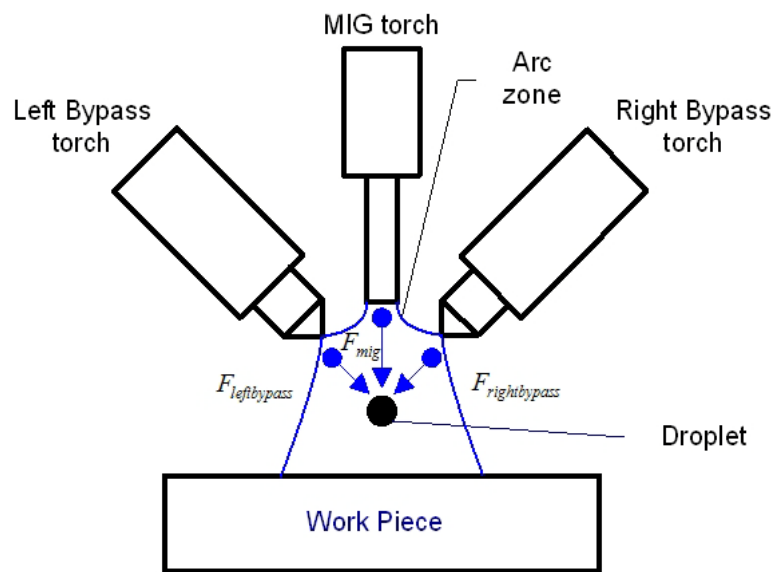


Fig. 2-11 Arc forces act on the droplet in DB-GMAW

The schematic diagram of DB-GMAW is shown in Fig. 2-12. As the bypass welding currents could be controlled, the current through the base metal is also well controlled. Heat input into work-piece is also reduced to a desired level.

Similar as the DE-GMAW, the metal transfer type in DB-GMAW is changed. Free flight metal transfer could be obtained with total welding current below the transition current. Much electric energy is used on the bypass torches without bringing many benefits to the metal transfer process.

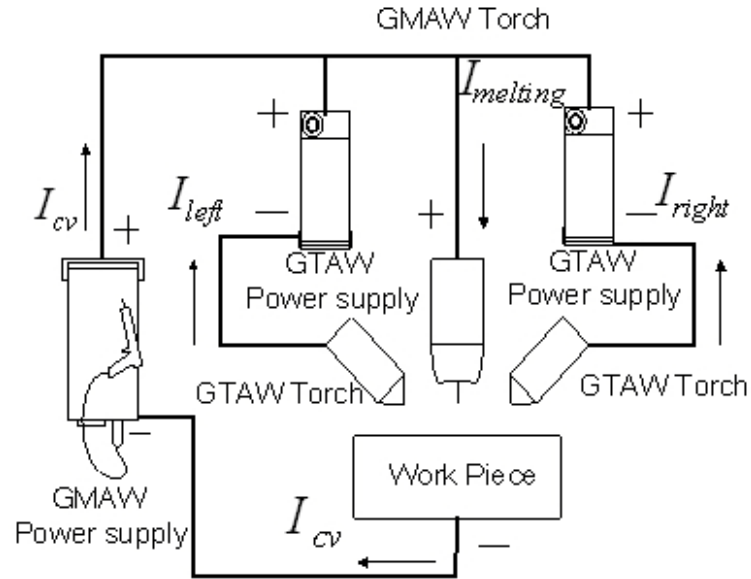


Fig. 2-12 Illustration of DB-GMAW

2.3.5 Other metal transfer control methods of GMAW

Pulsed spray metal transfer (GMAW-P) is a highly controlled variant of axial spray transfer, in which the welding current is cycled between a high peak current and a low background current level. In GMAW-P, the base current is used to keep the arc on while the peak current is adopted to melt the electrode and detach droplet. The heat input and average current will be lowered to an acceptable level. While the pulsed GMAW has been widely adopted in industry, it does have certain limitations. The fundamental cause of these limitations is that a peak current higher than the transition current [8] must be used in order to detach the droplet to complete the metal transfer. Vaporization occurs under high current and results in fumes. More critically, the arc pressure is proportional to the square of the amperage [11]. The high arc pressure may blow liquid metal away from the weld pool. For full penetration application where the work-piece has to be fully penetrated through the entire thickness, the high arc pressure may easily cause burn-through. This is the major reason why the less productive GTAW process, whose amperage can be set at whatever level needed, has to be used for the root pass in full penetration applications.

An improved method of gas metal arc welding (GMAW) is developed in the Center for Manufacturing at the University of Kentucky [23-24, 56]. The method includes utilizing a pulsed current having a variable waveform to ensure the detachment of one-droplet-per-pulse of current. During the welding process, the current is sufficient to produce a droplet at the end of a consumable electrode wire. After the droplet reaches a desired size, the current is lowered to induce an oscillation in the droplet. The current is then increased which, in combination with the momentum created by the oscillation, effects droplet detachment. The oscillation may be monitored by observing the arc voltage to determine a preferred detachment instant. A computer implemented method allows for the adaptive control of the current waveform to accommodate for anticipatable variations in the welding conditions, while maintaining ODPP transfer and a constant pulse period.

Methods based on mechanically assisted droplet transfer have also been proposed or developed to produce the spray transfer below the transition current [57-58] but the torch size and weight are greatly increased resulting in a set of special and costly equipment that is not suitable for other applications. Ultrasonic GMAW is recently developed to control metal transfer. However, a high ultrasonic power will be used and the process stability should be further developed.

To sum up, aforementioned methods are “neat” using smart approaches to resolve different issues and difficulties but being “neat” also restricts their applications in wider ranges. Toward the development of a more general method, the laser enhanced GMAW has been proposed and developed in this dissertation. It adds a relatively low power laser to a conventional GMAW and the objective is to provide an auxiliary force to help detach the droplet at a desired diameter with any desired current that most suits for the application including future adaptive control applications where the current needs to be adjusted freely as determined by the control algorithm.

2.4 Existing efforts on laser-enhanced GMAW

Laser enhanced GMAW has been studied at the University of Kentucky as the first part of the project [5-7]. Much of the materials in this subsection was published in [5-7] and summarized [5-7]. This subsection directly uses the materials in these papers that document the efforts in the first part of the project. The authors of these papers are credited for the presentation of these materials and are acknowledged for the summarization.

As can be seen in [5-7], a laser beam aims to the droplet. The intention is to detach the droplet using the laser recoil pressure as an auxiliary detaching force to compensate for the lack of the electromagnetic force associated with relatively small amperage that is needed for a particular application, rather than to provide an additional heat to speed the melting of the wire. The associated additional heat from the laser should be insignificant in comparison with that of the arc used.

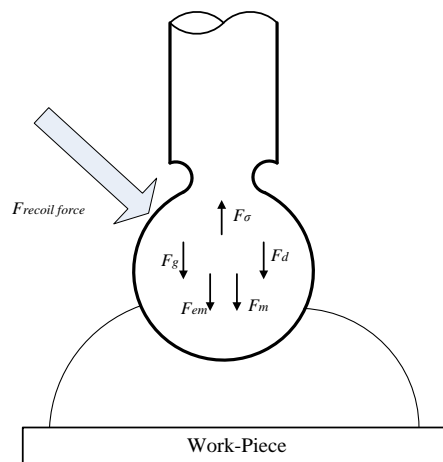


Fig. 2-13 Principle and major forces acting on the droplet in Laser Enhance GMAW

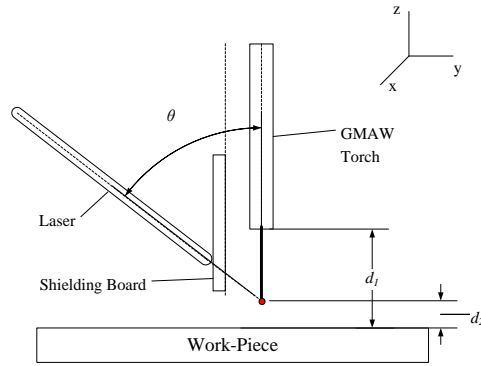
In conventional GMAW, the major forces acting on the droplet include the gravitational force F_g , electromagnetic force (Lorentz force) F_{em} , aerodynamic drag force F_d , surface tension F_{σ} , and momentum force F_m [12] as shown in Fig. 2-13. In Laser Enhanced GMAW, a laser is applied and an additional force is introduced as shown in Fig. 4. In

conventional GMAW process, the droplet is not detached when the retaining force F_σ is still sufficient to balance the detaching force F_T

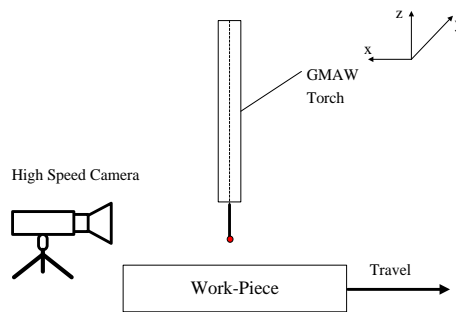
$$F_T = F_g + F_d + F_m + F_{em} \quad (1)$$

During metal transfer process, the major variables that change or can be changed to affect the detaching force are the droplet mass and the current. Because the surface tension is the major retaining force and it is fixed for the given wire, the droplet can only be detached either (1) by waiting the droplet to grow into a larger size such that the gravitational force is sufficient to break the balance; (2) by waiting the droplet to touch the weld pool such that an additional detaching force –surface tension between the droplet and weld pool- be added or (3) by increasing the current to increase the electromagnetic force. Since neither of these is ideal, a laser is introduced in this paper to increase the detaching force to a sufficient level. Because this laser force is controllable through laser intensity/power, droplets may be detached at a desired diameter at desired amperage.

System: Fig. 2-14 shows important parameters that specify a realization of Laser Enhanced GMAW system developed by Yi Huang to conduct the first part of research in the project. The GMAW torch and the laser head do not move. The work-piece moves at a constant speed. The direction of this movement will be perpendicular to plane shown in the Fig. 2-14(a). The camera was also placed in this direction with a distance about 1.2 m from torch. To conduct the Laser Enhanced GMAW process in an expected way, parameters need to be set appropriately. A high speed camera was used to capture the video of the welding process for off-line analysis. A band-pass filter centered at the laser waveform 808 nm was used to observe the process and record the images.



(a) Installation parameters



(b) Camera installation

Fig. 2-14 System installation

As shown in Fig. 2-14, three parameter used should be determined, and they are the contact tube to work-piece distance d_1 , angle between laser beam to GMAW torch θ , and the distance from the point where the laser interests the wire axis (d_2). Experimental results suggest that d_1 be set around 20 mm, θ be be around 60 degree, and d_2 be set at the range from 3 to 7 mm.

The laser used is Nuvonyx Diode laser ISL-1000L (see Fig. 2-15) whose focal beam dimension is $1\text{mm} \times 14\text{mm}$ and wavelength is 808nm. When this laser is used, only less than 1/14 of the laser beam can be applied onto the droplet to generate the recoil force to detach the droplet as the diameter of the wire is 0.8 mm and the diameter of droplet may be just slightly greater. However, in the first part of the efforts that focus on proving concepts, the efficiency of the laser is not a primary concern.

Fig. 2-15 shows the arrangement of the laser in relation with the torch. In this experimental setup, the laser beam is aligned with the wire. In order to protect the end of laser from contamination of possible fumes, a shielding board (not shown in Fig. 2-15) is added between the laser and torch and the laser is projected through a hole on the shielding board to the wire.



Fig. 2-15 Installation of GMAW and Laser (the shielding board is not shown in the picture)

A CV (constant voltage) continuous waveform power supply was used to conduct experiments. Pure argon was used as the shield gas and the flow rate was 12L/min (25.4 ft³/h). The work-piece was mild steel and experiments were done as bead-on-plate at a travel speed 6.6 mm/s (15.6 in./min). The wire used was ER70S-6 of 0.8 mm (0.03 inch) diameter. The distance from the contact tube to the work piece was 20 mm as aforementioned.

The welding voltage was set at four levels: 26, 28, 30, and 32 volts. For each voltage, four different wire feed speeds, 250, 300, 350, and 400 inches per minute, were used to produce different welding current levels resulting in 16 sets of experimental conditions. In all experiments, welding currents were not more than 135 amps which will generate short-circuiting or repelled globular transfer or non-wire-axis drop globular in the conventional GMAW. The laser beam was continuously applied along the wire (solid and droplet) at four different levels of laser intensities for each of the 16 experimental conditions: 0, 46 watts/mm², 54 watts/mm², and 62 watts/mm². There were thus totally

64 experiments conducted. For convenience, the parameters will be presented as a set (wire feed speed, voltage, laser intensity). Experimental results show that that all the currents were lower than the transition current that is approximately 150 amps [11] for the wire material and diameter. The current increases significantly as the voltage setting increases because of the reduced wire extension. However, the effect of the laser on the current is significant, no more than 5 amps.

Metal transfer: The diameter of the detached droplet is obtained from series of high speed images. All images presented as series have the dimension scale except for those presented individually. The time interval of consecutive images in the same series is constant. Fig. 2-16 illustrates the scene in a typical metal transfer image.

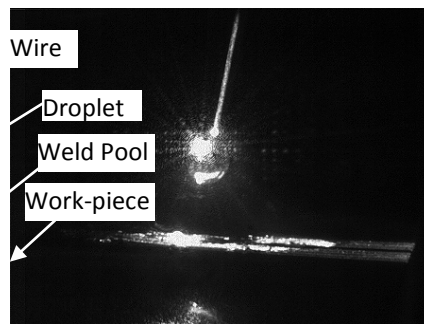
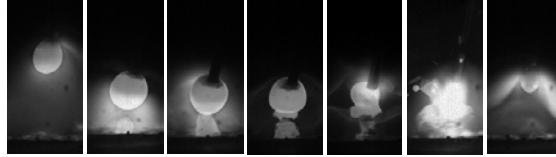
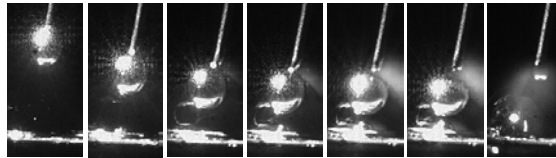


Fig. 2-16 Illustration of metal transfer image.

Fig. 2-17(a) shows a typical metal transfer cycle for the experiment conducted using (wire feed speed, voltage, laser intensity) = (300 in./min, 30 volts, 0). This is a short-circuiting transfer in which the second and third stages of the metal transfer are combined. From recorded currents, the current in this experiment is 110 amps approximately. In the cycle shown in Fig. 2-17(a), the combined detaching force from the electromagnetic and gravitational force was not sufficient enough to balance out the retaining force, i.e., the surface tension which is determined by the surface tension coefficient and diameter of the wire, before the droplet touched the weld pool. The transfer was short-circuiting and spatters were produced. Examination of recorded images during this experiment shows that the short-circuiting transfer dominated although the globular transfer also occurred occasionally.



(a) Without laser



(b) Laser intensity of 62 watts/mm^2

Fig. 2-17 Typical metal transfer in comparative experiments with and without laser under (300 in./min, 30 volts, 0) and (300 in./min, 30 volts, 62 watts/mm^2)

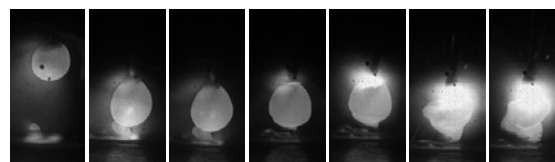
Fig. 2-17(b) is a typical metal transfer cycle from the comparative experiment with an application of the laser at intensity of 62 watts/mm^2 . As can be seen, the large droplet did not touch before detached and there were no spatters produced. This is a free flight transfer type, and it is drop globular. Examination of all images shows that the metal transfer all occurred as drop globular. It is apparent that it was the laser that made the difference in changing the metal transfer.

The recoil pressure is the major force the laser applies to the droplet. Application of a laser beam to a droplet at an appropriate direction ensures the recoil pressure to be a detaching force. The added detaching force from the laser recoil pressure reduces the need from other sources for the detaching force. When the current thus the electromagnetic force is given, the added detaching force from the laser recoil pressure reduces the needed gravitational force to balance out the surface tension. As a result, the needed diameter of the droplet for detachment is reduced. If the needed diameter is reduced sufficiently such that the droplet can grow to this diameter before it touches the weld pool, the short-circuiting transfer changes to a free flight transfer type as observed in Fig. 2-17(b).

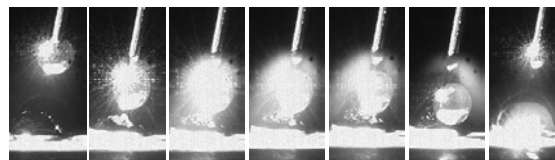
For these two comparative experiments, the laser does not change the mean welding current significantly as can be seen from the recorded currents. However, as the droplet does not touch the weld pool, the fluctuation of the welding current is reduced. Further, because the droplet is detached before touching the weld pool, the average transfer time is reduced from 183.3 ms without laser to 178.3 ms with laser. The average diameter of droplet decreases from 2.23 mm without laser to 1.89 mm with laser. The laser thus reduced the needed diameter (weight) of the droplet for detachment and changed the metal transfer type.

Figs. 2-18 to 2-20 are typical metal images from other three additional groups of comparative experiments using other different wire feed speeds also at 30 V of voltage setting. Because of the changes in the wire feed speed, the mean current will vary.

First, the typical metal transfer process as shown in Fig. 2-18(a) and Fig. 2-19(a) for 250 and 350 in./min without the laser was all the short-circuiting transfer and significant amount of spatters was produced. When the laser was applied, as can be seen from Fig. 2-18(b) and Fig. 2-19(b), the metal transfer changed to the drop globular transfer and spatters were not found. As the mean welding current did not increase, it was the laser recoil pressure that effectively changed the type of the metal transfer type. In addition, the changes in the metal transfer resulted in less fluctuating welding current and the metal transfer process was thus more stable.

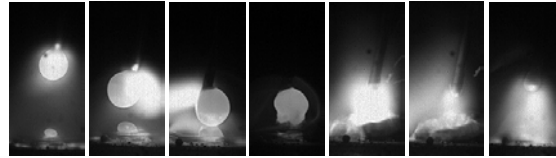


(a) Without laser

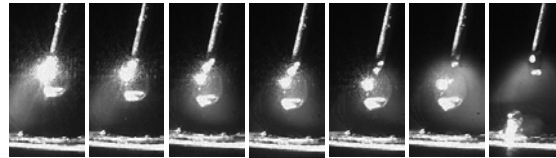


(b) Laser intensity of 62 watts/mm^2

Fig. 2-18 Typical metal transfer in comparative experiments with and without laser under (250 in./min, 30 volts, 0) and (250 in./min, 30 volts, 62 watts/mm^2)

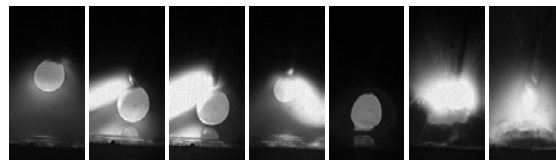


(a) Without laser

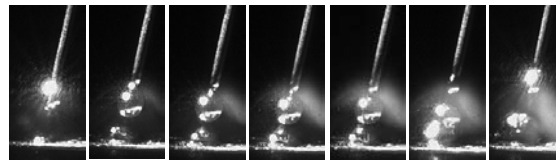


(b) Laser intensity of 62 watts/mm²

Fig. 2-19 Typical metal transfer in comparative experiments with and without laser under (350 in./min, 30 volts, 0) and (350 in./min, 30 volts, 62 watts/mm²)



(a) Without laser



(b) Laser intensity of 62 watts/mm²

Fig. 2-20 Typical metal transfer in comparative experiments with and without laser under (400 in./min, 30 volts, 0) and (400 in./min, 30 volts, 62 watts/mm²)

Second, when the wire feed speed increased to 400 in./min such that the current increased, the short-circuiting transfer no longer dominated. Fig. 2-20(a) shows a consecutive transfer process where a short-circuiting transfer followed a drop globular transfer. This was typical in the experiment with 400 in./min without the laser, different from other experiments in the series at the same voltage but lower wire feed speeds where the shorting circuiting transfer dominated. The increased mean current was the major reason for the frequent occurrence of the drop globular transfer but the fluctuation of the welding

current into relatively low levels also produced short-circuiting transfers from time to time. When the laser was introduced, short-circuiting transfers no longer occurred and transfers became totally free flight ones, as shown in Fig. 2-20(b). The diameter of droplet became similar as that of the electrode wire and the transfer is close to the drop spray. As can be seen from the recorded currents, the mean current and current levels did not increase by the laser. It was the laser recoil pressure that effectively changed the metal transfer mode from a mix of short-circuiting and drop globular to the drop spray and reduced the fluctuation in the welding current.

Findings: Analysis has been performed for the recorded metal transfer images and electrical signals. Analysis shows that the laser aiming at the droplet in laser enhanced GMAW can apply an auxiliary detaching force on the droplet without a significant additional heat or current change. Free flight transfers could be successfully produced at continuous currents from 90 amps to 135 amps with a 0.8 mm diameter steel wire without spatters. Laser enhanced metal transfer process is also governed by the established physics of metal transfer except for there is a need to include the additional detaching force caused by the laser. If it is short-circuiting transfer in conventional GMAW, laser enhanced GMAW may change it to drop globular transfer. If conventional and laser enhanced GMAW both produce drop globular, the latter reduces the diameter of the droplet. If it is short-circuit or drop globular transfer in conventional GMAW, laser enhanced GMAW may become the drop spray. The established physics of metal transfer can explain all these changes by counting the additional detach force caused by the laser. The droplet can be detached at a given/desired diameter in a reasonable range by applying appropriate laser intensity under a given current (arc variable) in a reasonable range.

However, while the feasibility of the method proposed for this project is experimentally verified, the length of the laser stripe is aligned with the wire and droplet and the laser is continuously applied. As mentioned earlier, the laser energy is wasted and adversely applied onto the work-piece. More critically, because of the presence of the continuous force due to the laser, the detachment occurs anytime when the surface tension is

balanced out by the combined detaching force due to the laser, droplet mass (gravitational force) and electromagnetic force. The detachment time and mass are not controlled although smaller droplets can be detached with relatively small currents. As a result, this dissertation research continues.

CHAPTER 3 Pulsed Laser Enhanced GMAW

In this dissertation research, a pulsed laser-enhanced GMAW process is developed as the second part of the project. In this process, the metal transfer process is monitored in real-time. When the droplet enters the location the laser aims at, a laser pulse is applied. To reduce the need for laser energy to a level achievable using our existing spot laser, the current is pulsed simultaneously with the laser. To make sure the pulses of the laser and current are correctly synchronized, the monitoring of the metal transfer process is done using high speed imaging system and real-time image processing algorithm. The accurate monitoring of the droplet using the image method can eliminate the effect of the variations in the wire feed speed, melting speed, and contact-tube-to-work distance such that the synchronization can be accurately assured.

3.1 Metal Transfer Control

The proposed method, i.e., the pulsed laser enhanced GMAW proposed, can be illustrated using Fig. 3-1 and Fig. 3-2. In Fig. 3-1, a laser spot with a relatively small diameter is generated to aim at the position where the droplet will be detached. Fig. 3-2 illustrates the waveforms of the current and laser energy with variable defined below:

I_p : peak current

I_b : base current

T_p : peak period during which the peak current laser pulse are applied and the droplet is detached

T_b : base period during which the laser pulse is not applied

E_p : peak laser energy which is applied together with the peak current to detach the droplet during the peak period.

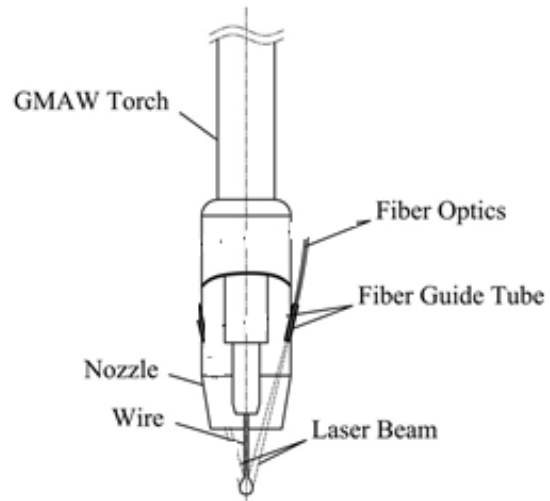


Fig. 3-1 GMAW Enhanced with a Laser Spot

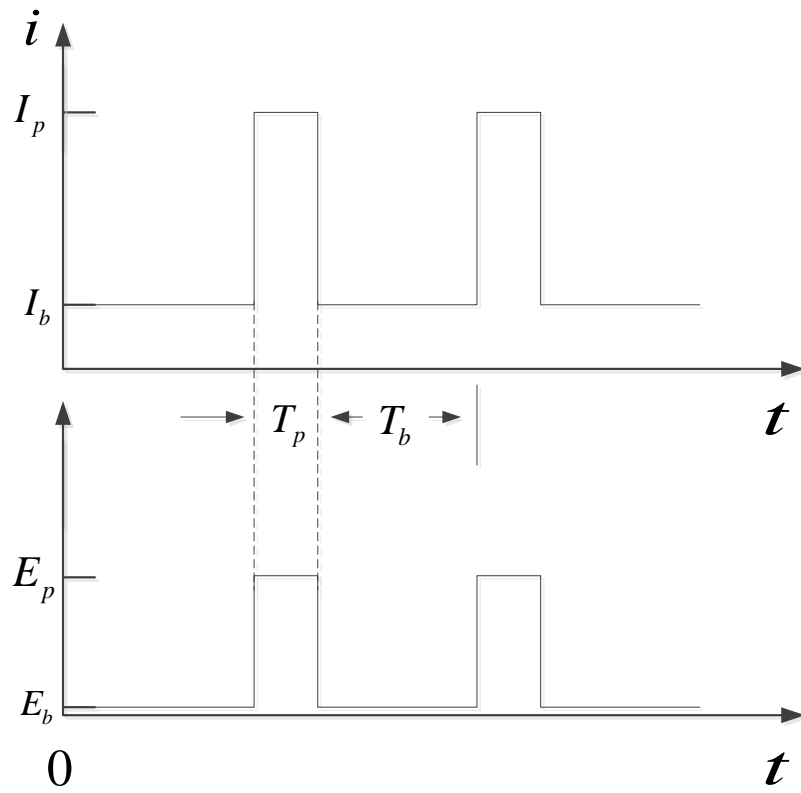


Fig. 3-2 Current and Laser Waveforms in Pulsed Laser Enhanced GMAW

The application given dictates the amperage of the peak current I_p . The difficulty we try to resolve is to reduce I_p needed to detach the droplet by using the auxiliary laser recoil laser. The peak current and laser pulse should be applied when the droplet moves to the direction aimed at by the pre-placed laser. If the droplet is not appropriately aimed by the laser, the laser will be applied either to the solid wire or will miss from underneath the droplet. As a result, there will be not laser recoil force of the liquid droplet to combine with the increased electromagnetic force during the increased current. This will be equal to a pulsed GMAW without laser enhancement. Hence, the real-time accurate measurement of the droplet which is approximately 1 mm in diameter is the key to effect the pulsed laser enhanced GMAW. This will be done by using a high speed imaging and image processing system to be introduced.

As such, the base period T_b will be a variable rather than be fixed. The peak current I_p and peak period T_p will be fixed. If the base current I_b is also fixed, the average anode power that controls the melting speed of the wire

$$P_{average} = \frac{I_p T_p + I_b T_b}{T_p + T_b} V_{anode} \quad (3-1)$$

will not be able to be controlled to balance the wire feed speed. In this equation, the anode voltage V_{anode} is in general considered a constant which does not change with the current. To balance the wire feed speed, this average power can be adjusted by changing the base current I_b . Hence, if the arc length is too short as measured by the average arc voltage such that the melting speed needs to be increased, I_b can be increased. Otherwise, I_b can be reduced.

If the arc length is in the appropriate range such that the wire tip will rise above the laser beam axis after the droplet is detached and will go through the laser beam axis in a reasonable long T_b , I_b can be fixed. In this case, the droplet is detached by the synchronized laser and current pulses when it crosses the laser beam axis. The feeding and melting of the wire is automatically balanced and no adjustment on I_b would be needed.

In the proposed method, the intersection of the laser beam axis and the wire axis is calibrated. A high speed camera monitors the wire and droplet. The calibration gives a desired location to detach the droplet in the camera coordinate system. By processing the high speed images to acquire the droplet in real-time, the instant at which the pulses need to be applied can be determined.

3.2 Metal Transfer Waveform Control

Detaching the droplet by monitoring the droplet movement and applying the pulses of the laser and current when the droplet moves across the correct position aimed by the laser assures the proposed method to work. However, the mass of the droplet detached and the time intervals between detachments are subject to the effect of the variations in the process including the contact-tube-to-work distance and wire feed speed.

Metal Transfer Frequency Control: In a typical conventional setting for GMAW, the wire feed speed V_w is pre-set. The mass needing to be melted and transferred into the work-piece in a unit time can be calculated. Hence, the mass that needs to be melted and transferred, denoted as ΔM , in the given time period ΔT can be determined. Denote the transfer frequency as f and the mass of the droplet is m , the following equation can be obtained:

$$mf = \frac{\Delta M}{\Delta T} = kV_w \quad (3-2)$$

where k is a fixed constant that is determined by wire diameter and material.

Assume that the application requires that the transfer frequency f be accurately controlled at $f = f^0$ where the desired transfer frequency f^0 is given. This would require that the position of the droplet be moved to cross the laser aiming line in a time period $T^0 = 1/f^0$ after the droplet last time crossed and then was detached. Reset the time the droplet last time crosses the aiming line as zero. Then the droplet needs to cross the aiming line again in T^0 .

Denote the location of the droplet as $y(t)$ and the coordinate of the laser aiming line as y^0 . A control is needed to assure $y(T^0)$ in order to control the mass transfer frequency. When the wire feed speed is given, this control is approximately governed by the following equation if the change in the droplet diameter can be omitted (this change, not itself, can indeed be omitted):

$$\frac{dy(t)}{dt} = V_w - \left(\frac{1}{k}\right) \frac{dm}{dt} \quad (3-3)$$

where $\frac{dm}{dt}$ is the melting speed of the wire and coefficient $\frac{1}{k}$ converts from mass/time to length/mm where k is the same fixed constant as in eq. (3-2).

The melting of the wire in GMAW has been a well explored area and many valuable results have been obtained [48-50]. Basically, the wire is melted by the anode and resistive heat which are proportional to the current and its square respectively. While the anode heat is determined by its power

$$P_{anode} = V_{anode}I \quad (3-4)$$

with the anode voltage as a constant that does not change with the current, the resistive heat also depends on the length of the wire extension (L). In literature the power which melts the wire is often simplified as

$$P = c_1I + c_2LI^2 \quad (3-5)$$

where c_1 and c_2 are coefficients. The melting speed can be considered proportional to the melting power. Hence,

$$\frac{dy(t)}{dt} = V_w - k_1I - k_2LI^2$$

where k_1 and k_2 are positive constants.

In the proposed control, $y(t)$ is controlled to follow a trajectory $y^*(t)$ to approach y^0 at T^0 by adjusting the amperage of the base current $I_b(t)$ that is relatively small. Hence, we may use a simplified model to predict the process output $y(t)$:

$$\frac{dy(t)}{dt} = V_w - k_1I_b(t) \quad (3-6)$$

Then the standard linear model predictive control algorithm can be used to determine how to adjust the amperage of the base current such that the droplet crosses the laser

aiming line at $t = T^0$. As a result, a control system shown in Fig. 3-3 can be established to control the metal transfer frequency when the wire feed speed is given.

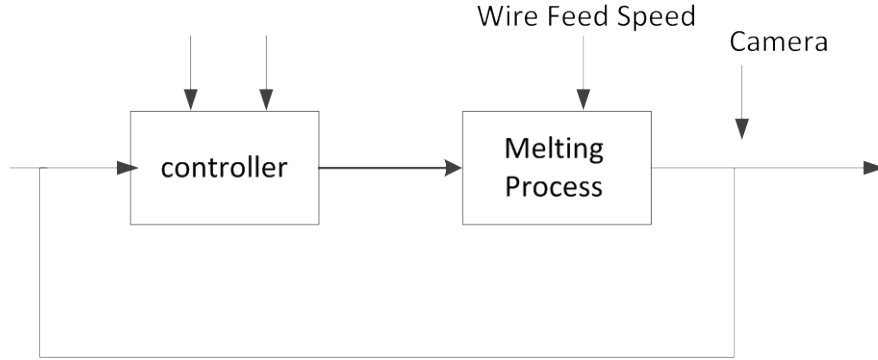


Fig. 3-3 Metal Transfer Frequency Control System

Metal Transfer Frequency and Droplet Mass Control: If both the mass and transfer frequency need to be controlled at the desired values (f^0, T^0) , a fixed wire feed speed V_w would not be sufficient. One may propose the following models

$$\frac{dy(t)}{dt} = V_w(t) - k_1 I_b(t) \quad (3-7a)$$

$$\frac{dm(t)}{dt} = c_1 I_b(t) \quad (3-7b)$$

These models suggest that the mass growth can be adjusted by I_b from (3-7b). Once I_b is determined, (3-7a) can be used to determine the wire feed speed with I_b as a given constant. However, this method would not work because the adjustment on V_w is very slow and the time needed is much longer than the transfer cycle T^0 which is typically below 50 ms.

As such, we propose to still control the metal transfer frequency using the system shown in Fig. 3-3. The adjustment on the wire feed speed for the mass control is set as an outer loop as shown in Fig. 3-4. While the speed for the inner loop should be done with a millisecond level control period, the speed for the outer loop control is much slower. In this control system, the mass of the droplet detached (only available at the discrete time k

when the droplet is detached) $m(k)$ is used as the feedback to determine how to adjust the wire feed speed.

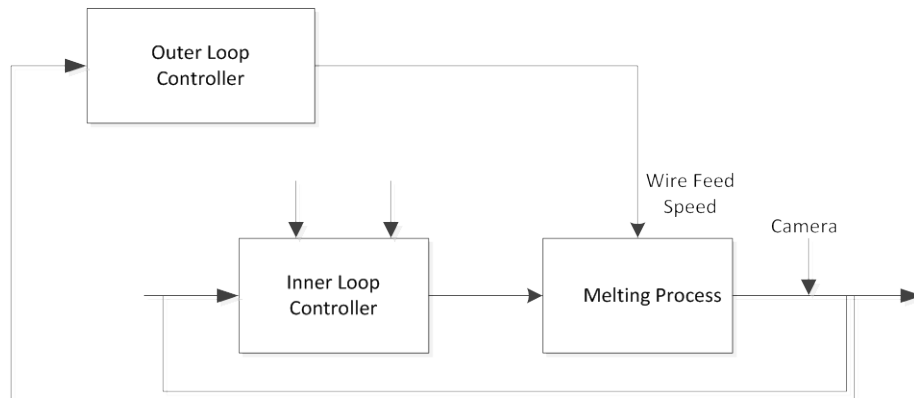


Fig. 3-4 Double-loop control for metal transfer waveform

3.3 Requirements from Proposed Controls

It is apparent that the proposed controls require (1) the ability to real-time monitor the location of the droplet to acquire the feedback $y(t)$; (2) the ability to real-time monitor the mass of the droplet when it is detached. To provide these capabilities, we will need high image system and develop high speed image processing algorithm to obtain the droplet at the speed approximately 1 ms per measurement. If the hardware does not provide the needed speed needed, we believe the needed hardware will be made available at a later time. Hence, even though not all of the control method proposed/developed would be implemented in this dissertation research, the foundation needed may still be established.

CHAPTER 4 EXPERIMENTAL SYSTEM

Fig. 4-1 is the diagram for the experimental system established to implement the pulsed laser-enhanced GMAW (Pulsed LE-GMAW) and conduct pulsed LE-GMAW experiments. This is a computer based feedback control system that uses the feedback for the droplet location from a real-time imaging and image processing subsystem to operate the laser and the CC (constant-current) power supply. It involves high speed imaging, high speed data transfer from the camera to the computer, high speed reliable image processing for accurate location of the droplet, and relies on these advanced capabilities to control the operation of the laser and power supply, thus to control the metal transfer process. To our knowledge, this will be the first system that real-time monitors the droplet and uses the monitoring result to adaptively control the metal transfer process – a process that has up to 100 cycles of metal transfer per second.

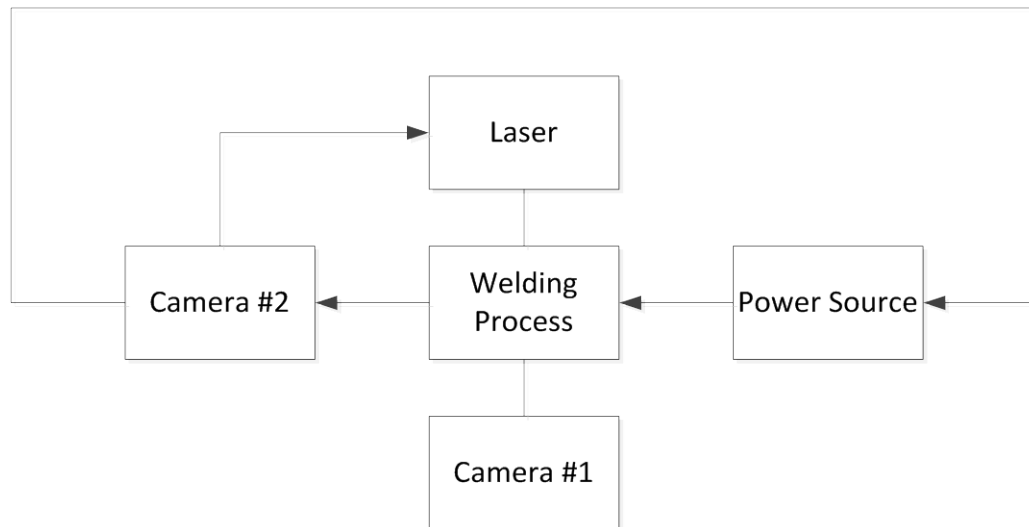


Fig. 4-1 Experimental system diagram

In addition to being computer based feedback control, this system differs from the previous LE-GMAW in the following areas:

1. Laser Mode: the laser is changed from a continuously applied one that did not require any controls to a pulsed one which requires controls to function in desirable ways. The change from continuous to pulsed mode is to minimize the laser energy waste and un-intentional effects on the weld pool.
2. Laser Dimension: the laser beam is changed from a 14 mm X 1mm stripe to a spot of 1 mm diameter. This change is to improve the utilization efficiency from previous 1/14 to 100 percent approximately. In addition, this change also reduces the un-intentional application of the laser on the weld pool from 13/14 to 0 approximately.
3. Laser Alignment: the previous laser stripe (14 mm X 1 mm) can easily be aligned along the wire to assure the application on the droplet. The small laser spot in the present system requires fine tuning for the alignment. Hence, a new laser fixture has been built to flexibly adjust the laser orientation and locations to allow the easy alignment.
4. Fixture for Monitoring Camera: the previous system uses a recording camera which is a commercial package for video recording for off-line analysis. High speed images can be recorded despite the use of high resolutions allowing the droplet be easily recorded. However, for the monitoring camera whose data will be processed to provide the droplet, high speed images can only be obtained at reduced resolutions. The camera needs to aim at the droplet to reduce the field of view in order to still maintain a sufficient resolution. To this end, a flexible fixture has been built to allow the camera to aim at the droplet and wire rapidly.
5. Motion System: In the previous system, a linear motion is used. To introduce relatively large variations in the contact-tube-to-work, a major variation that affects the arc length and requires the proposed control method to overcome using the feedback of the droplet position, a rotation system is used to rotate a pipe in this dissertation research. By rotating a pipe, the distance from the work-piece surface (pipe surface) to the fixed torch varies when the pipe is rotated because of the imperfect alignment of the pipe longitudinal axis with the axis of the rotation.

The imperfect roundness of the pipe introduces an additional source to affect the alignment.

In this chapter, this newly established experimental system will be described except for the real-time imaging and image processing system which will be discussed in Chapter 7.

4.1 Hardware

GMAW System

The conventional GMAW system used in this pulsed LE-GMAW system includes a CC power source, a GMAW torch, a wire feeder and a welding positioner and motion system.

In particular, a Miller Maxtron 450 CC/CV welder is used as the power source. The wire feeder is a Hobart Heavy Duty 2460 Wire Feeder 4-roll drive 6877B-1 wire feeder that is capable of feeding wire from 40 – 600 inch per minute. A 2-roll drive version of this wire feeder was tried first but later it was proved to be un-stable when feeding the wire of the diameter of 0.8mm. Steel pipes are fixed to a Panjiris mini-pro welding positioner that rotates the pipe. The wall thickness of the pipe used is 2.1mm.

Laser

A small spot laser with a lower power output is used to replace the previous laser of much larger stripe to generate the auxiliary detaching force to the droplet. What needs to be noted is that the laser used in the process is to provide an auxiliary detaching force solely rather than to provide any intentional heat to be transferred into the weld pool. The process is thus different from Laser-GMAW hybrid process where a high power density laser is projected directly to the weld pool and provides significant amount of heat input intentionally.

The laser used in this new system is a DLR-50 fiber laser manufactured by IPG Photonics with maximum output power of 50 watts. The power can be adjusted in real-time by providing an analog voltage signal. The laser has a guide laser module and a fiber laser

module. The two lasers have identical trajectories. The focused area of the laser spot is approximately 1mm in diameter. The wavelength of the fiber laser is between 960 nm and 980 nm. This infrared laser is invisible and the guide laser is thus used to help it to aim.

Fig. 4-2 shows the laser and installation in relation to the welding torch and wire. The flexile fixture can be seen. The bottom in the picture of the positioner with a pipe installed.

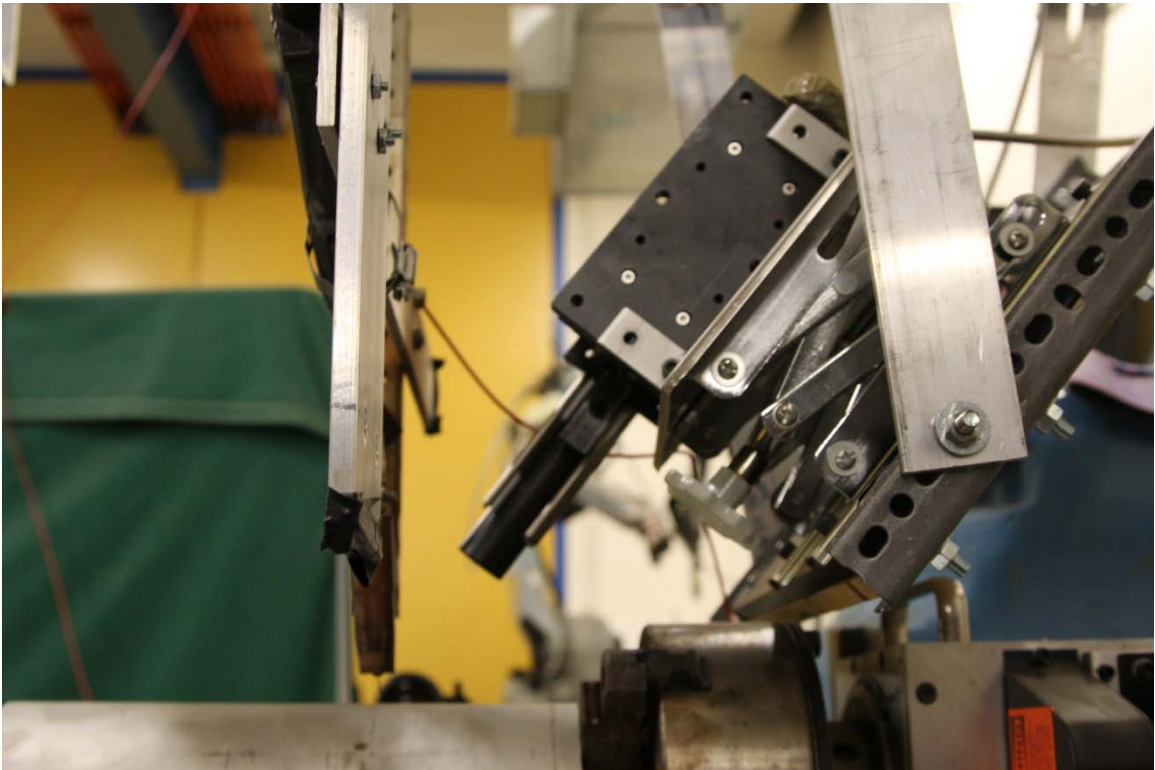


Fig. 4-2 Laser and its installation in relation to the welding torch

Machine Vision Control System

The high speed machine vision system used to monitor the droplet in real-time consists of a micro lens which allows to aims at a small object from a long distance, a high speed camera and a frame grabber. The long distance prevents the camera and lens from being damaged by possible spatters from a GMAW process.

The high speed camera is a Gazelle gzl-cl-22c5m high speed camera (see Fig. 4-3), made by PointGrey, equipped with a nikkor 200mm f/4D micro lens to capture the images reflecting the droplet growth process from a relatively large distance. The gzl-cl-22c5m camera has a CMOS CMV2000 sensor with the diagonal size of 1.7 cm. Its fastest shutter speed is 5.5 μ m. For 2048 x 1088 pixels resolution, the highest frame rate is 280 fps. For this dissertation research where the frame rate needs to be relatively high, , the resolution is set to be 200 x 800 pixels. The camera can thus capture the images at 1200 frames-per-second.

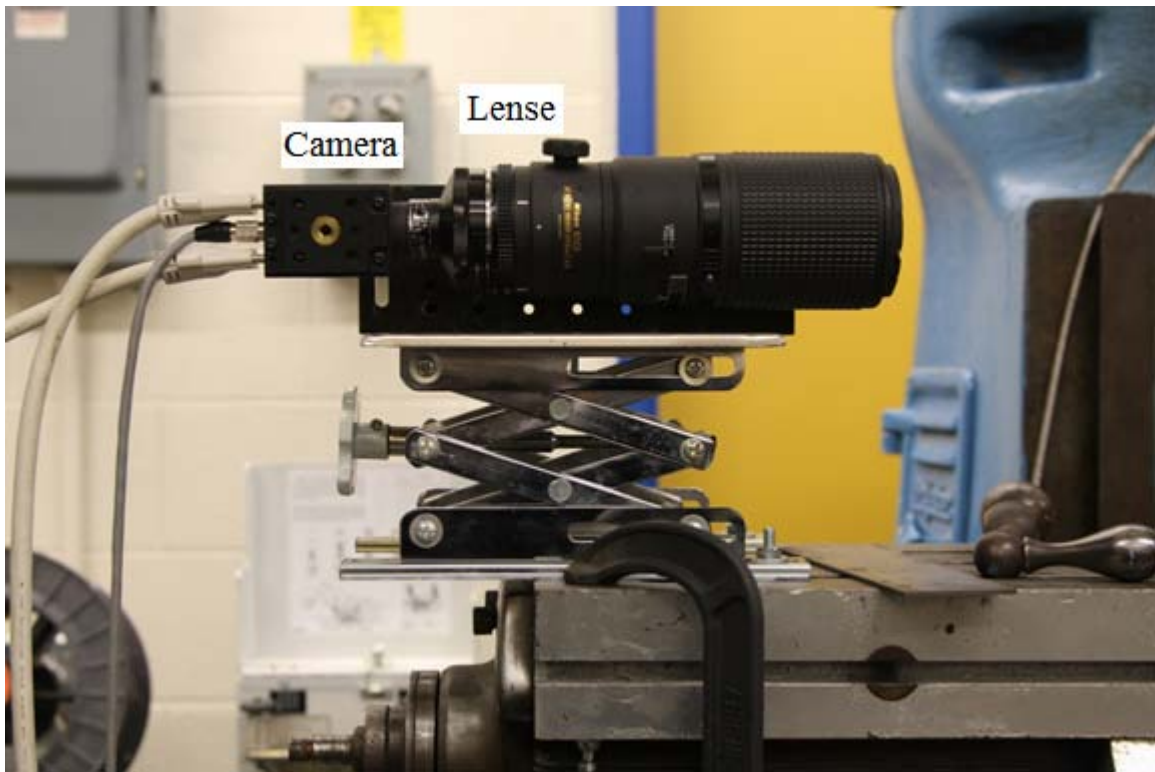


Fig. 4-3 High speed camera and installation fixture

The frequency response characteristic of the gzl-cl-22c5m camera is given in Fig. 4-3. In the new experimental system for this dissertation research, the wavelength of the laser is around 970 nm. The frequency response is thus not ideal as the quantum efficiency (QE) is only 5% approximately. This means that the projected laser cannot be identified on the camera during the experiment. As a result, the trajectory of the laser has to be pre-identified by projecting the guide laser (wavelength of 650nm/50% of QE). Once the

guide laser is set to a certain point, a length of metal wire will be melted at the same position to ensure the effect and the presence of the fiber laser. This recorded position will provide the position to decide when to apply the pulsed current and pulsed laser to detach the droplet.

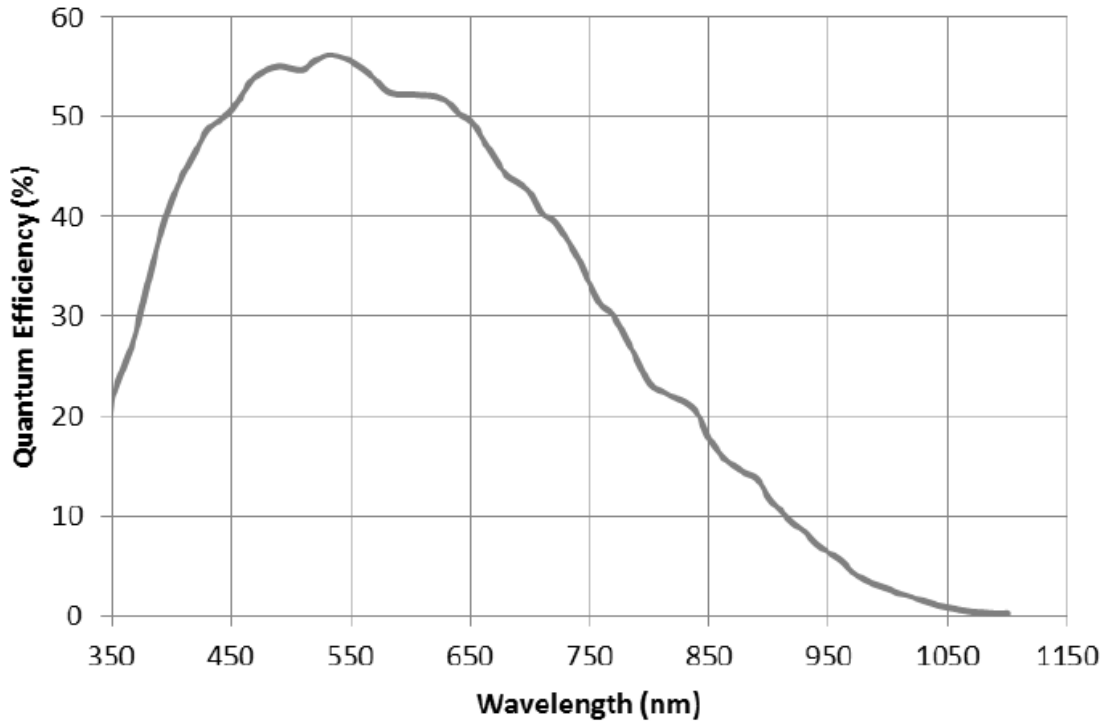


Fig. 4-4 Response Characteristic of the GZL-CL-22C5M Camera Image Sensor

The gzl-cl-22c5m camera needs to work with a frame grabber to achieve the high frame rate for the images to be accessed by the computer for processing. From the recommended list provided by the camera manufacturer, the BitFlow KBN-PCE-CL2-F frame grabber is chosen for this research. Of all the three recommended frame grabbers, this KBN-PCE-CL2 has the lowest rating of lost-of-package, which means this is the most reliable choice for our pulsed LE-GMAW system which depends on the results from the machine visions system to function properly.

A second high speed camera was also used to record images for off-line analysis. Fig. 4-5 shows this Olympus iSpeed-2 high speed camera which is capable of recording the metal transfer at 33,000 frames per second. A band-pass filter centered at 810 ± 2 nm with full

width at half maximum $10\pm 2\text{nm}$ was used to observe the process and record the images. All images presented in this dissertation were recorded using this high speed camera with this band-pass filter unless being specified otherwise. The frame rate was set to 3000 fps.



Fig. 4-5 Second high speed camera for image recording and off-line analysis

Control Interface

An NI-data-acquisition card NI 6221 data acquisition board with 2 16-bit analog input channels with the sample rate of 250KS/s, 2 16-bit output channels with update rate of 833KS/s and 8 Maximum clock rate of 1MHz digital input/output channels is used to interface with the welding power supply to control its current waveform.

Software

The main program for the control system, i.e., the pulsed LE-GMAW system, is written with Visual C++. This includes the control algorithm for the current waveform and the real-time image processing algorithm.

Matlab is used to provide off-line analysis. Labview 2009 is adopted to provide controls for some verification experiments and an independent control program for the diode laser.

4.2 System Set-Up

4.2.1 Experimental system

The experimental system is set up as in Fig. 4-6. The GMAW torch is placed above the pipe. The pipe is installed/fixed at the positioner. The weld positioned sits on a steel platform. The height of the platform is adjustable to allow the Contact Tube to Work Distance (CTWD) to be easily adjusted.

The controlling high speed camera (left in the picture) is installed on a Bridgeport travel stage that is capable of moving in three axes. This travel stage allows a precision control on the position of the camera. A common calibration for tripod mounted camera usually takes 5 to 10 minutes and a lot more calibration work needs to be done each time before experiment, while this travel stage mounted camera only takes less than 1 minute to calibrate. In addition, this travel stage provides a stable installation without being affected by ground vibration. Calibration for the camera is nearly no longer needed once the recording position is settled.

The Olympus i-speed camera views the droplet from a transverse direction parallel with the axis of the pipe rotation. There thus will be laser being directed viewed by this camera. Possible damage on this camera due to laser may thus be avoided.

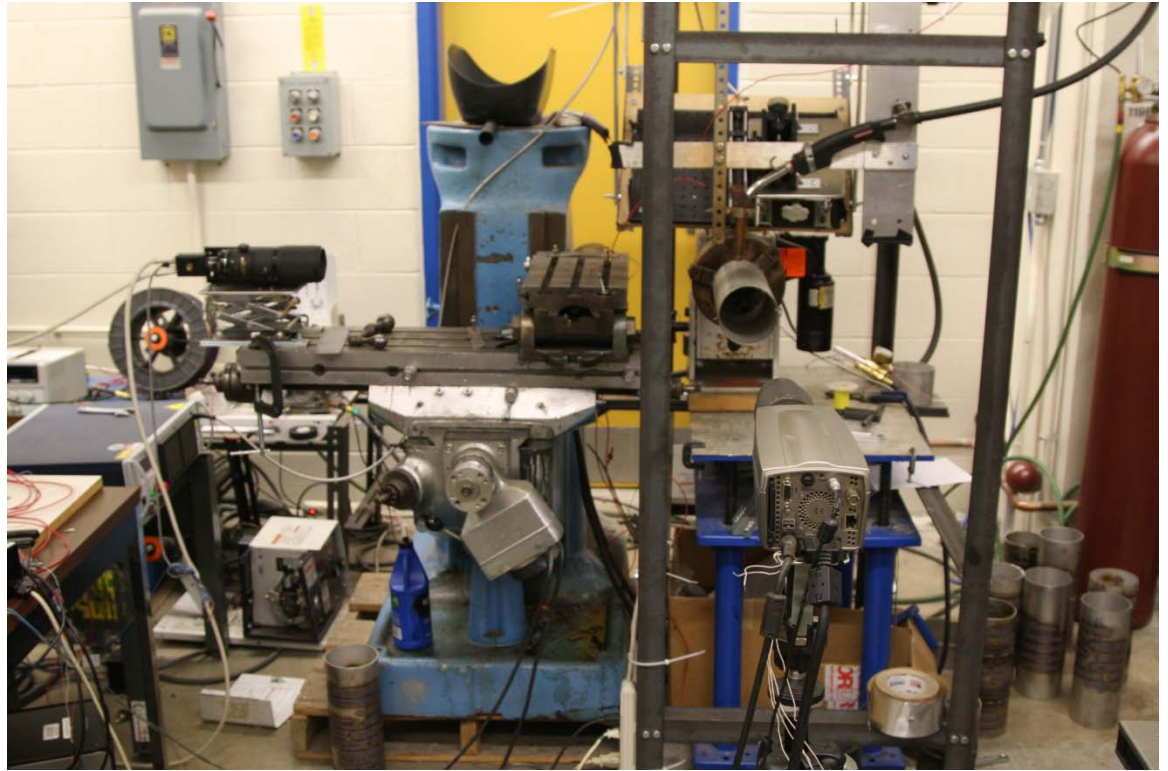


Fig. 4-6 Experimental system

The diode laser is fixed on a three-way adjustable platform/fixture and placed with the GMAW torch with an angle. The installation of the laser in relation with the torch is shown in Fig. 4-7.

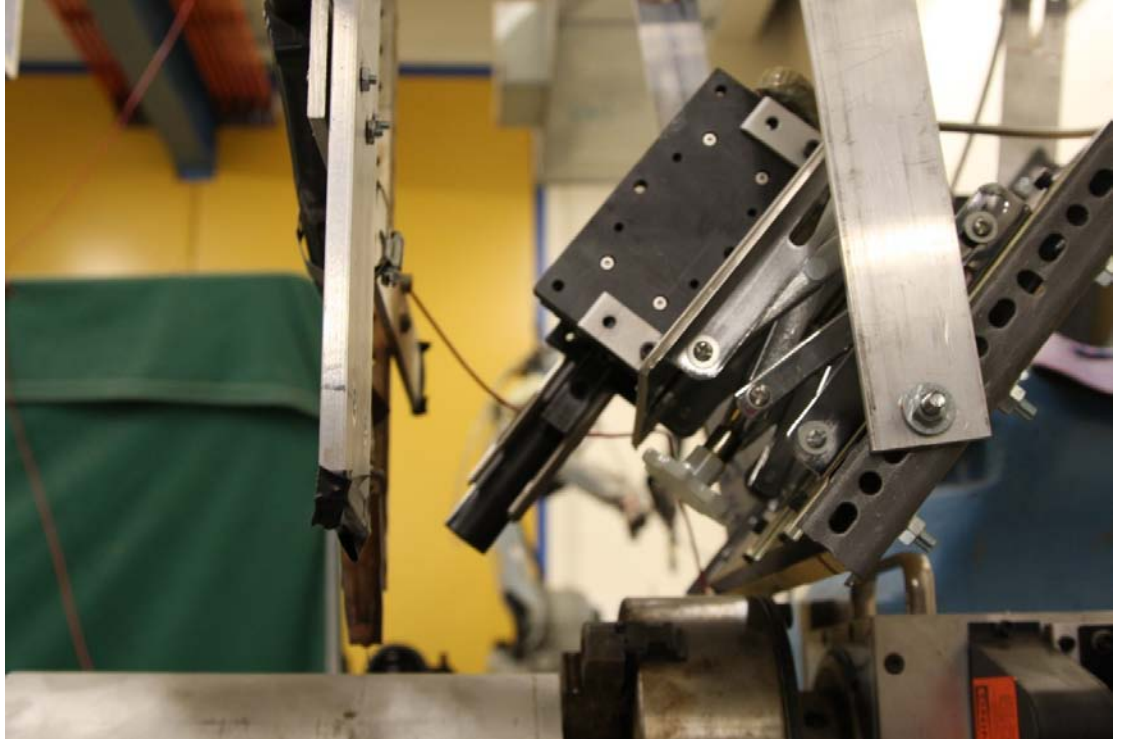


Fig. 4-7(a) Laser installation in relation with the torch: view 1

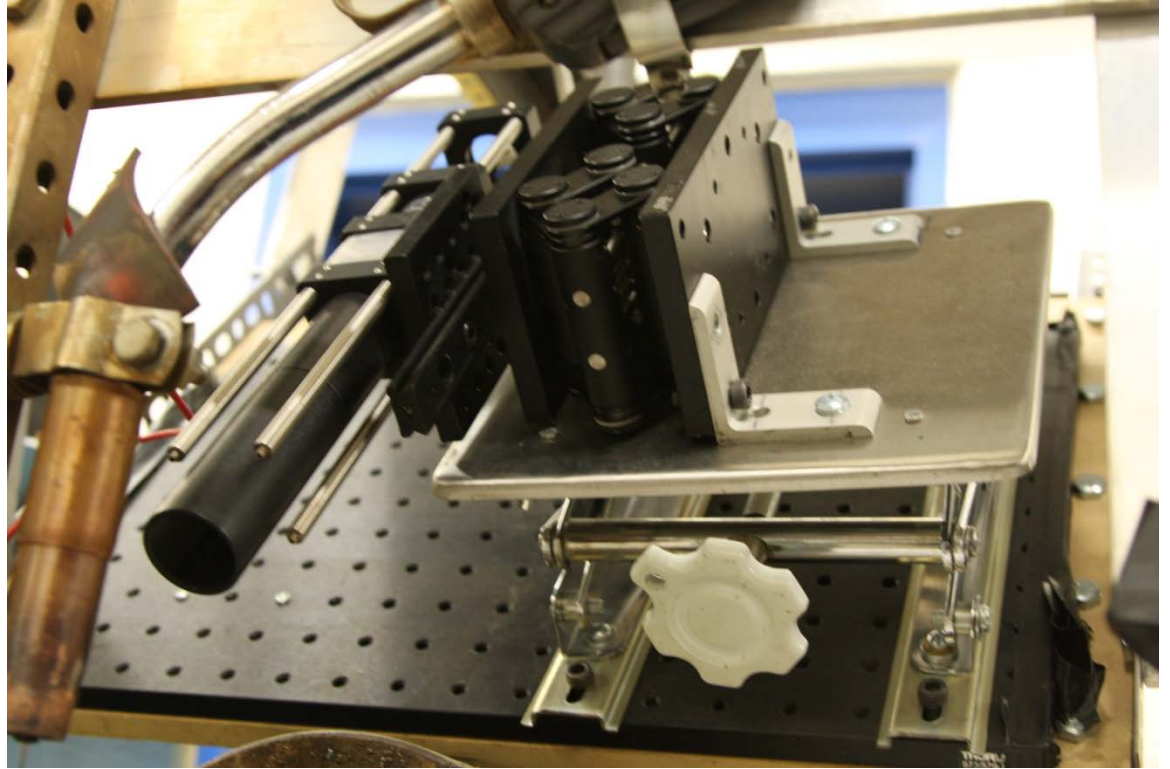


Fig. 4-7(b) Laser installation in relation with the torch: view 2

4.2.2 Installation parameters

Fig. 4-8(a) and (b) show the important parameters for the proposed laser enhanced GMAW system. Because the laser needs to be applied on the droplet precisely, most positions of the components in the proposed system have been pre-decided. Most of the parameters thus need to be constant for the proposed system. During the experiments, the GMAW torch and the laser remain stationary, while the work-piece positioner rotates clock-wise about x-axle. Camera #1 records the process in front of the whole system with the distance between camera #1 and the torch to be approximately 1.5m. The view direction of camera #1 is parallel with the y-axle. Camera #2 is placed along x-axle and sits 1.2m away from the torch.

Contact tube-to-work-piece distance (CTWD): The CTWD is denoted as d_1 in Fig. 4-8(a) and (b). In conventional GMAW, this parameter determines the stability of the process. The CTWD is set around 15 mm similarly as in conventional GMAW.

Wire extension: The wire extension is denoted as d_2 in Fig. 4-8 (a) and (b). The wire extension cannot be too small when the laser is projected at an angle. Otherwise, the gas nozzle may block part or entire laser beam before the laser reaches the droplet. In this research, the wire extension is approximately 10 mm.

Angle between Laser Beam to GMAW torch: θ determines the orientation of the laser recoil force as a vector in relation to other forces and its component/projection along the wire extension direction as an effective detaching force. It also affects the compactness and realizability of possible future system for industry use. While a large angle would reduce the effective detaching force along the wire axis and affect the compactness of the system, a small angle would require the gas nozzle to be modified such that the laser can reach the droplet. In this proposed system, the nozzle is not modified and the angle is selected to be around 30 degree for easy installation.

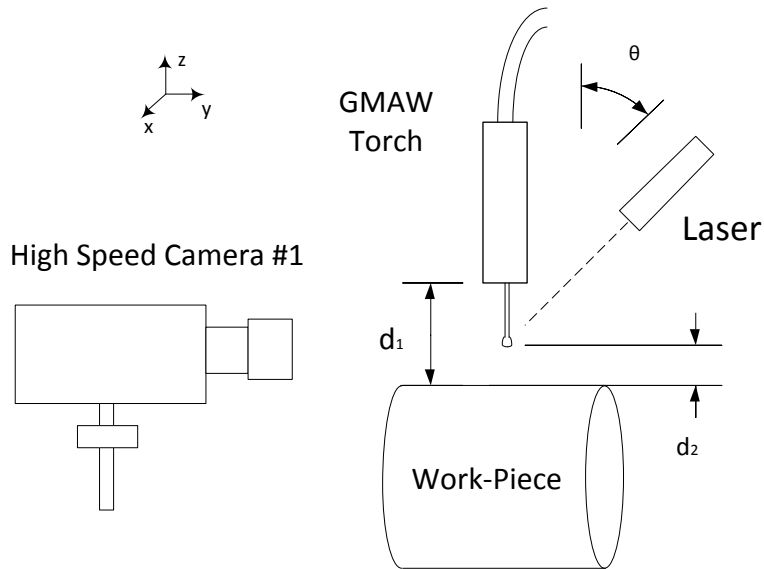


Fig. 4-8(a) Installation of the Proposed System: View 1

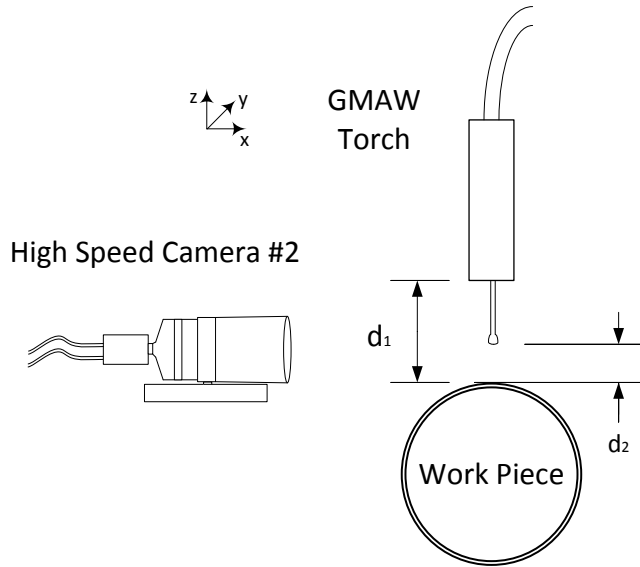


Fig. 4-8(b) Installation of the Proposed System: View 2

With the experimental system established and as specified in this chapter, the ability to experiment the pulsed laser-enhanced GMAW is partially developed. In following chapters, the image processing ability and control ability will be further developed before experiments for the pulsed LE-GMAW are established.

CHAPTER 5 Image Processing

As can be seen in Chapter 3, any realization of any of the control system proposed for the pulsed laser-enhanced GMAW depends on a real-time detection of the droplet in order to function appropriately. There are two levels of requirements for the detection of the droplet: droplet contour and droplet position. The contour of the droplet can provide full information about the droplet from shape, size, to position. However, its accurate detection may require significant computation power even though we may have done our best to optimize the algorithm. For the present computation power reasonably affordable, its real-time implementation in controlling the ultra-high speed metal transfer process may not be ready yet. However, as micro-processor frequencies increase, its real-time implementation may soon become realistic. Since this study is to establish the foundation for pulsed laser-enhanced GMAW, the detection of the droplet contour is of a core interest and thus will be addressed in this chapter in addition to the detection of the droplet position that determines when the laser is applied.

Another issue to be discussed before the image processing algorithms are developed is what environmental conditions we should consider for our algorithms. One major parameter that may affect the effectiveness of the algorithm is the robustness of the image processing algorithm with respect to the visibility of the laser in the image. In the pulsed laser-enhanced GMAW, the laser may be visible or not visible on the droplet depending on if it is applied and the visibility of its wavelength for the camera. We need the algorithm to work correctly despite the condition with the laser – applied or not applied and visible or not visible wavelength.

In this chapter, the basic algorithm is first developed to detect the contour of the droplet with the presence of visible laser. Then its effectiveness for the droplet image without visible laser will be checked to see if any modification is needed. Then a simplified algorithm that can effectively detect the droplet position will be developed to provide a basic realization of the control for the pulsed laser-enhanced GMAW process if the

contour detection requires computation power significantly greater than our current capability.

5.1 Basic Algorithm

As stated, the basic algorithm will be developed to detect the droplet contour with the presence of a visible laser. To this end, the previous continuous laser whose wavelength is visible for the camera used is applied continuously. In addition, this laser is 14 mmX1 mm which assures that the laser is always projected on the droplet.

In particular, in this subsection, an Olympus i-speed high speed camera was used to image the metal transfer process at 3,000 fps with a band-pass filter centered at 808 nm. A CV (constant voltage) continuous waveform power supply was used to conduct experiments. The wire used was ER70S-6 of 0.8 mm (0.03 inch) diameter. Pure argon was used as the shield gas and the flow rate was 14 L/min (25.4 ft³/h). The work-piece was mild steel and experiments were done as bead-on-plates at a travel speed 10 mm/s (24 in./min). In the experiments conducted in this subsection to acquire the needed images, the power of the laser was set at 864 watts and 1/14 of this laser beam (i.e. 61 watts of laser power) was applied to the wire continuously. For the wire diameter and material, the transition current for the spray transfer is approximately 150 amps (see table 4.1 in reference [8]). Table 5-1 shows the experimental conditions designed to conduct Laser Enhanced GMAW and comparative conventional GMAW whenever needed. The current shown in the table is the actual measurements from the conventional GMAW experiments. It is apparent that in the experiments, the currents were lower than the transition current that is approximately 150 amps [8] and short-circuit metal transfer should be expected in conventional GMAW.

Table 5-1 Experimental condition and welding current

Voltage (Volts)	Wire Feeding Speed (inches/min)	Welding current Measured in Conventional GMAW (amps)
29	200	82.6±21.0

5.1.1 Measurement of the growth of the droplet

By observing the recorded video, it is seen that due to the wire feed speed is relatively low approximately at 200 inch per minute; the growth of the droplet is also slow. The reflection of the laser is strong throughout the entire growth-detaching cycle. A brightness based droplet locating and edge detection based droplet extracting algorithm is thus proposed.

Region of Interest

Region of Interest (ROI) is defined first to expedite the processing and simplify the processing by removing most of unwanted information. To automate the algorithm and processing, the selection of ROI is based on the brightness of the regions in the captured images. Fig. 5-1 gives six consecutive images captured during metal transfer in laser enhanced GMAW. As can be seen, the regions containing droplets are above the regions of weld pool and both regions are bright. Hence, it is feasible to automatically find the topmost brightest region as the region of interest. In this study, the size of the ROI has been selected as 100×100 pixels by off-line analysis. Fig. 5-2 gives an example of ROI automatically selected. It is seen that the region of interest contains three bright regions: (1) region (0:15, 45:55) corresponds to the reflection of the laser from the wire; (2) region (15:50, 20:50) is the reflection of laser from the droplet, and (3) region (45:70, 35:60) is the anode spot on the droplet. It is clear that the droplet is included completely in the ROI. The remaining task is to extract the droplet automatically from the background within the ROI.

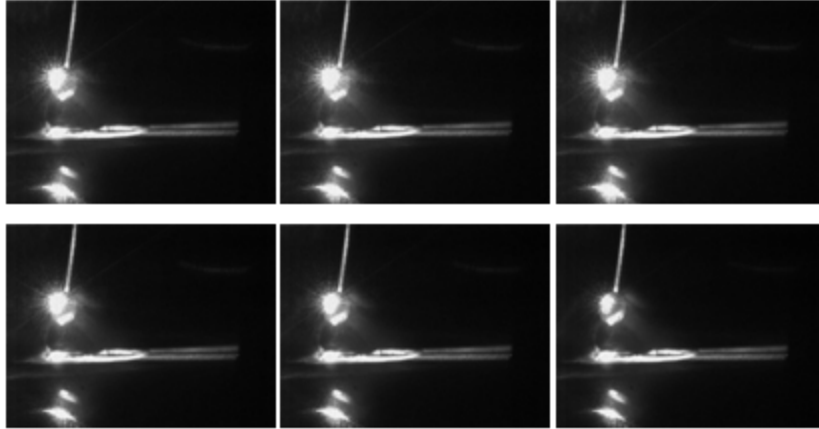


Fig. 5-1 Original images

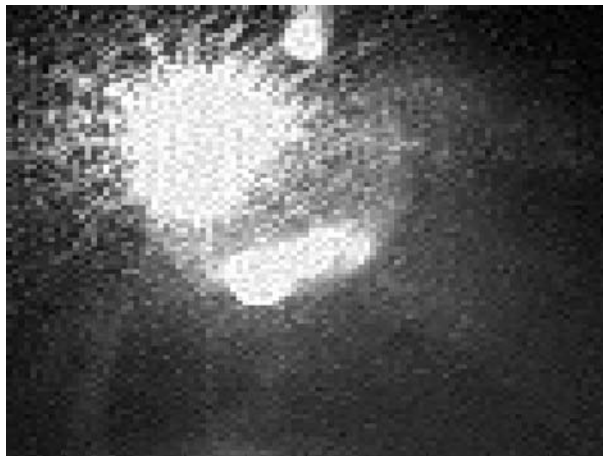


Fig. 5-2 ROI of an original image

Interpolation

Interpolation is a useful method using existing data points as reference to construct new data points within a certain range. For GMAW process monitoring, it is typical that a high speed camera is used to capture images with relatively low resolutions in order to achieve sufficient frame rates. For images of relatively low resolutions, interpolation can be an effective step to ease the processing.

The bilinear interpolation [66] for point (x, y) to be interpolated is formulated by the following equation:

$$f(x, y) = ax + by + cxy + d \quad (5-1)$$

Where coefficients a, b, c and d are obtained using the four neighbor points as:

$$\begin{bmatrix} a \\ b \\ c \\ d \end{bmatrix} = \begin{bmatrix} x-1 & y-1 & (x-1)(y-1) & 1 \\ x+1 & y-1 & (x+1)(y-1) & 1 \\ x-1 & y+1 & (x-1)(y+1) & 1 \\ x+1 & y+1 & (x+1)(y+1) & 1 \end{bmatrix}^{-1} \begin{bmatrix} f(x-1) & (y-1) \\ f(x+1) & (y-1) \\ f(x-1) & (y+1) \\ f(x+1) & (y+1) \end{bmatrix} \quad (5-2)$$

Fig. 5-3 shows an example of the bilinear interpolation which increases the image resolution from 100×100 to 200×200 . As can be seen, the details of the droplet in the interpolated image become more pronounced.

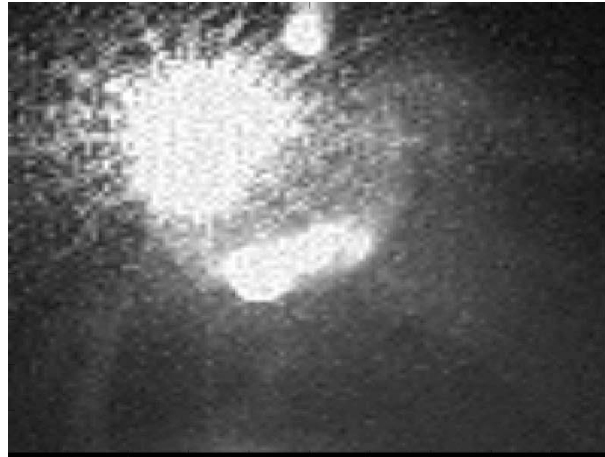


Fig. 5-3 Interpolated image

Filtering

To eliminate the noises and improve the quality of the raw image, the authors choose to filter [66] the ROI with a Gaussian filter. The filter is designed with a 5×5 kernel κ defined by following equations:

$$G(x, y) = \frac{1}{2\pi\sigma^2} * e^{-\frac{x^2+y^2}{2\sigma^2}} \quad (5-3)$$

$$K = \begin{bmatrix} G(-2,2) & G(-1,2) & G(0,2) & G(1,2) & G(2,2) \\ G(-2,1) & G(-1,1) & G(0,1) & G(1,1) & G(2,1) \\ G(-2,0) & G(-1,0) & G(0,0) & G(1,0) & G(2,0) \\ G(-2,-1) & G(-1,-1) & G(0,-1) & G(1,-1) & G(2,-1) \\ G(-2,-2) & G(-1,-2) & G(0,-2) & G(1,-2) & G(2,-2) \end{bmatrix} \quad (5-4)$$

To filter the interpolated ROI, just convolute the kernel with the image. Fig. 5-4 demonstrates the filtering effect on the interpolated ROI. It is seen that sharp noises have been decreased obviously.

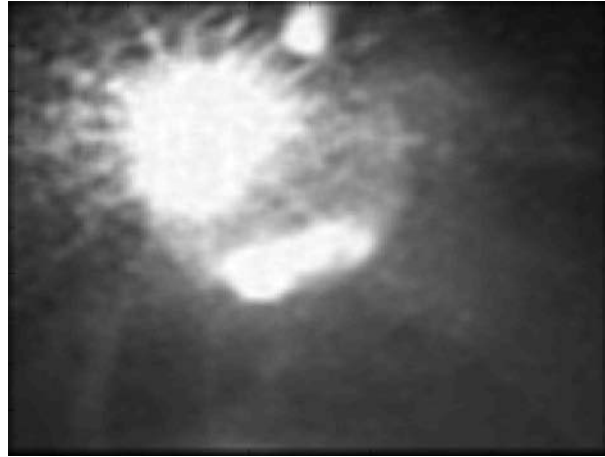


Fig. 5-4 Filtered image

Edge Detection

To extract the droplet from the background, an edge detection algorithm [66-68] is applied to the filtered image to find the edges of the droplet. First, the Sobel operator is used and the result of edge detection is shown in Fig. 5-5. As can be seen, the edges in the top right region of the droplet are missing due to the great grayscale variety introduced by the strong laser light. Hence, we also experimented with the Canny operator. The result is shown in Fig. 5-6. It is seen that not only the edges of the droplet but also many additional edges in the gaseous region under strong laser illumination are detected. The subsequent automatic clustering of droplet edges will be definitely affected. To resolve this issue, we propose to combine these two edge detection operators. For the

regions affected greatly by the laser illumination, the Sobel operator is chosen to decrease the detected non-droplet edges. For the darker areas, the Canny operator is used to preserve the edges belonging to the droplet. Based on off line analysis, the ROI, that has been interpolated and filtered, is divided into four 100×100 square sub-regions. The edges in the top left region and bottom right region are detected with the Canny operator and those in other regions are detected using the Sobel operator. Fig. 5-7 presents the computed edges in all four sub-regions and their combination is given in Fig. 5-8. As can be seen, not only the edges of the droplet are preserved well, non-droplet edges are also significantly reduced. Preserved droplet edges and reduced non-droplet edges in the background (in relation to the droplet) form a basis to successfully identify the droplet boundary.



Fig. 5-5 Droplet edges detected by the Sobel operator



Fig. 5-6 Droplet edges detected by the Canny operator

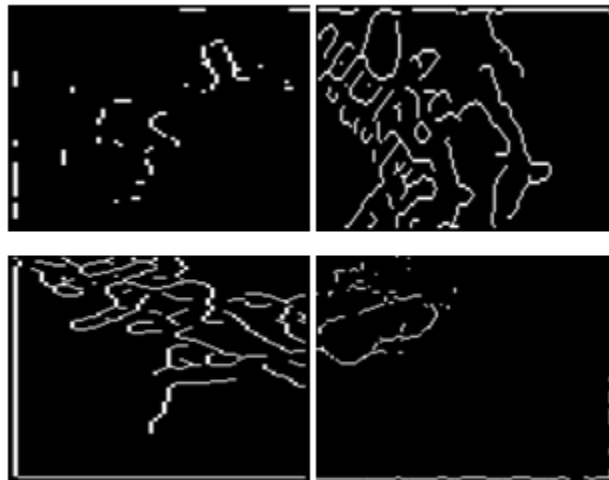


Fig. 5-7 Edge detection in four sub-regions



Fig. 5-8 Edge detection result with two operators combined

Gradient descent based center searching and K means clustering

Since the center of the droplet changes obviously from frame to frame, it should be computed instead of being pre-specified. A straightforward method to compute the center of droplet is to compute the mean value of all the detected edges, which will give an approximate center of the droplet. Assuming the computed approximate center is (x, y) , the distance d_{ij} of the any detected edge point (i, j) to this center is computed as:

$$d_{ij} = \sqrt{(i-x)^2 + (j-y)^2} \quad (5-5)$$

The mean value of all the computed distances is defined as the radius of the droplet, denoted as r . For the K means clustering, just compare the distance of d_{ij} with r : if $(r-c) < d_{ij} < (r+c)$ where c is defined as a ninth of r , the point belongs to the droplet edges. However, the center is computed as the mean value of all the detected edges and its accuracy directly depends on the accuracy of the detected edges. The unevenly distributed detected edges will lead the computed center to deviate to the higher density part of the edges. Consequently, the clustered droplet edges will deviate the true edges toward the direction of the deviation of the center. To decrease this deviation, the gradient decent based center searching algorithm has been proposed [67] to compute a

new center after the droplet edges are clustered until the difference between the current center and the previous center is zero or less than a specified value. The computed center converges to the true center when the gradient equals zero.

The means of all detected edges in the two directions are calculated as an approximate estimate of the droplet center. Clustering [69] the image with this estimated center gives the results in Fig. 5-9. For the edges remaining in Fig. 5-9, the means can be calculated again as a new estimate of the droplet center. Clustering can be done again using the new center. The results are given in Fig. 5-10. It is seen that the noise is reduced significantly after the second pass of center estimation and clustering.



Fig. 5-9 Result of clustering after center approximation



Fig. 5-10 Result of clustering after second pass center estimation

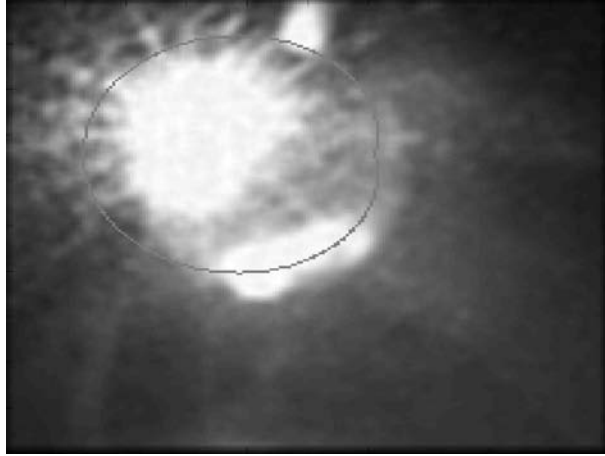


Fig. 5-11 Comparison of the detected edge with the original droplet

Fig. 5-11 shows the comparison of the detected/identified edges with the original droplet boundary. It is seen that the detected edges can accurately depict the actual droplet.

5.1.2 Droplet Tracking and Measurement Algorithm

In subsection 5.1.1, the four sub-regions in the ROI were pre-defined manually using the center of the ROI. While such a manual setting is not preferred, it also creates a potential problem, i.e., the droplet may not always appear in the center of the ROI pre-defined. As a result, some sub-regions may contain most of the droplet while others contain little or none. The effectiveness of using different operators for different sub-regions of different characteristics would be affected. Hence, an improved algorithm is proposed to adaptively estimate the droplet center and then use it to divide the ROI into four sub-regions (Fig. 5-12).

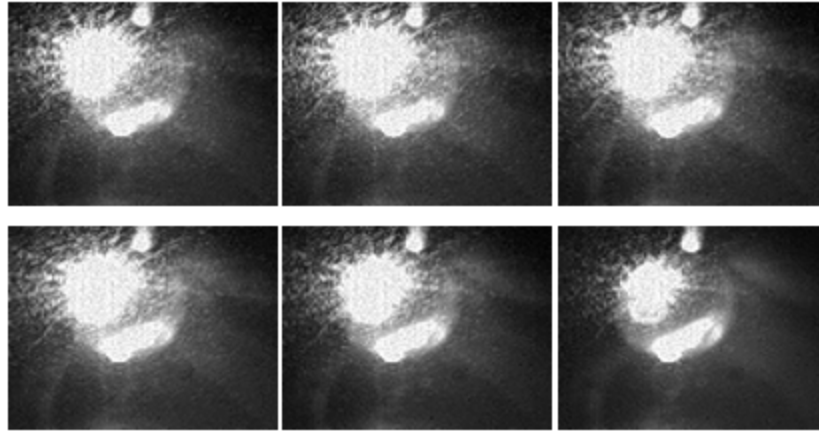


Fig. 5-12 ROIs of a series of consecutive images

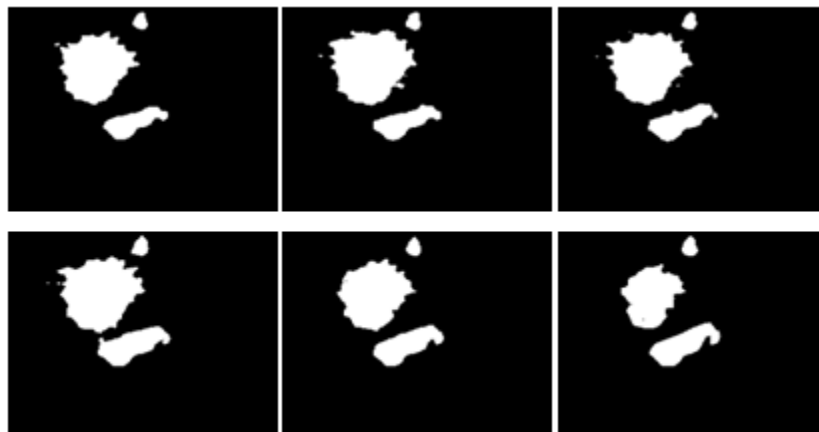


Fig. 5-13 Binarized images

Binarizing the series of images being processed (as given in Fig. 5-1) gives the result of three most bright regions as shown in Fig. 5-13. It is found that the computed geometrical center of these bright regions is close to the center of the droplet. In particular, the geometrical centers computed in the six frames are (69.5802, 72.0106), (67.4819, 72.4866), (69.6867, 73.4382), (72.1843, 75.1229), (74.5197, 76.7668) and (78.0540, 79.6191) respectively. Off line analysis shows that the computed positions are indeed

close enough to the center of the droplet and thus can be used as the center to divide the ROI into four sub-regions.

Repeat the edge detection algorithm proposed in subsection 5.1.1 but with the adaptively computed center (x, y) of the three bright regions as the droplet center to divide the ROI into four sub-regions. The results are shown in Fig. 5-14. As can be seen, the maximum noise (in terms of the distance from the actual edge of the droplet) in the detected edges is less than that of the detected edges shown in Fig. 5-8.

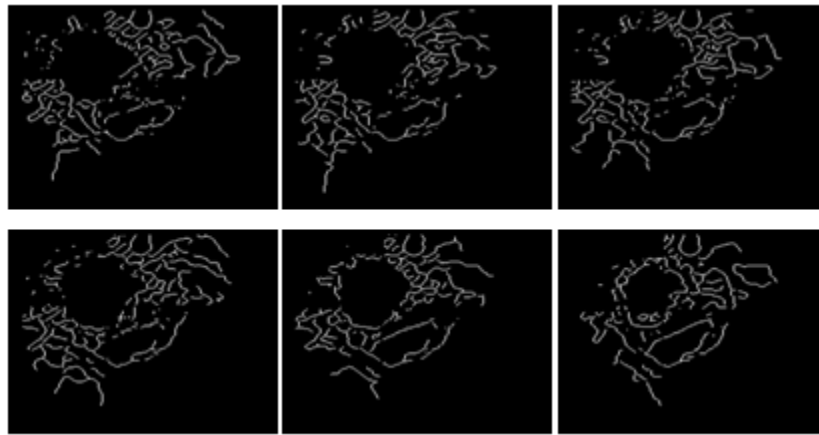


Fig. 5-14 Edges detected based on estimated droplet center

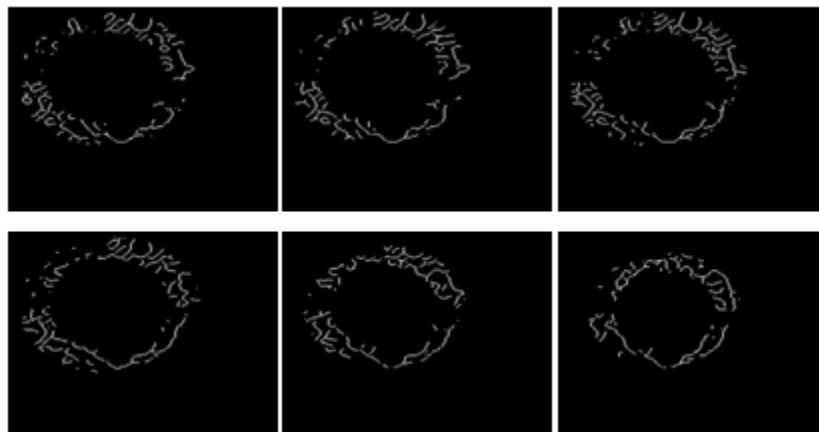


Fig. 5-15 First calculation results after second pass center estimation

Fig. 5-15 shows the results of the K means clustering after the second pass. It is seen that the detected edges are not evenly distributed around the droplet. Consequently, the computed center with the mean distance of the edges will deviate to the higher density part of the edges. To further decrease this deviation, the median value of the edges of the droplet are computed and chosen as the center instead of the mean value. Denote (p, q) as the new center of the droplet, C_h as the horizontal coordinates of droplet and C_v as the vertical coordinates of the droplet, the median value is computed as the new estimate of the droplet center:

$$p = \frac{Max(C_v) + Min(C_v)}{2} \quad (5-6)$$

$$q = \frac{Max(C_h) + Min(C_h)}{2} \quad (5-7)$$

Then the K means clustering is repeated. The results are shown in Fig. 5-16.

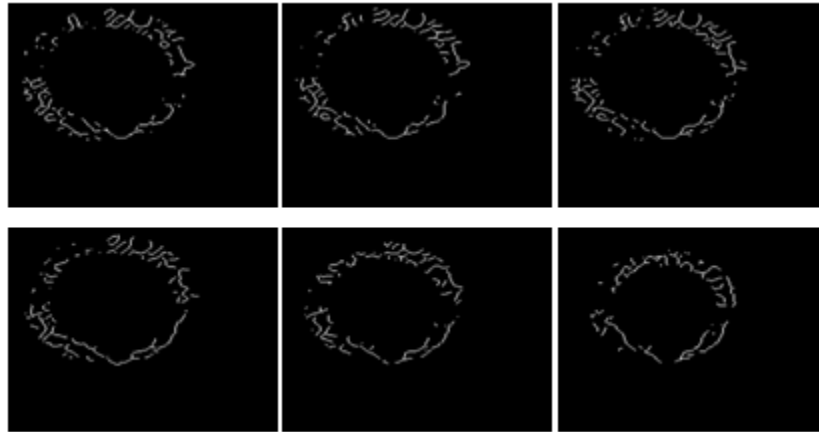


Fig. 5-16 Second pass clustering results with the new center (p, q)

After the edges of the droplet are determined, it is desirable to fit a model for the droplet boundary from the detected edges to calculate the area of the droplet (in the image). In

most cases, the shape of the droplet may not be a perfect circle. Hence, the authors propose a method to fit the edge of the droplet with a second order curve to measure the size of the droplet.

Denote r_i ($i = 1, 2, \dots, N$) as the radius from the calculated center point (p, q) to the detected edge point (x_i, y_i) and θ as the angle from the x-axis to the line that connects the center to (x_i, y_i) . Formulate the second order curve as follow:

$$r = a_0 + a_1\theta + a_2\theta^2 \quad (5-8)$$

Using Least Square Method (LSM) the coefficients can be calculated by the following equation where Y is the collection of the radius, and ϕ represents the vector of the coefficients:

$$\phi = (\psi^T \psi)^{-1} \psi^T Y \quad (5-9)$$

$$Y = [r_1, r_2, \dots, r_N]^T \quad (5-10)$$

$$\psi = \begin{bmatrix} 1 & \theta_1 & \theta_1^2 \\ 1 & \theta_2 & \theta_2^2 \\ \vdots & \vdots & \vdots \\ 1 & \theta_n & \theta_n^2 \end{bmatrix} \quad (5-11)$$

$$\phi = [a_0 \quad a_1 \quad a_2]^T \quad (5-12)$$

Solving the equations (5-9)-(5-11) gives the value of the coefficients and the second order curve can thus be fitted to calculate edges. The results are shown in Fig. 5-17.

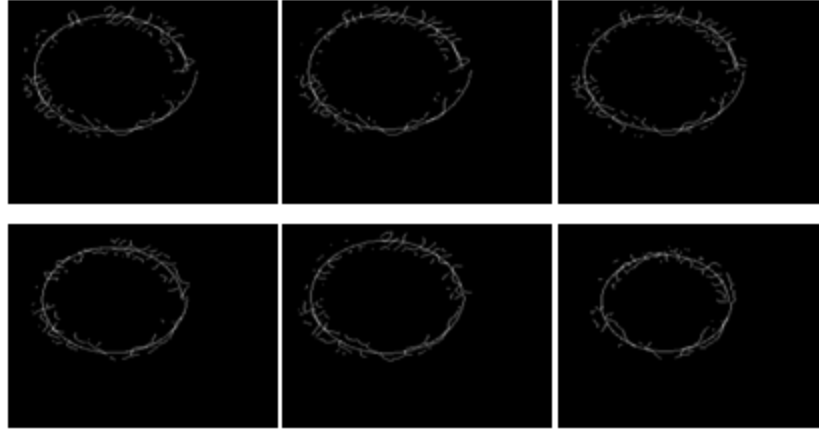


Fig. 5-17 The fitted second order curve as the estimated boundary of the droplet

For the droplet boundary, the model needs to be established with $r(0) = r(2\pi)$ as a constraint that is referred to as the closure constraint in this study. That is, when θ equals zero, equation (5-8) gives

$$r(0) = a_0 \quad (5-13)$$

When $\theta = 2\pi$, equation (5-8) generates

$$r(2\pi) = a_0 + 2a_1\pi + 4a_2\pi^2 \quad (5-14)$$

Hence, the constraint $r(0) = r(2\pi)$ gives

$$a_0 = a_0 + 2a_1\pi + 4a_2\pi^2 \quad (5-15)$$

Thus:

$$2a_1\pi = 4a_2\pi^2 \quad (5-16)$$

$$a_1 = -2a_2\pi \quad (5-17)$$

Bring equation (5-17) in equation (5-8):

$$r = a_0 + a_1\left(\theta - \frac{1}{2\pi}\theta^2\right) \quad (5-18)$$

Use the least square fitting method and equation (5-18) again to fit the modified second order curve for the detected edge of the droplets. The results are shown in Fig. 5-18.

After the coefficients a_0 and a_1 in Eq. (5-18) are known, the size of the droplet (the area of the droplet on the image) can be computed:

$$A = \frac{1}{2} \int_{-\pi}^{\pi} r^2 d\theta = \frac{1}{2} \int_{-\pi}^{\pi} \left(a_0 + a_1\left(\theta - \frac{1}{2\pi}\theta^2\right)\right)^2 d\theta \quad (5-19)$$

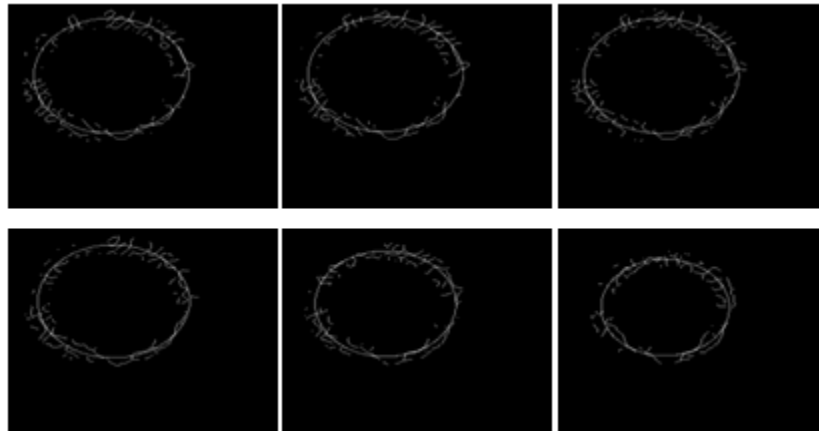


Fig. 5-18 Revised fitted second order curve

As can be seen, although the fitted curves in Fig. 5-17 fit the droplet boundaries adequately and confirmed the effectiveness of the proposed second order model in the polar coordinate system, the closure of the fitted droplet boundary is not assured. To be realistic, the fitted boundary of the droplet must be closed. After the closure constraint is applied and the estimation algorithm is revised accordingly, the closure of the fitted boundary is assured as can be seen in Fig. 5-18. Comparison of the fitted boundaries with

the original droplet images as demonstrated in Fig. 5-19 confirmed that the second order model in the polar coordinate system with the closure constraint modeled the droplet boundary with adequate accuracy.

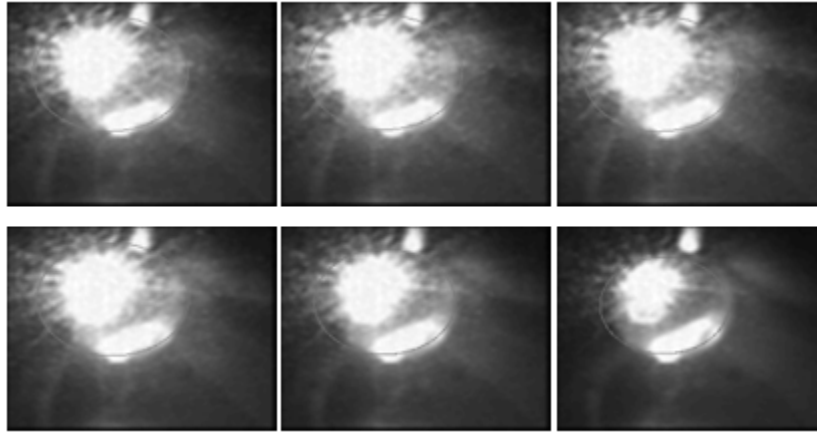


Fig. 5-19 Compare the revised fitting result with the droplet boundary

5.1.3 Summary

As can be seen, under the environment of the presence of visible laser,

- An effective image processing algorithm has been proposed to extract the droplet boundary edges (contours) satisfactorily for the laser enhanced GMAW.
- The proposed polar coordinate model with the closure constraint provides a reasonable modeling approach for the droplet.
- Experimental results verified the effectiveness of the proposed image processing algorithm and polar coordinate model with the closure constraint.
- The proposed algorithm and model form part of the foundation to measure and feedback control the size of the growing droplets in the laser enhanced GMAW for possible applications in precision joining.

5.2 Algorithm without Visible Laser

In section 5.1, an image processing algorithm has been developed to measure the contour of the droplet when for the laser is constantly applied to the droplet in laser enhanced GMAW as the basic algorithm. In such a condition, the bright reflection spot and the anode spot on the droplet can be easily recognized by image processing algorithm, and hence provide ideal decision making criteria for droplet tracking algorithm. However, there is also the condition for pulsed laser-enhanced GMAW without a visible laser. For example, this would be the case when the wavelength of the chosen laser for the process is out of the frequency response range of the camera's sensor. This would also be the case that the bright reflection spot is not visible during the base current time. For this reason, a new image processing algorithm for the droplet contour detection needs to be developed for such a condition in order to assure the robustness of the machine vision based control system. This subsection is thus devoted to the development of such an algorithm as a modification of the basic algorithm.

The pulsed laser-enhanced GMAW experiments conducted to acquire images in this section are performed using a CC (Constant Current) power supply with 150 amp peak current 28 amp base current. The diameter of the steel wire used is also 0.8 mm. The laser pulse is synchronized with the current peak pulse. The laser power is set to its maximum output - 50 watts. However, the wavelength of the laser is invisible for the Gazelle high speed camera used to record the images to be processed. Gazelle high speed camera is the camera we will be using in the real-time control system.

Fig. 5-20 shows a series of captured frames by the Gazelle high speed camera. These frames are captured from uncontrolled GMAW process showing a droplet growth period during the base current time.



Fig. 5-20 Droplet growth period during the base current time.

To increase the processing speed, a region of interest also needs to be selected from the image. For such a purpose, the droplet must be identified from the image automatically. The mean and maximum value of the brightness in the frame is first calculated. Since the light in the image is uniquely contributed by the arc and the arc only exists beneath the electrode, the region with maximum brightness value can only be the anode spot on the

droplet. The droplet can thus be identified from the captured image. The region above the droplet is eliminated from the region of interest. Fig. 5-21 shows the selected regions of the interest for each frame in Fig. 5-20.

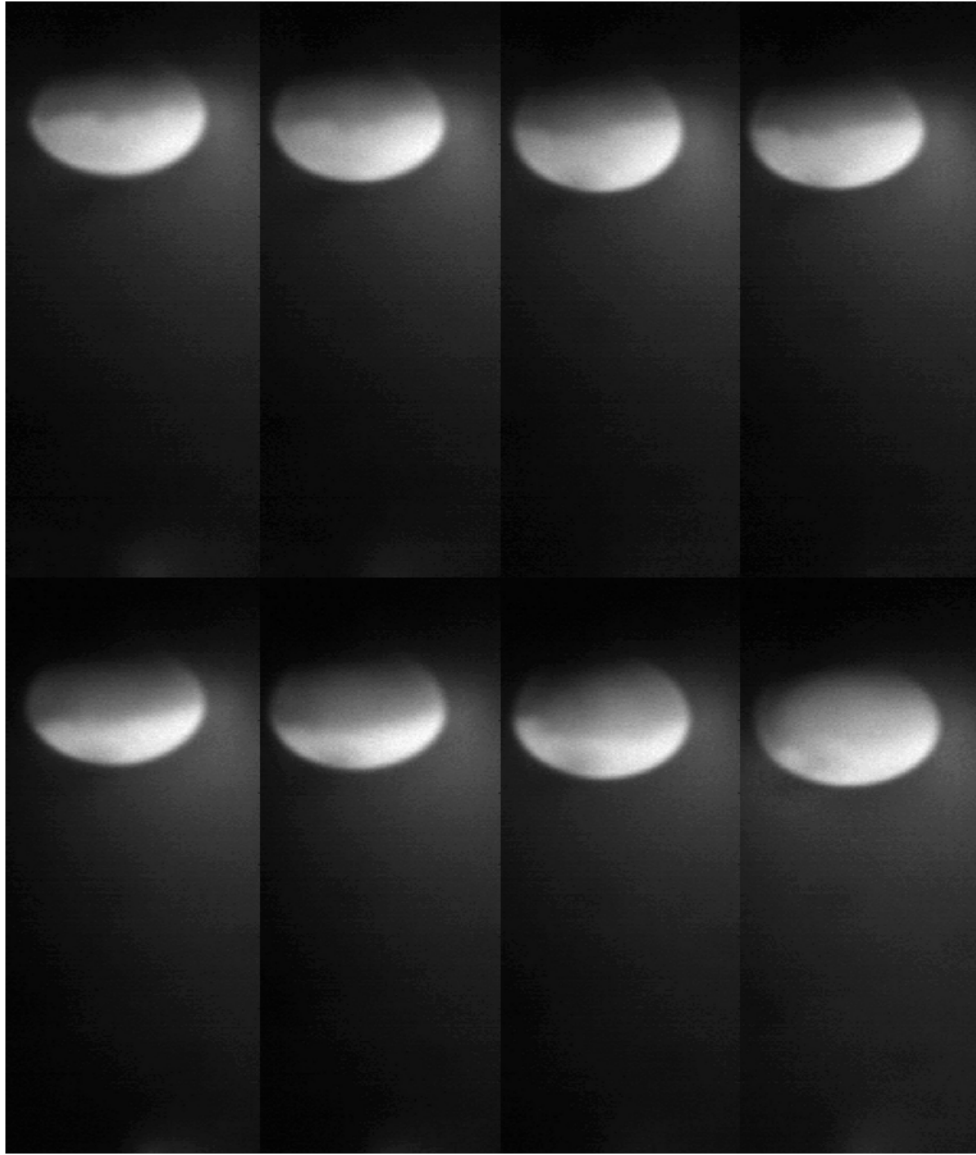


Fig. 5-21 Selected regions of interest for images in Fig. 5-20.

An edge detection algorithm then needs to be used. Because there is no visible laser (not applied during the base period), few noises exist in the selected region of interest. The edge points of the droplet can thus be easily determined using any existing edge detection

algorithm introduced in the previous section. However, it is found that the Sobel operator provides the most desirable results for the edge detection. The edge detection results for the images in Fig. 5-21 are shown in Fig. 5-22.

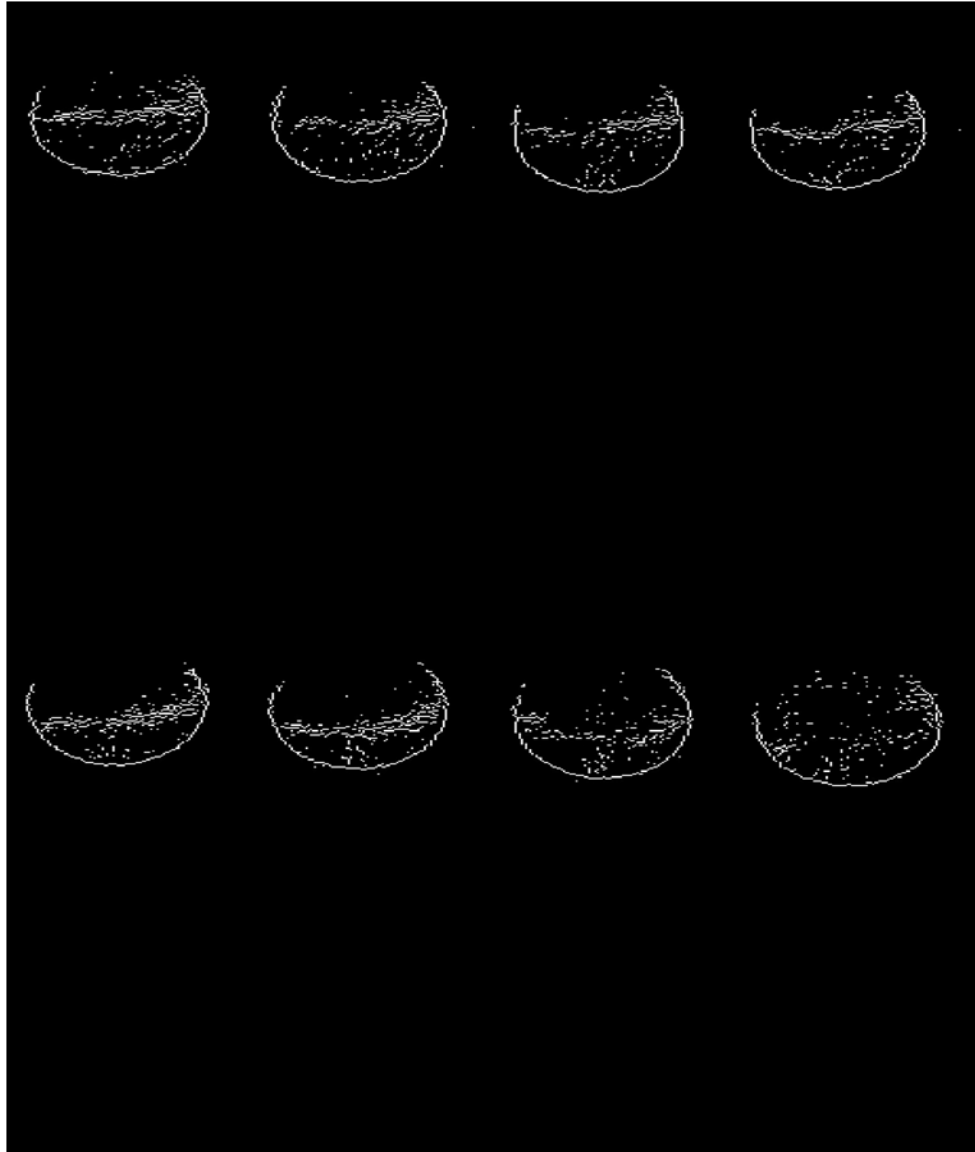


Fig. 5-22 Edges detected for images in Fig. 5-21 using the Sobel operator

To determine the upper edge of the droplet, the detected edges with the largest coordinate (most close to the contact tip) are chosen to represent the upper edge of the droplet. The lowest coordinate with the maximum brightness value in the region of the interest can be

used as the lower edge of the droplet. Hence, the center of the droplet can be estimated. Thus, the distance from the estimated center of the droplet to the upper edge and lower edge of the droplet can be estimated. Calculating the mean value of these distances gives an approximated radius of the droplet. Using this estimated radius of the droplet as a reference, any edge detection result with an either too large or too small distance to the center of the droplet can be treated as noises and thus be eliminated from the edge detection results. The resultant noise reduction can be seen by comparing Fig. 5-23 with Fig. 5-22.

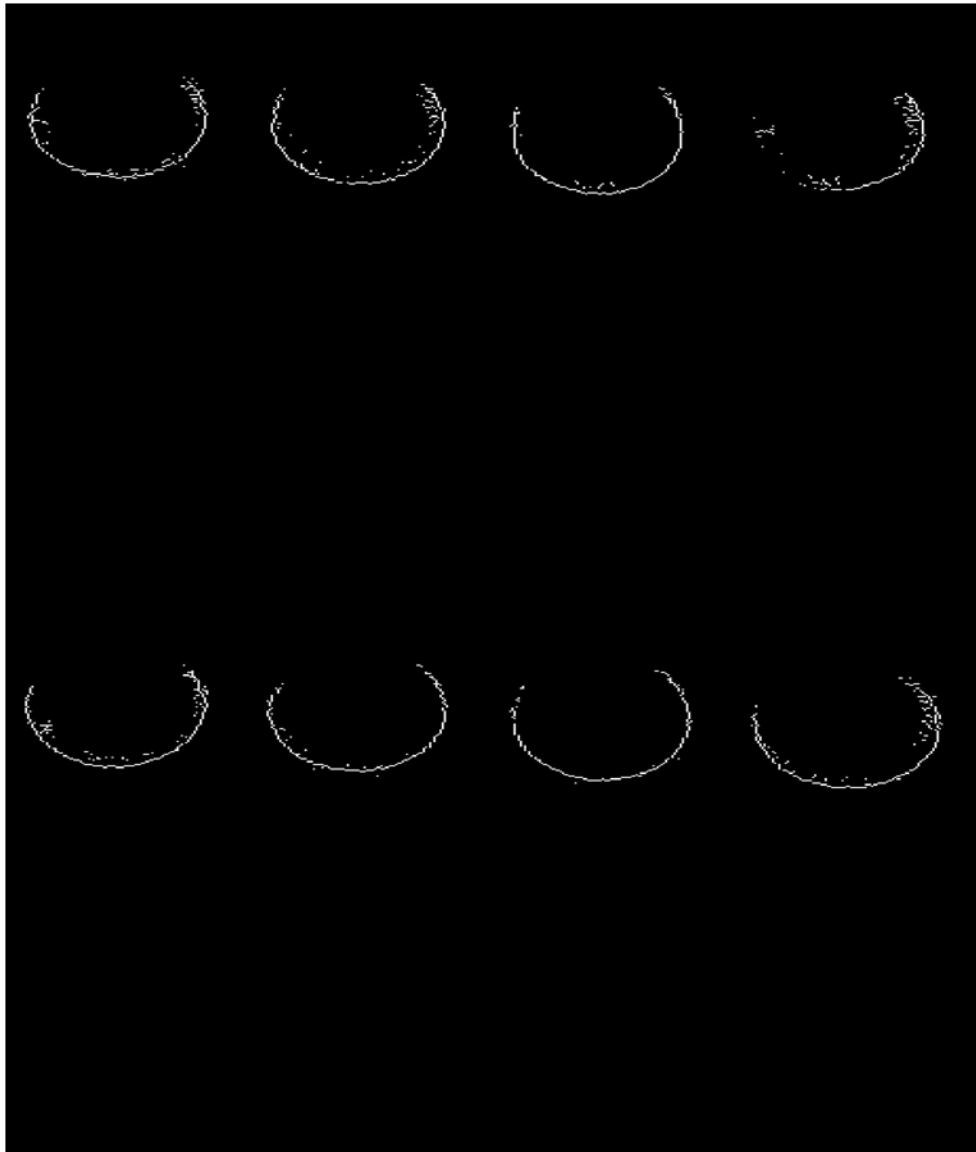


Fig. 5-23 Noise reduction results for edges detected for images in Fig. 5-21 using the Sobel operator

Repeating the least square method introduced in the previous algorithm, an closed-loop eclipse can be fitted to the calculated edges. Fig. 5-24 shows the fitted result.

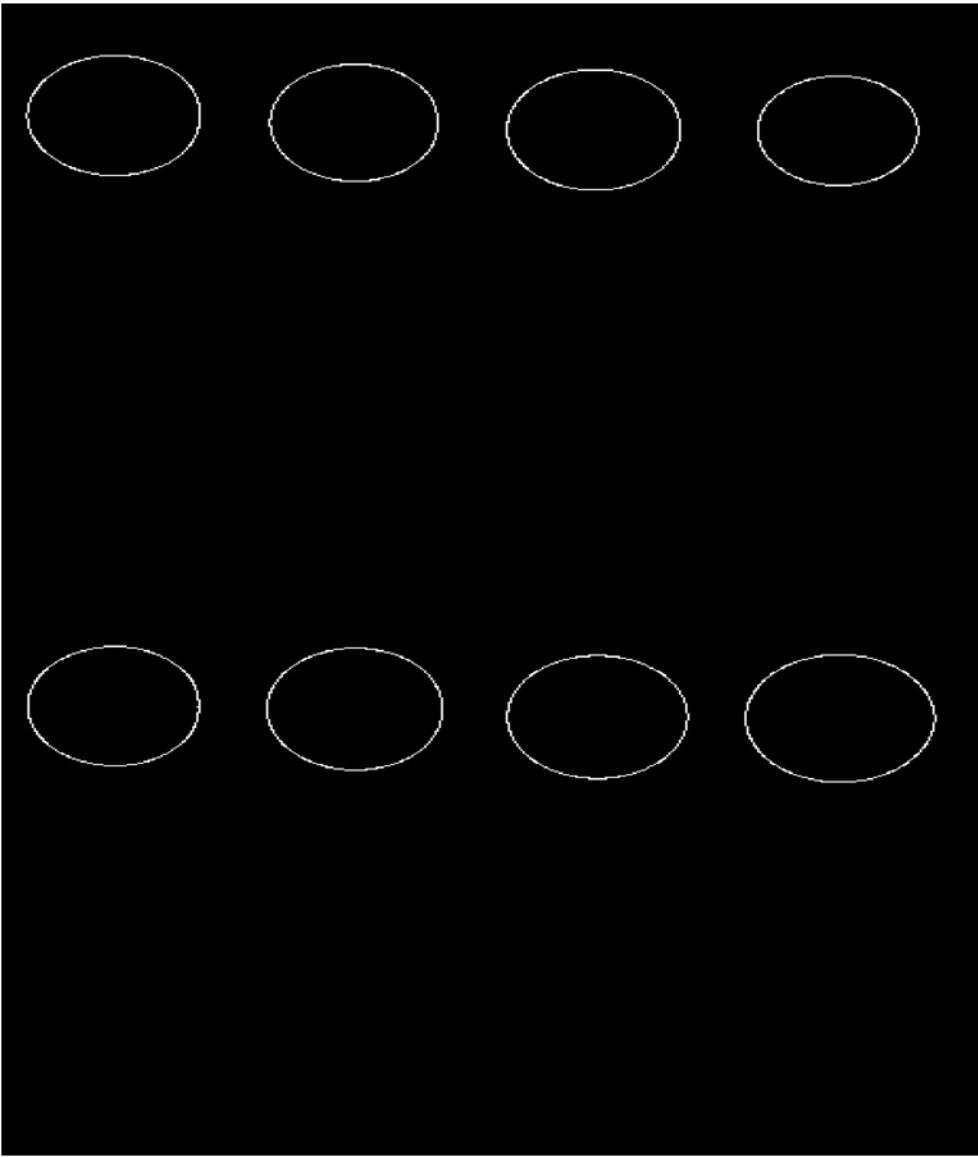


Fig. 5-24 Fitted edges

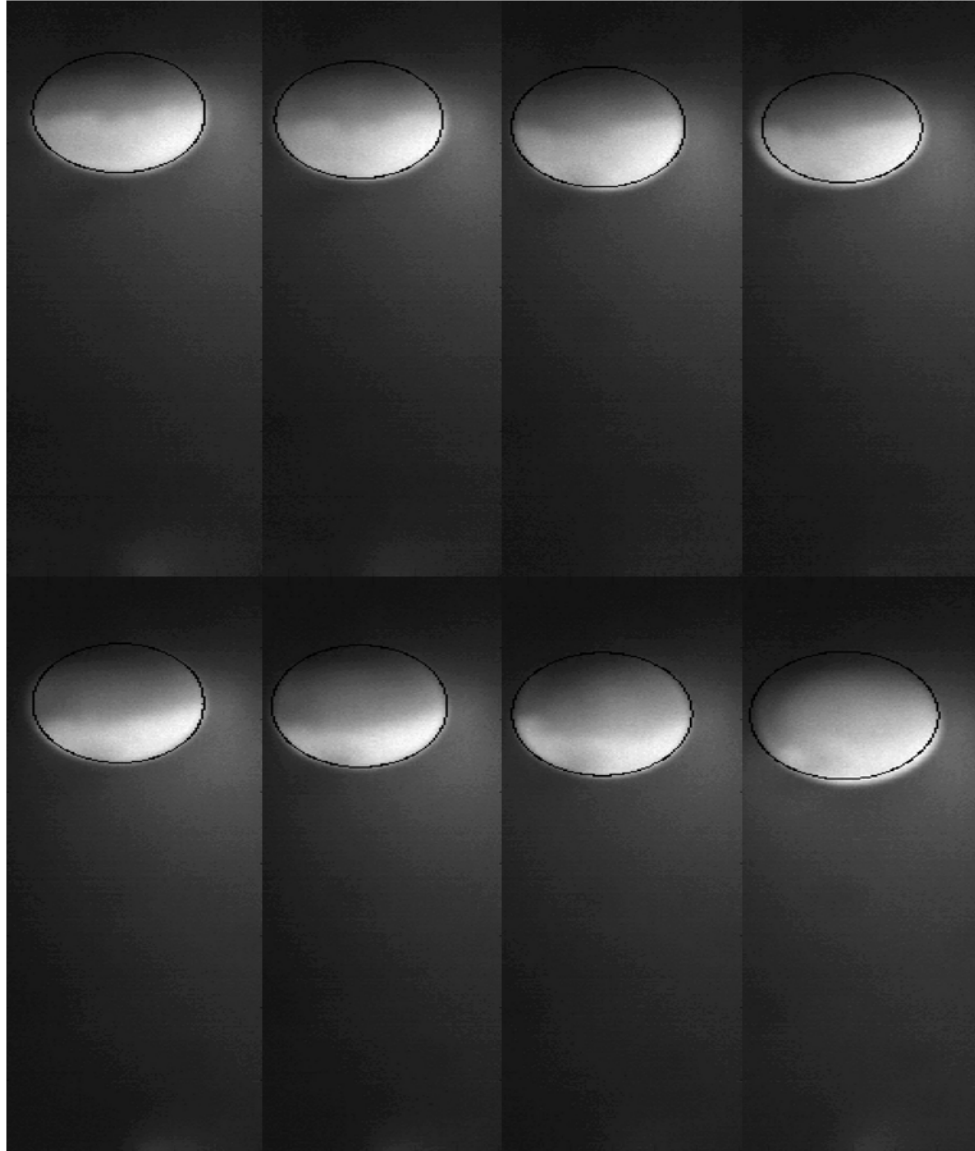


Fig. 5-25 Comparison of the fitted edges with the original images

Fig. 5-25 shows the comparison of the fitted edges with the original images. The result shows that during the base current time, the proposed algorithm can identify the position and the edge (contour) of the droplet when laser is not applied. An effective algorithm is thus developed for the condition without visible laser. As can be seen, it resembles similarity with the algorithm for the condition with a visible laser. These two algorithms may be applied for corresponding conditions accordingly.

However, although the proposed image processing algorithm suggests the processing results are accurate, the processing speed is not fast enough to satisfy the need for the control system to calculate the contour and the position of the droplet. Hence, a modified image processing algorithm needs to be developed for real-time processing for the droplet position only.

5.3 Simplified Algorithm for Real-time Implementation

In the developed laser enhanced GMAW, the metal transfer speed is around 20 droplets/second. Before a droplet is detached, it will grow on the tip of the electrode and being pushed towards the weld pool. To monitor the droplet for control, the acquisition speed of the control camera is set at 1,000 fps. The image processing algorithm has to be both accurate and fast enough to measure the position of the droplet at 1000Hz. It is found that the full algorithms developed to monitor the droplet contours in previous two sections are not capable of achieving such a high speed. Hence, to achieve this ultra-high image processing speed, the algorithms have to be simplified and be tailored toward effectively extracting the minimal information needed to determine when to apply the laser. This minimal information should be the position of the droplet rather than its shape and size. The objective of real-time on-line image processing is thus to monitor the droplet position during the base current period at 1,000 Hz.

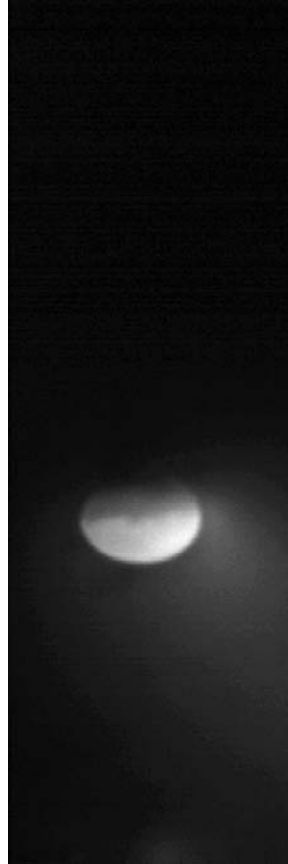


Fig. 5-26 Captured image for simplified real-time processing algorithm

Fig. 5-26 shows a captured frame in laser enhanced GMAW. The image window is reduced by two pixels from its boundary on all four sides to eliminate possible noises. The area below the weld pool is also removed from the region to be processed using the *a priori* information in order to increase the processing speed.

To identify the position of the droplet, we wish to also determine the upper and lower edges of the droplet as we did in the previous sections. However, to speed the processing, a simplified method is proposed. This method first calculates the mean of the brightness in the window. This mean can be used as an estimate of the brightness of the droplet edge. The set of the points with this brightness forms the estimated edge. It is true that the

accuracy using the mean as the edge's brightness may not high. However, the brightness of all points in the window is approximately lie in two ranges: low brightness and brightness. There are actually no many points whose brightness is close to this mean (estimated brightness of the edge). Hence, this relatively low accuracy in the estimation of the droplet edge brightness will not affect the edge points derived from this estimation. This proposed algorithm thus effectively reduces the computation without affecting the edge detection accuracy significantly.

Further, the point whose brightness is the maximal is used as the estimation of the arc anode/spot which should locates at the bottom of the droplet. The bottom of the droplet can be used as a characteristic parameter to represent the position of the droplet. This is considered as the arc spot. From the upper edge points of the droplet and the arc spot, the droplet size can be estimated. However, the most reliable measurement from the image processing is still the arc spot unless the estimated edge points can be further modeled to remove possible noises. In addition, even though the edge of the droplet can be accurately detected in real-time, using it for real-time control for the droplet growth will still require computation. Hence, at the present time in this dissertation research, only the arc spot estimated is used to determine the position of the droplet to determine when to apply the laser pulse in order to absolutely assure the real-time speed. Other information may be further verified and be used in the future.

Fig. 5-27 marks the arc spot and boundary of the upper edge on the original image. As can be seen, both the upper and lower edge of the droplet are identified with an acceptable accuracy, in comparison with the diameter of the laser.

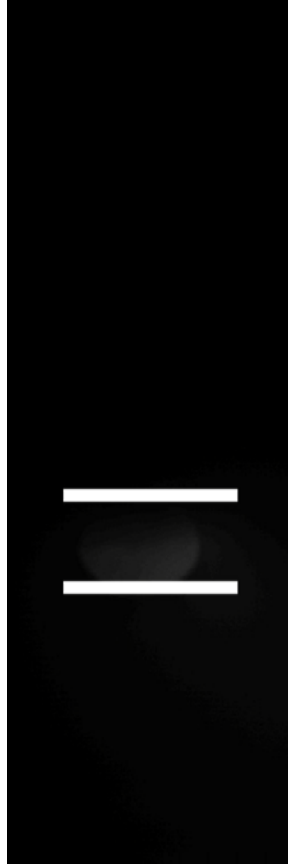


Fig. 5-27 Processing result of the simplified image processing algorithm

5.4 Summary

- An effective image processing algorithm has been proposed to extract the droplet boundary edges satisfactorily when laser is applied for the laser enhanced GMAW.
- An effective image processing algorithm has been proposed to identify the position and estimate the size of the droplet when laser is invisible in the laser enhanced GMAW.
- Experimental results verified the effectiveness of the proposed image processing algorithm and polar coordinate model with the closure constraint.
- The proposed algorithm and model form part of the foundation to measure and feedback control the size of the growing droplets in the laser enhanced GMAW for

possible applications in precision joining.

- A high speed image processing algorithm has been proposed for real-time monitoring and controlling of the metal transfer process in the pulsed laser-enhanced GMAW.

CHAPTER 6 Control System

The success of the proposed process, i.e., the pulsed laser-enhanced GMAW, depends on real-time accurate detection of the position of the droplet during its growth process. The goal is to control the droplet detachment in each of its growth period such that the droplet is detached when it passes the laser aiming line by applying synchronized laser and current pulses through combining the laser recoil force with the increased electromagnetic force.

6.1 Background

To monitor the welding process in real-time, many methods have been developed. Traditional methods include arc sensing, infrared sensors, ultrasonic sensors, and machine vision systems [Real-time Weld Process]. Most of these conventional methods are low cost and easy to install. They are also often fast and accurate enough to monitor major variables in the welding process. These methods have been widely used to monitor the weld seam, weld profile, weld penetration and weld pool surface.

Monitoring droplets in the welding process is also an important area of research interest in welding community. Researchers have used high speed machine vision systems to observe the droplet through directly viewing and laser back lighting. At the University of Kentucky, Dr. Zhengzhou Wang in the Welding Research Lab proposed droplet tracking algorithms using brightness based separation algorithms in 2008. However, most of the works in this area have been based on off-line analysis and feasibility studies. .

As aforementioned, the pulsed laser enhanced GMAW relies on the real-time accurate detection of the droplet to function. Machine vision should be the most direct method to detect the droplet accurately. Only after the droplet can be monitored, appropriate controls may be done to perform the pulsed laser-enhanced GMAW in the desirable ways.

6.2 Control System

The Machine Vision Control System used for this dissertation research consists of an optical system and an acquisition and processing system. The optical system includes a gz1-cl-22c5m high speed camera made by PointGrey and a Nikkor 200mm f/4D micro lens. An $810\pm 2\text{nm}$ band pass filter is installed on the inner side of the lens. The acquisition and processing module includes a desktop and a BitFlow KBN-PCE-CL2-F frame grabber,

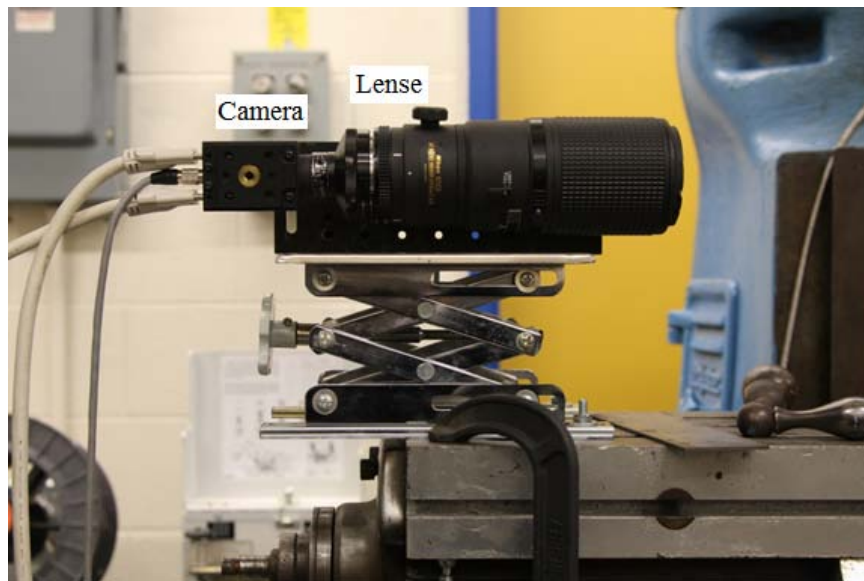


Fig. 6-1 Optical System

Fig. 6-1 shows the optical system where the lens is fixed on a height-adjustable platform. The camera is attached to the lens. The camera is powered by a 12v DC power supply. Two cables connect the camera with the frame grabber.

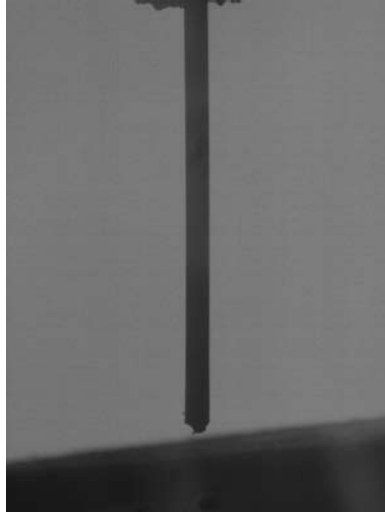


Fig. 6-2 captured frame of the consumable electrode

Fig. 6-2 shows a captured frame with the resolution of 800 x 600 pixels for the metal wire coming down from the torch. On the top side of the frame, the end of the contact tube is visible; below the metal wire is a pipe installed on the rotation weld positioner. This frame is captured by the high speed camera working at the calibration mode. A 100 watt light bulb has been used as the back-lighting source in order to provide sufficient illumination despite the use of the band pass filter in the optical system that makes the environmental lights to be almost invisible.

When the maximum frame resolution (2048 x 1088 pixels) is used, the frame rate can only be up to 280 fps. The frame rate achievable needs to be increased by reducing the frame resolution. A conventional GMAW process may have a droplet transfer rate up to 100Hz in the short-circuiting transfer mode where the arc length is short. In this research, the droplet transfer rate is confined to 20 Hz for spray transfer at very low currents and reasonable arc length. Such a droplet transfer rate requires a minimum frame rate of 1000 fps to provide a reasonable monitoring and control time resolution. In order to achieve this frame rate, the line resolution of the camera is reduced from 2028 to 200. (For this camera, its column resolution does not affect the frame rate. Also, the frame rate does not increase proportionally with the reduction in the line resolution.) For observation and analysis convenience, the column resolution is reduced from 1088 to 800. Hence the resolution of the images acquired is 200 x 800 pixels. To monitor the droplet and wire, the camera is rotated 90 degrees and makes the resolution of the camera to become 800 x

200. At this resolution, the camera's highest frame rate can reach 1300 fps. To be repeatable, the frame rate for this research is set to 1200 fps. This allows each droplet growth cycle to be imaged 60 times approximately for analysis, monitoring, and control. Fig. 6-3 shows part of a droplet growth/transfer cycle being imaged.

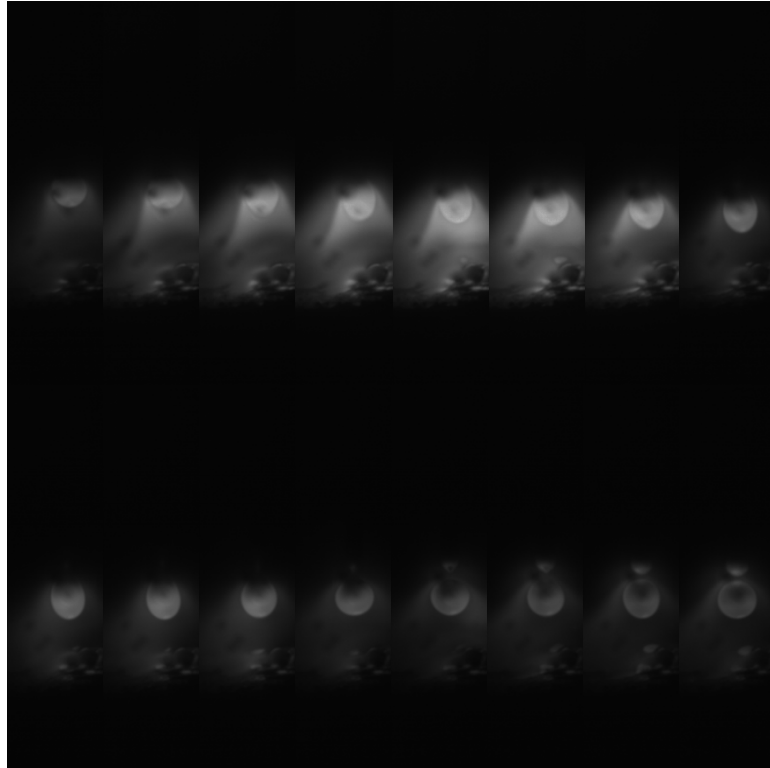


Fig. 6-3 Recorded metal transfer process

A KBN-PCE-CL2-F frame grabber made by BitFlow and a computer form the acquisition and processing module. The Karbon frame grabber has an input pixel clock frequency range of 20 – 85 MHz. This allows a camera with even higher frame rates to be used.

6.3 Control Algorithm

GMAW typically runs at a constant voltage (CV) mode. A desirable voltage is set at the power supply. The actual voltage is measured by the power supply to determine how the current needs to be adjusted to maintain the voltage at the desired level being set. This is a conventional way to operate the GMAW process in which a wire is continuously fed. If the current is insufficient to melt the wire at the speed it is fed, the arc length (the distance between the wire and work-piece) will reduce such that the wire dips into the weld pool to extinguish the arc. Otherwise if the current is excessive to melt the wire at a speed higher than the feeding speed, the arc length will increase such that the wire tip and arc anode approach the contact tube. The contact tube will be burnt. In the CV mode, the arc voltage that proportionally increases and reduces as the arc length increases and reduces will be used as the feedback to adjust the current such that the voltage is maintained the desired set-point. The arc length will thus be maintained at an appropriate level. The CV mode thus provides an automatic control to melt the wire at the speed the wire is fed.

While the CV mode is convenient for easy operation, it lacks an accurate control on the current that is the major parameter controlling the production of the welds and determining the metal transfer process. To accurately control the metal transfer such as when the droplet is detached, we use a CC (constant current) power supply that outputs the current per control command. Because the current is accurately controlled, unless the peak current pulse is applied with the laser pulse, the droplet will not be detached. Using the machine vision based monitoring, the peak current pulse and the laser pulse are applied when the droplet crosses the desired location to detach the droplet. The droplet thus does not detach if it is not at the desired location and will be detached when it is at the desired position. The metal transfer process is thus accurately controlled.

In this research, the proposed control system utilizes the computer to finish both image acquisition and functions as the controller. The block diagram of the control algorithm is given in Fig. 6-4.

Before the experiment, several initialization tasks need to be done. First, the communication among the computer, the camera and the frame grabber will need to be initialized. Then, a set of buffer needs to be allocated in the computer's RAM. These buffers will store the captured images through the whole experiments. If the buffer is large enough, all of the captured images will be stored and no re-writing will occur.

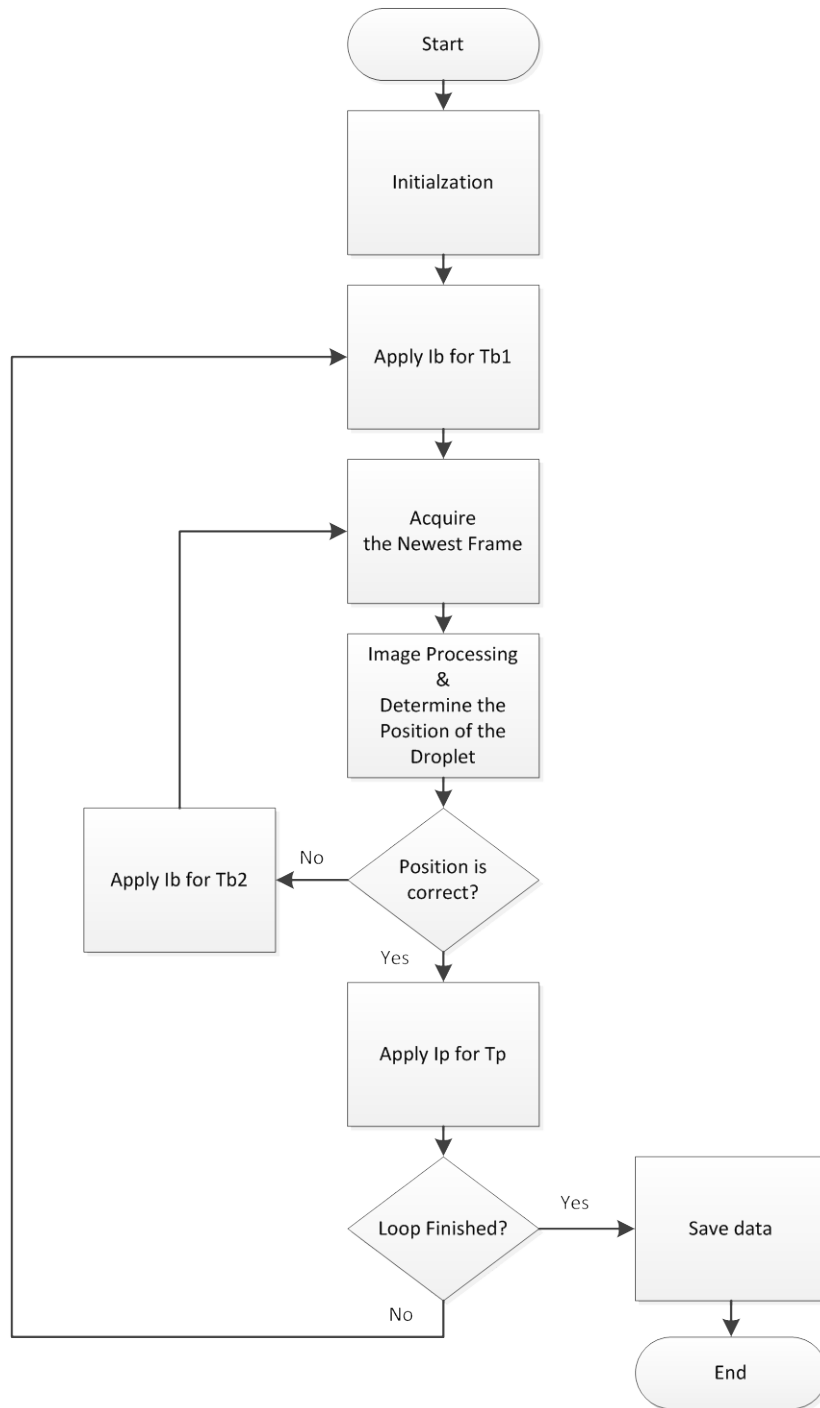


Fig. 6-4 Block diagram of proposed control algorithm.

Before the experiment, the desired position for droplet detachment needs to be defined. In this study, the desired detaching position is restricted to the position where laser is applied on the electrode. Fig. 6-5 shows a captured frame of the electrode in a calibration

mode. For the calibration mode of the camera, a low frame rate at 30fps is used to ensure the exposure time is long enough. Also, a back-light is applied to help make sure that the focal point of the lens is on the electrode.



Fig. 6-5 Captured image of the electrode in calibration mode

Fig. 6-6 shows a captured frame when the guide laser is applied on the electrode. Because the sensor of the camera has a very low (less than 10%) frequency response for the wavelength of the diode laser, the laser itself is invisible on the camera. The position of the laser can be determined from the guide laser. Another way to calibrate the detaching position is to apply the laser at its full power laser (50 watts) on the electrode. The location where the wire is being melted as can be seen from the image will be the detaching location. Thus, the detaching position of the droplet during the laser enhanced GMAW is defined.



Fig. 6-6 Laser on the electrode

In Fig. 6-6 the vertical coordinate of the spot being illuminated by the laser is (500:580, 1:200). During the welding process, this coordinate will be used as the criterion to decide when to apply the peak current pulse and the laser to detach the droplet.

An arc start program will first commence to establish a stable arc between the electrode and base metal before the control algorithm starts to function. After this arc starting period, the control system will take over and gives out a voltage signal to the CC power supply to apply the base current. In the meantime, the camera will capture images and store them in the pre-allocated buffers through the frame grabber.

The frame grabber supports two kinds of work mechanism: continuously transmit new frames from the buffer or work in a wait-done mode. In the normal mode, the frame grabber will work continuously to refresh the pointer to grab each frame to the upper level of the control system; regardless of the time it takes for the image processing algorithm to finish the task. If the speed of the image processing algorithm is relatively slow, the differences between the speed of the image grabbing and the speed of the image processing will build up over the time such that the control will inevitably fail over time. While in the wait-done mode, if the image processing algorithm takes too long to finish processing a frame, the frame grabber will wait until it is finished and then give the upper level the newest frame; all other frames stored during the waiting time will be neglected.

This may cause discontinuities in the processing results and undesirable controlling results. However, the controlling process itself will continue as the welding process runs. In this study, the speed of the simplified image processing algorithm is adequate for the normal mode. The normal mode is thus used. In case more complex algorithms are needed, the wait-done mode may be considered.

When the camera begins to capture images, the captured data/images will be written into the buffers. After an entire frame is written, the pointer will jump to the current frame and the image will be analyzed by the image processing algorithm. If the position of the droplet is not low enough, the system will wait again with a shorter period of base current time. If the position of the droplet is about the same with the pre-defined position, the control system will send the signals to apply the peak current and the laser. The combined detaching forces will detach the droplet and the control loop will restart. Otherwise, if for some reason the position of the droplet is lower than the pre-defined position, or the image processing algorithm fails to give a valid result, after a certain period of waiting time, a peak current that is larger than the normal peak current will be applied to detach the droplet without the alignment with the laser. This allows the electrode to burn back and a new control cycle will start.

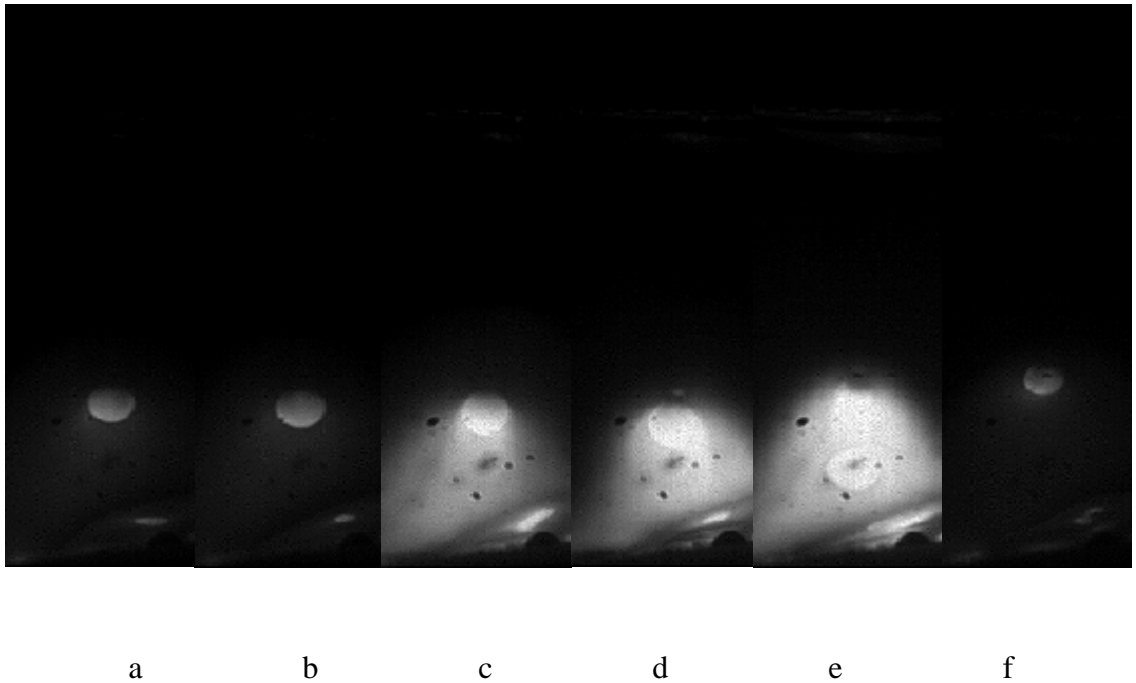


Fig. 6-7 Droplet transfer in laser enhanced GMAW

Fig. 6-7 shows a series of frames in part of a metal transfer cycle during the pulsed laser-enhanced GMAW. These frames are captured by the Olympus high speed camera at the frame rate of 3000 fp. Although the frames are not cropped to the same resolution compared to the frames captured by the Gazelle high speed camera, the reference detaching point is the same with previous captured frames. Frame a in Fig. 6-7 shows the droplet in the base current time. During the base current period, the arc is burning at a relatively low level. The brightness of the frame is not too extreme. This provides a good chance to measure the size of the droplet in real-time.

During the base current time, the base current is only 28 amp and no much of the electrode is melted such that the wire feed speed is larger than the electrode melting speed. As a result, the droplet continuously moves down towards the base metal. In frame b, the position of the droplet is lower than the droplet position in frame a, and it has

reached the reference detaching point. Thus, the control algorithm sends out signals to apply a peak current and laser. Frames c, d and e show that the droplet is being detached.

After the droplet is detached by the peak current and laser, the consumable electrode lost a significant amount of melted metal. The electrode consuming speed is thus larger than the wire feed speed during the peak current period. For this reason, the position of the droplet bounces back a length above the reference detaching point when the next base current time begins. The image processing algorithm again starts to work and continues to measure the position of the droplet.

6.4 Summary

In this chapter, the machine vision based control system and algorithm are introduced. The machine vision system successfully captures the images in real-time. The high speed image processing algorithms analyze the images and provide the processing result for the position of the droplets in real time. This control system successfully controls the pulsed laser-enhanced GMAW process in real time and provides a solid foundation for the process to compete with the GTAW process in precision joining in the future.

Although, due to the hardware limitations, the images captured by the Gazelle high speed camera cannot be stored for off-line verification currently, the second high speed camera record the images that can verify the controlling results of the metal transfer process in the pulsed laser-enhanced GMAW.

CHAPTER 7 Experimental Verification

The pulsed laser-enhanced GMAW is to combine the laser recoil force and the increased electromagnetic force to effect a droplet detachment. It also assures that the detachment does not occur randomly as in the laser-enhanced GMAW, an advantage over the latter. The pulsed laser-enhanced GMAW is thus a controlled process that delivers a controlled metal transfer. Its advantage over the conventional GMAW is that it uses a laser to reduce the amperage needed to provide a sufficient electromagnetic force.

To verify the effectiveness of the proposed modification for the laser-enhanced GMAW, the system developed has been used to perform the pulsed laser-enhanced GMAW process. The major result we wish to verify is: if a pulsed GMAW with the application of a certain peak current for certain duration is unable to detach the droplet in each pulse, adding a laser pulse synchronized with the pulse of the peak current for the same pulse duration may be able to detach in each pulse. This would verify the proposed principles of the pulsed laser-enhanced GMAW: (1) the effectiveness of the laser in introducing an auxiliary detaching force; (2) the laser can be applied in a pulsed way such that the waste during the base period can be eliminated. This would also verify the effectiveness of the developed system: (1) all elements developed for the system works; (2) the system developed is able to perform the pulsed laser-enhanced GMAW. The ideas proposed and the work performed in this dissertation can thus verified experimentally.

7.1 Experimental Conditions

A CC (Constant Current) power supply is to conduct the experiments. The current to output to perform GMAW is specified/adjusted by the control system which sends a command signal to the power supply.

The diameter of the steel wire used is 0.8 mm. Pure argon is used as the shielding gas and the flow rate is 14 L/min. The bead-on-plate experiments are conducted on stainless steel 304 pipes. The diameter of the pipe is 11.43cm (OD) and the wall thickness is 2.1mm.

The travel speed (converted from the rotation speed) is 6 mm per second. The peak current is lower than the transition current [??] in the conventional GMAW because a peak current higher than the transition current will be able to detach the droplet to produce spray transfer without laser as long as the duration of the peak current is sufficient. Hence, for experiments without the laser, multiple pulse one droplet phenomenon with globular transfer should be expected. For experiments with the laser, the laser is set to pulse mode, i.e. the laser is controlled to be applied on the droplet and synchronized with the peak current pulse. The peak power of the laser is set to its maximum output - 50 watts.

The CTWD (contact-tube-to-work distance) is around 1.5 cm but it varies as the pipe surface is perfectly symmetrical about the rotation axle and the torch position is fixed. The longest wire extension at which the laser needs to be applied is 1cm. In conventional CV GMAW, the fluctuation in CTWD affects the current and the metal transfer process. In the proposed process – pulsed laser enhanced GMAW – this effect of this fluctuation will be compensated by the real-time vision system.

Table 7-1 lists major parameters used in experiments conducted to verify the proposed principles and developed system. The resultant metal transfer process that needs to be used to perform analysis is video recorded using an Olympus i-speed camera (second high speed camera) at 3000fps. All the images presented are from the recorded high speed videos.

Table 7-1 Major Parameters in Verification Experiments

Experiment Number	Peak Current (amp)	Peak current time (ms)	Base Current (amp)	Minimal Base current time (ms)	Laser Power (watts)
1	150	6	28	30	N/A
2	150	6	28	30	50
3	145	8	28	30	N/A
4	145	8	28	30	50

7.2 Experimental Methods

In all experiments, with laser or without laser, the process is monitored in real-time using the vision system and then be controlled in exactly the same ways except for the application of the laser. That is, after the base current is applied for the specified minimal base current time as shown in Table 8-1, the vision system starts to monitor the position of the droplet. When the droplet reaches the desired position, i.e., 10 mm below the contact tip, as determined from the vision system, the peak current specified in Table 7-1 is applied for the period specified in the table with or with the application of the laser. During the application of the peak current (with or without laser) and the following minimal base current application period, the metal transfer process is not monitored. After the minimal base current application period, the monitoring resumes to detect the position of the droplet. If the droplet has exceeded the desired position (greater than 10 mm from the contact tip), a detaching pulse (with a current of 160 A for 8 ms) is applied to assure the droplet be detached. Otherwise, the peak current with the duration, both specified in the table, is applied again.

A successful metal transfer control is the so-called one droplet per pulse, i.e., the droplet is successfully detached every time by the applied peak current for the specified period when it reaches the desired position. Otherwise, if the detaching pulse is used or a droplet

is not detached by the specified peak current for the specified period, the metal transfer control is considered unsuccessful.

7.3 150 A Peak Current without Laser

150 A is considered the transition current for 0.8 mm steel wire [8]. The transition current [8] may be a fuzzy concept in literature. The accepted definition is that a current higher/lower than the transition current may/may not detach the droplet with a diameter similar with that of the wire. The application duration of this current is not concerned but the application duration affects the ability of a specified current to detach the droplet. Hence, in this study, the peak current and its application time will be both included into the discussion and analysis. The exact value of the transition current and if a used current is higher/lower than the transition current will not be emphasized.

In experiment 1, the peak current is 150 amp and its duration is 6 ms while the base current and its minimal duration are 28 amp and 30 ms respectively. This corresponding average welding current is 48.3 amp. No laser is applied to the droplet in this experiment. The wire extension to trigger the peak current pulse is 10mm away from the contact tip.

The images of the metal transfer process are displayed in a series in Fig. 7-1 through 7-4. All the images shown have been zoomed in, in order to emphasize on the droplets. The sizes of the images are thus different from the captured images that are used for real-time image processing, which have been given in Chapter 5.

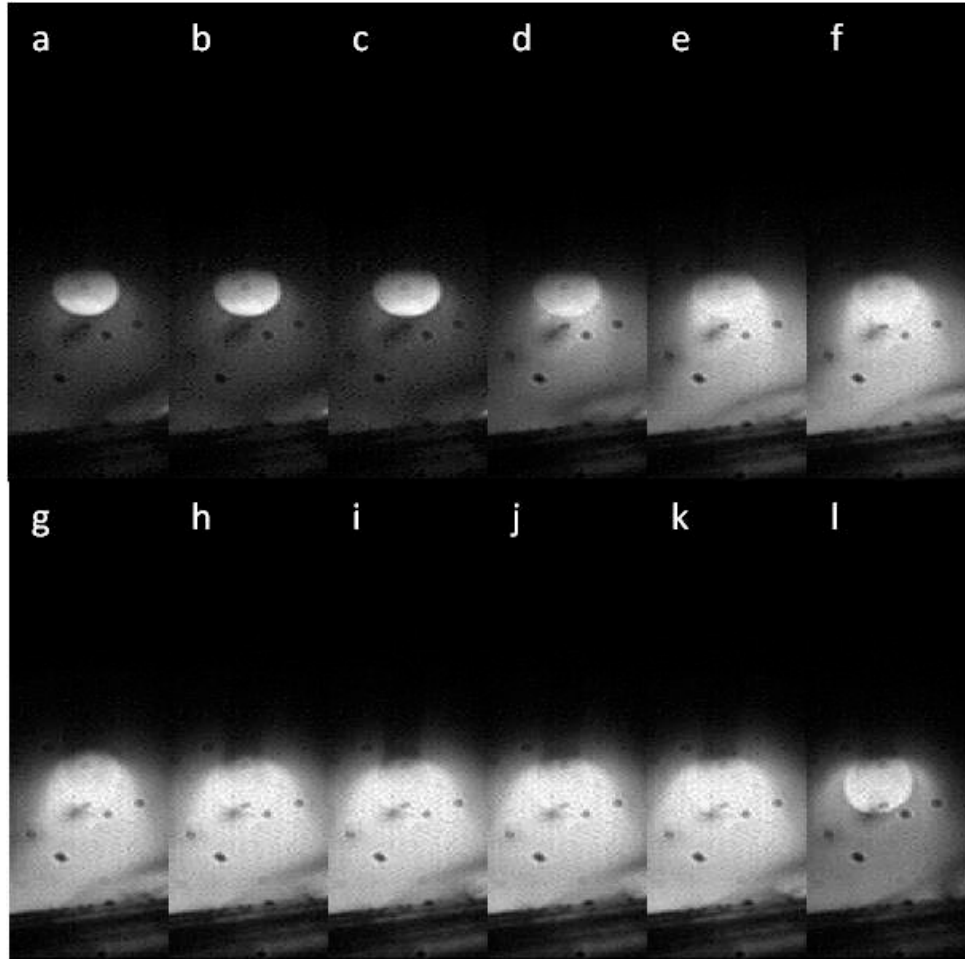


Fig. 7-1 Typical first pulsing cycle to detach a droplet without laser using 150 A current for 6 ms

Fig. 7-1 shows a droplet being detached in experiment 1. Frame a through d show that the droplet is being pushed down by the metal wire step by step. When the droplet reaches the desired point at frame e, a peak current of 150 amp is applied. However, at this time the size of the droplet is not sufficient for its corresponding gravitational force to compensate for the insufficiency of the electromagnetic force in detaching the droplet. As a result, after the peak current is applied for the specified duration (from frame e to frame k), the droplet is still not detached. The one droplet per pulse needed to qualify for a successful metal transfer control is not achieved.

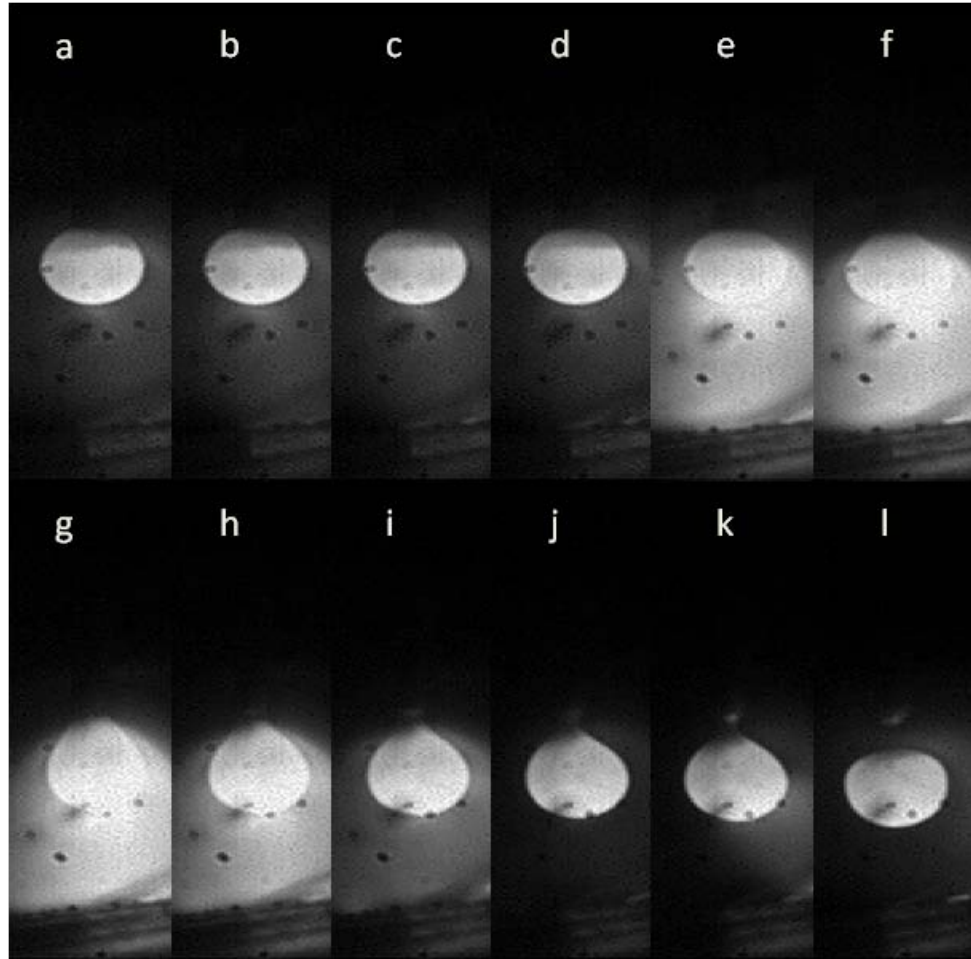


Fig. 7-2 A typical second pulsing cycle to detach a droplet without laser using 150 A current for 6 ms

Fig. 7-2 shows the next cycle that follows that in Fig. 7-2. After the previous peak current period and another 30 ms minimal base current period, the droplet has grown much larger when it is pushed to the desired position as can be seen by comparing frame d with frame d in Fig. 8-1. Unfortunately, despite the much increased droplet size, the peak current pulse still failed to detach the droplet. By the end of the peak current time, the droplet grew much further. The gravitational force became the dominant force exceeding the retaining force provided by the surface tension at the interface between the solid wire and molten droplet. As a result, the droplet was detached into the weld pool in the beginning of the following base current period.

Repeating experiments have been conducted with exactly the same nominal experimental parameters. The recorded videos are analyzed carefully. It is found that the multiple pulse – one droplet phenomenon observed in Fig. 8-1 and 8-2 occurs continuously. No There are almost no detachments of small droplets, as desired within a single pulse period, observed.

7.4 150 A Peak Current with Laser

In experiment 2, all the nominal parameters remain the same. The average welding current is still 43.9 amp; however, a 50watt laser is applied to the droplet when it reaches the desired position. This position for applying the laser and current pulses to detach the droplet is still 10 mm away from the contact tip.

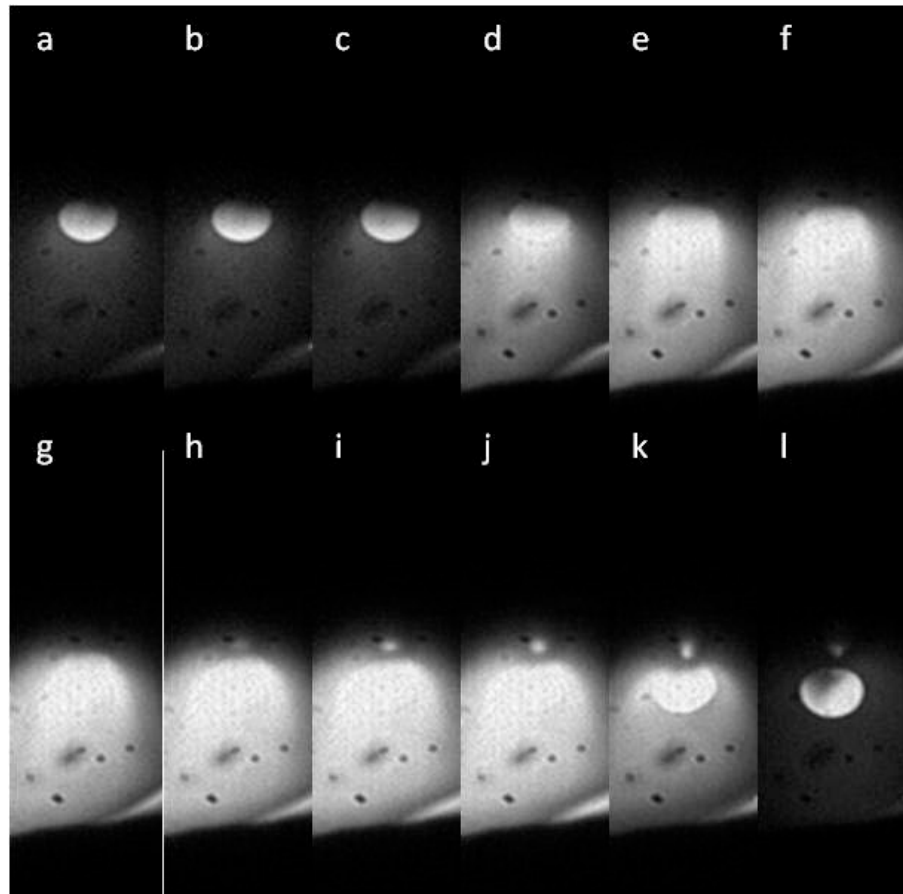


Fig. 7-3 A typical pulsing cycle to detach a droplet with laser using 150 A current for 6 ms

Although a laser has been applied to the droplet, neither camera is able to capture the light of the laser because the 960 nm wavelength of the laser is too high for the sensors of the high speed cameras. Hence, the aiming position and power of the laser has been pre-calibrated and pre-tested as mentioned previously.

Fig. 7-3 shows the metal transfer phenomenon in experiment 2. At the beginning of the cycle, the size of the droplet is at an average level. When the peak current is applied, the laser is simultaneously applied to the pre-defined aiming point. . This time, although the size of the droplet before the peak is applied is similar as that in Frame d in Fig. 7-1 (please compare frame c in Fig. 803 with frame d in Fig. 7-1), the droplet is successfully detached as can be seen in frame l in Fig. 7-3.

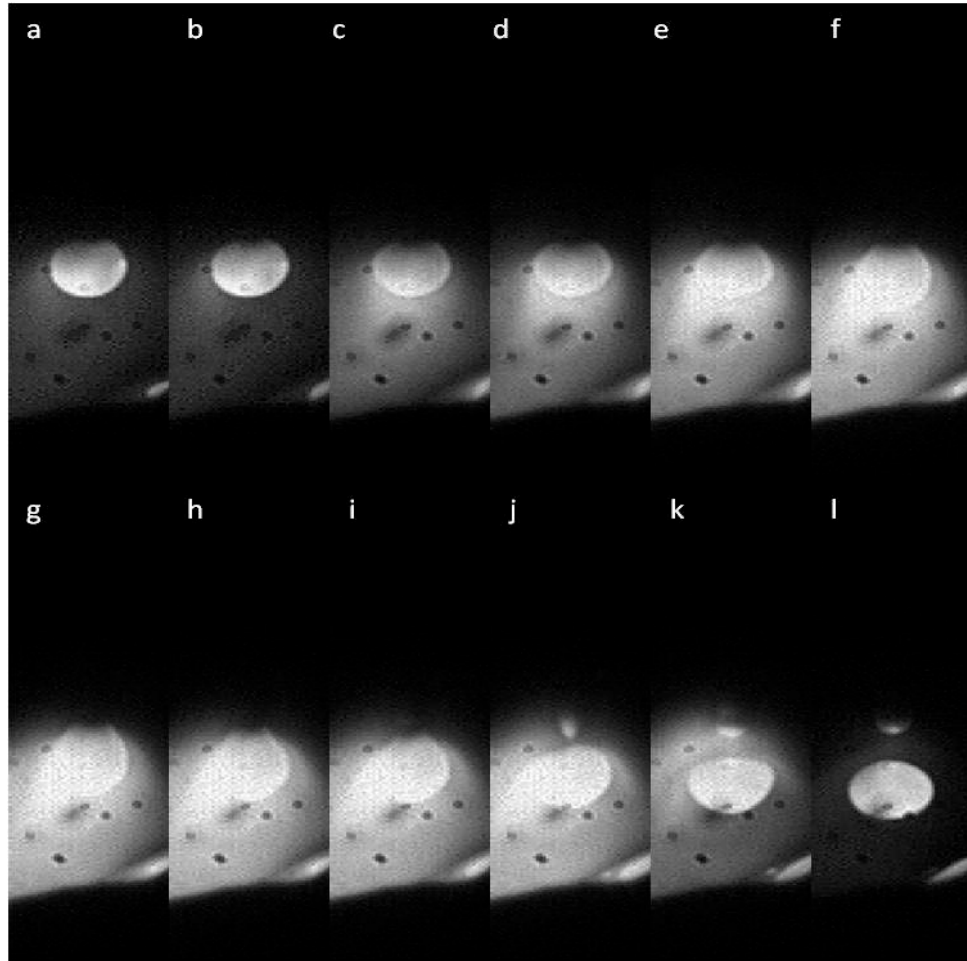


Fig. 7-4 A typical pulsing cycle to detach a droplet with laser using 150 A current for 6 ms after a successful detachment

Fig. 7-4 shows the metal transfer in the next cycle that follows. Because the previous droplet has been detached, after the base current period, the size of this droplet is the same in Fig. 7-3 and is considerably smaller than the size of the droplet in Fig. 7-2. This time, when the peak current and the laser are applied, the droplet is again detached as can be seen in Fig. 7-4 (j) .

Repeating experiments have been conducted with exactly the same nominal experimental parameters. The recorded videos are analyzed carefully. It is found that the desired one-droplet per pulse in Fig. 7-3 and 7-4 continuously repeat. The application of the laser thus made the difference to change the metal transfer from the undesirable multiple-pulse one-droplet of large droplet to the desired one-droplet per pulse with small droplets.

7.5 145 A Peak Current without Laser

After verified the effectiveness of the laser in helping detach the droplet in the pulsed laser enhanced GMAW, further experiments with a lower peak current have been conducted with the hope to verify that with the auxiliary detaching force from the laser, the peak current may be further lowered. As has been stated, the purpose to use a laser and introduce the laser-enhanced GMAW is to reduce the current needed to detach droplets. Ideally, we wish to detach the droplets of reasonable sizes at any reasonable given arc variables (reasonable welding currents) such that the GMAW may also freely choose the arc waveforms as the GTAW.

In experiment 3, the peak current is reduced to 145 amp and the peak current time is increased to 8 ms. The base current and the minimal base current period are still 28 amp and 30 ms without changes. The average current is increased to 52.6 amp due to the increase in the peak current period. Although the average welding current is slightly increased, the electromagnetic force is lower. In comparison with experiment 1 and 2.

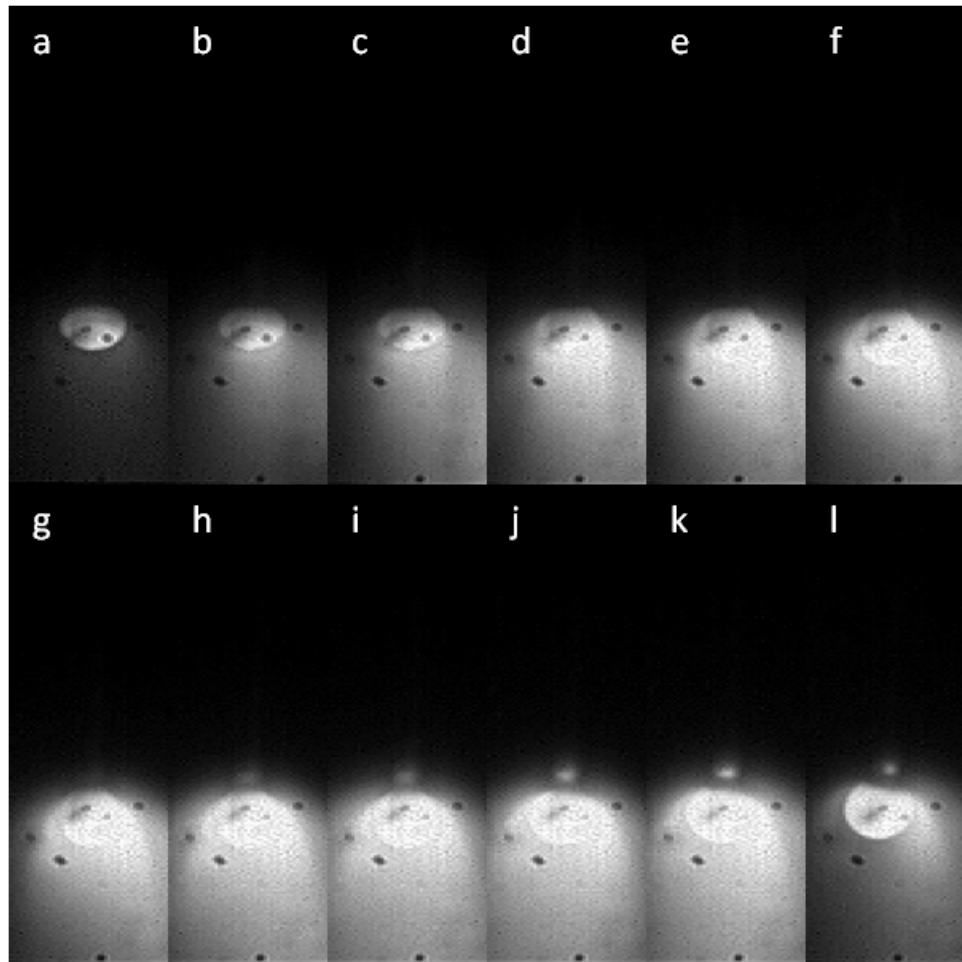


Fig. 7-5 A typical first pulsing cycle to detach a droplet without laser using 150 A current for 8 ms

Fig. 7-5 shows a typical metal transfer cycle in experiment 3 when the peak current has been reduced to 145 amp. When the droplet reaches the desired detaching point, a peak current is applied without the laser. The 145amp of peak current is considered to be lower than the transition current for the wire used in this study. It can be observed that although the peak current time has been extended 2 ms the surface tension still retains the droplet firmly. The necking phenomenon that is typically observed before the detachment starts is not observed. This indicates that when the peak current is lower than the transition current, simply extending the peak current time by a small additional period may still not detach the droplet because the combined detaching force may still not be sufficient to overcome the surface tension. This may also implies that the dynamic

response time needed for the droplet to reach the steady-state response under the given electromagnetic force may be smaller than 6 ms. To detach the droplet, the detaching force needs to be increased. When the current is given, the detaching force increases as the droplet grows due to the increased gravitational force.

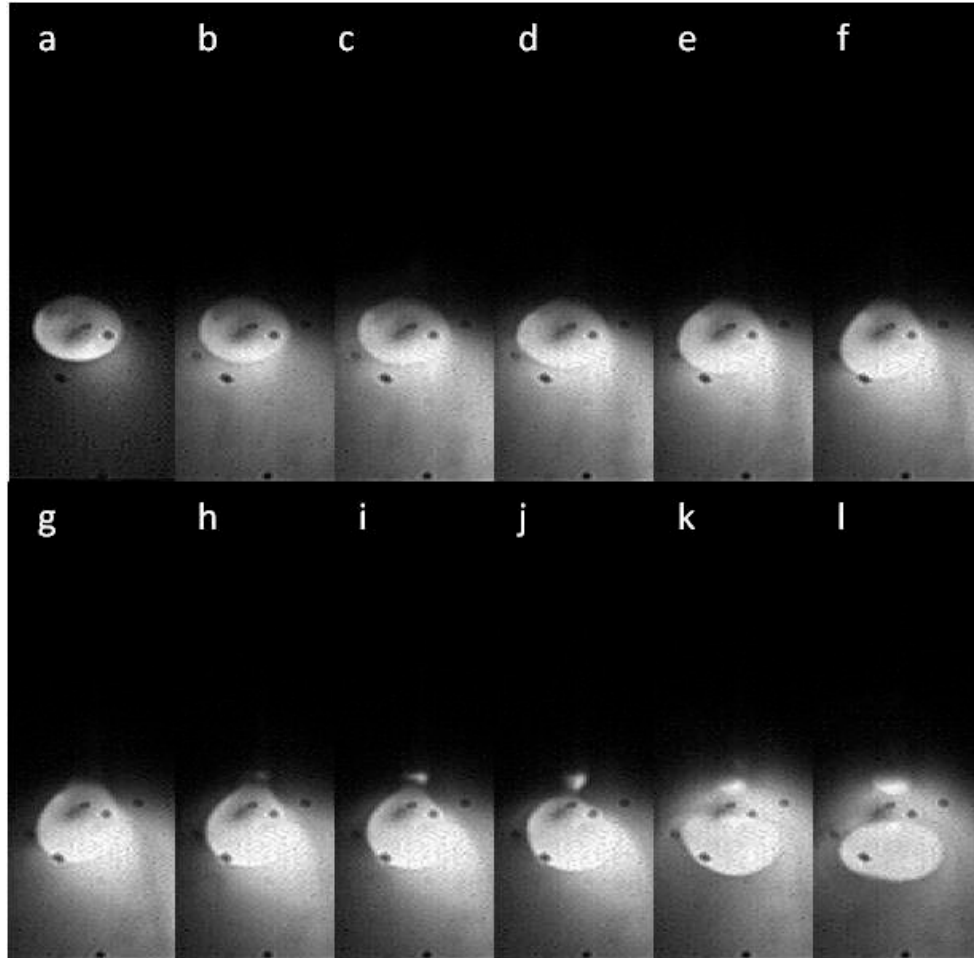


Fig. 7-6 A typical second pulsing cycle to detach a droplet without laser using 150 A current for 8 ms

Fig. 7-6 shows the metal transfer cycle following the one in Fig. 7-5 in which no droplet is detached. When the droplet reaches the desired detaching position and the peak current is applied, the droplet has grown significantly greater than it was before the peak current was applied in Fig. 7-5. The gravitational force has much increased such that the combined detaching force exceeds the retaining force. As can be seen, the droplet is detached during this second peak period (see Fig. 7-6 (k) and (l)). Hence, the undesirable

multiple-pulse one-droplet phenomenon is observed again. Repeating experiments under the same nominal parameters confirm this finding.

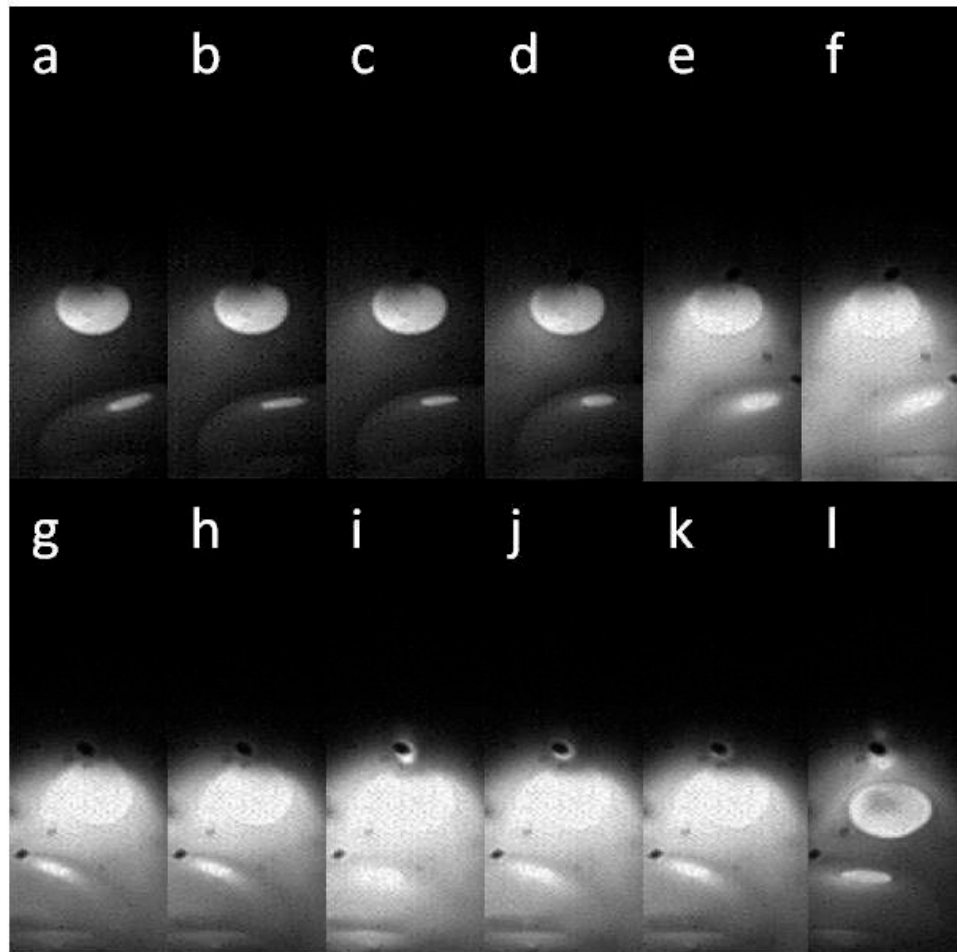


Fig. 7-7 A typical pulsing cycle to detach a droplet with laser using 145 A current for 8 ms

7.6 145 A Peak Current with Laser

In experiment 4, the nominal values for all the welding parameters remain the same with those in experiment 3 except for the application of the laser onto the droplet. As can be seen in Fig. 8-7, when the peak current and laser pulses are applied, the droplet is successfully detached during the peak current time. The droplet is transferred with a smaller size compared to the size of the droplet that was transferred in experiment 3.

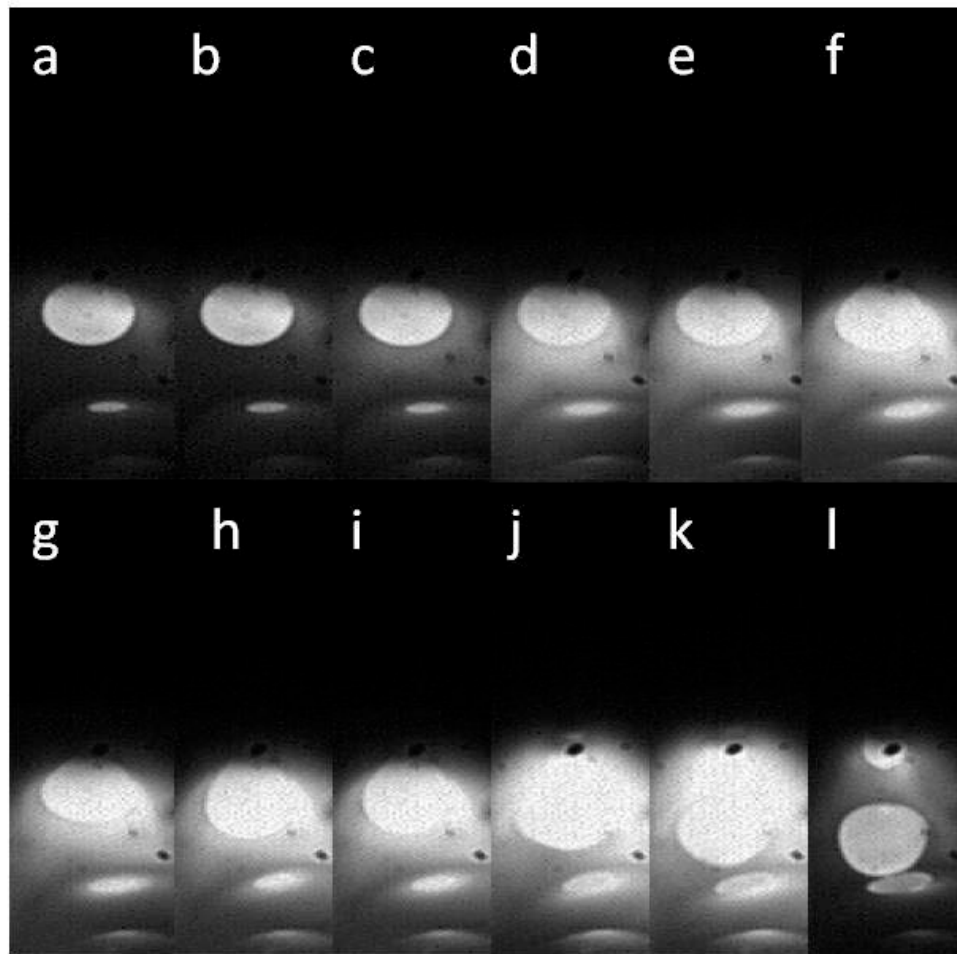


Fig. 7-8 A typical pulsing cycle to detach a droplet with laser using 145 A current for 8 ms after a successful detachment

Fig. 7-8 shows the metal transfer cycle that follows the one in Fig. 7-7 where a droplet has been successfully detached. It can be observed that when the peak current is applied with the laser, the droplet is detached in the middle of the peak current period. A careful observation shows that the droplet is greater than that in Fig. 7-7 when the pulses are applied. An observation of Fig. 7-7 shows that the droplet detached in Fig. 7-7 has actually formed approximately in Fig. 7-7(i). Hence, the metal melted later during the peak current period is accumulated to the initial droplet in Fig. 7-8. The increased initial mass of the droplet reduces the time to detach the droplet. From this point of view, 8 ms may

be slightly greater than needed to detach the droplet with the laser while the effect of the laser is also verified.

7.7 Summary

In this chapter, the effectiveness of the laser in helping detach the droplet and the effectiveness of the developed control system are verified through comparative experiments conducted with and without laser. The experiments also confirm that the pulsed laser-enhanced GMAW is feasible. That is, the laser does not need to be applied for an unnecessarily long time. It is also effective to be applied as a pulse when the detachment is needed together with the current pulse. Unnecessary over heating due to the laser is eliminated.

CHAPTER 8 Peak Current Reduction

As stated, the specific objective of the present dissertation research is to apply a pulsed laser spot onto the droplet at the right location where the detaching force from the laser is needed and at the right time when the detaching force from the laser is needed. This can eliminate the waste of the laser energy and the effect of the unintentional laser application on the work-piece and provide accurate control on the droplet mass and detaching time. As can be seen from the verification experiments in Chapter 8, this objective is realized.

The goal to apply a laser is to detach each droplet with desired size at desired time at any given arc variables in order to provide the ability to freely control the inputs into the work-piece where the welds are formed. “Any arc variables” here primarily imply any currents. Since the droplet can always be detached using a current higher than the transitional current, “any currents” here implies any currents lower than the transition currents. Further, since the ability to detach the droplet increases as the current increases when other variables are given, the effectiveness for the laser enhanced GMAW process can be evaluated by how much amperage can be reduced in order to detach the same droplet.

For the pulsed laser-enhanced GMAW, the detachment is also affected by other parameters including the pulse duration. Since the ability to detach a droplet in general should increase as the pulse duration increases, how much the pulse duration may be reduced may also be an evaluation for the effectiveness of the pulsed laser-enhanced GMAW. However, as has been seen in Chapter 7, increasing the peak pulse duration may not always increase the detaching capability if the duration is longer than the dynamic response time for the droplet to respond to a force (electromagnetic force) change. Further, increasing the peak pulse duration unnecessarily actually increases the heat input and reduce the control resolution for the detachment time.

As such, this dissertation will use the reduction in the peak current for effective detachment using a given pulse duration as the major evaluation for the effectiveness of the pulsed laser-enhanced GMAW. From Chapter 7, 6 ms should be used as the given peak pulse duration.

8.1 Experiments

A series of experiments have been done using exactly the same welding parameters except for the peak current. The experiment series begins with using 150 A peak current. When a peak current is confirmed to be able to detach each droplet, the amperage is reduced by 5 amps to see if the peak current may be further reduced while still being able to detach each droplet. Experiments in which each droplet is detached per pulse are the successful ones. Table 8-1 shows the parameters for the successful detachment experiments. The parameters in each successful detachment experiment in Table 8-1 have been used to conduct repeating experiments in order to accept as success.

The lowest peak current in Table 8-1 is 135 amp. Experiments have been conducted using 130 amp peak current. However, the desired one-droplet per pulse is not achieved. Hence, 135 amp is considered as the lowest peak current for successful detachment.

In Chapter 7, experimental results have shown that 150 amp is not sufficient to detach the each droplet in 6 ms. Further experiments have been done by increasing the peak current at 5 amp increment. It is found that 160 amp is the lowest peak current for successful detachment.

Fig. 8-1 to Fig. 8-4 give typical two consecutive cycles. Each of these figure has (a) and (b) with the cycle in (b) to follow the one in (a). As can be seen, the droplet is detached in each cycle during the peak current period by the synchronized peak current and laser

pulses. The size of the droplet when it reaches the detaching position may vary. However, the success in the detachment is not affected. The detachment is thus assured by the combined detaching forces from the electromagnetic force (due to the current) and the recoil force (due to the laser). The needed gravitational force, if any, can be provide by the mass from the droplet formed during the present base and peak period without dependence on the accumulation from previous cycles.

Table 8-1 Parameters for Successful Detachment Experiments

Experiment #	Peak Current (amp)	Peak current time (ms)	Base Current (amp)	Minimal base current time (ms)	Laser Power (watts)
1	150	6	28	30	50
2	145	6	28	30	50
3	140	6	28	30	50
4	135	6	28	30	50

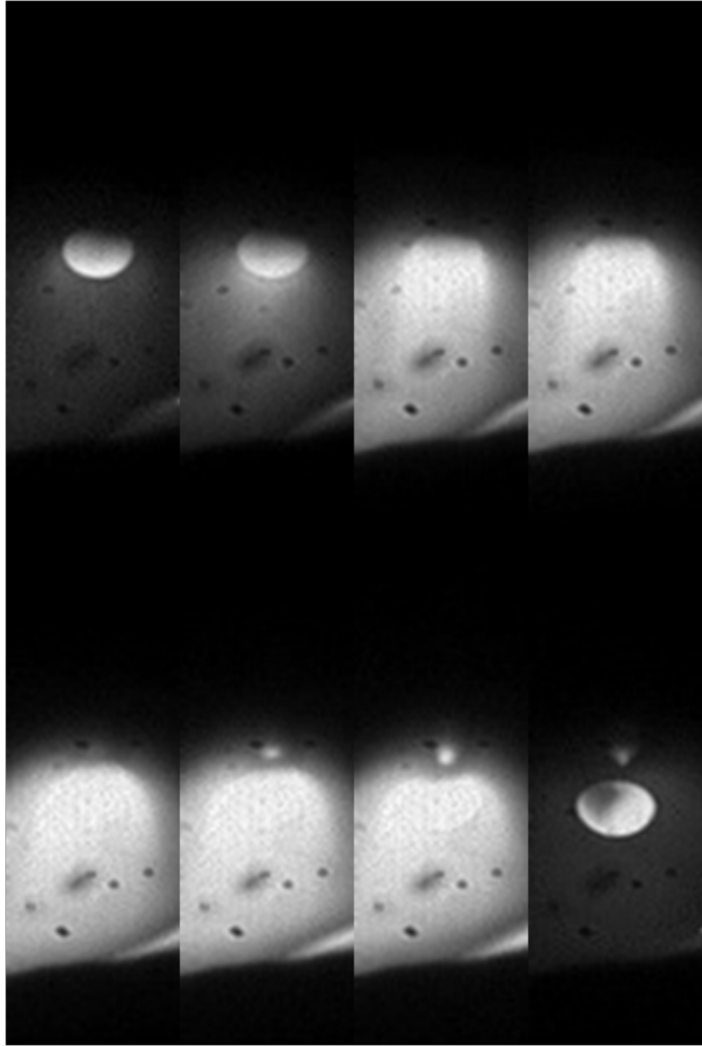


Fig. 8-1(a)

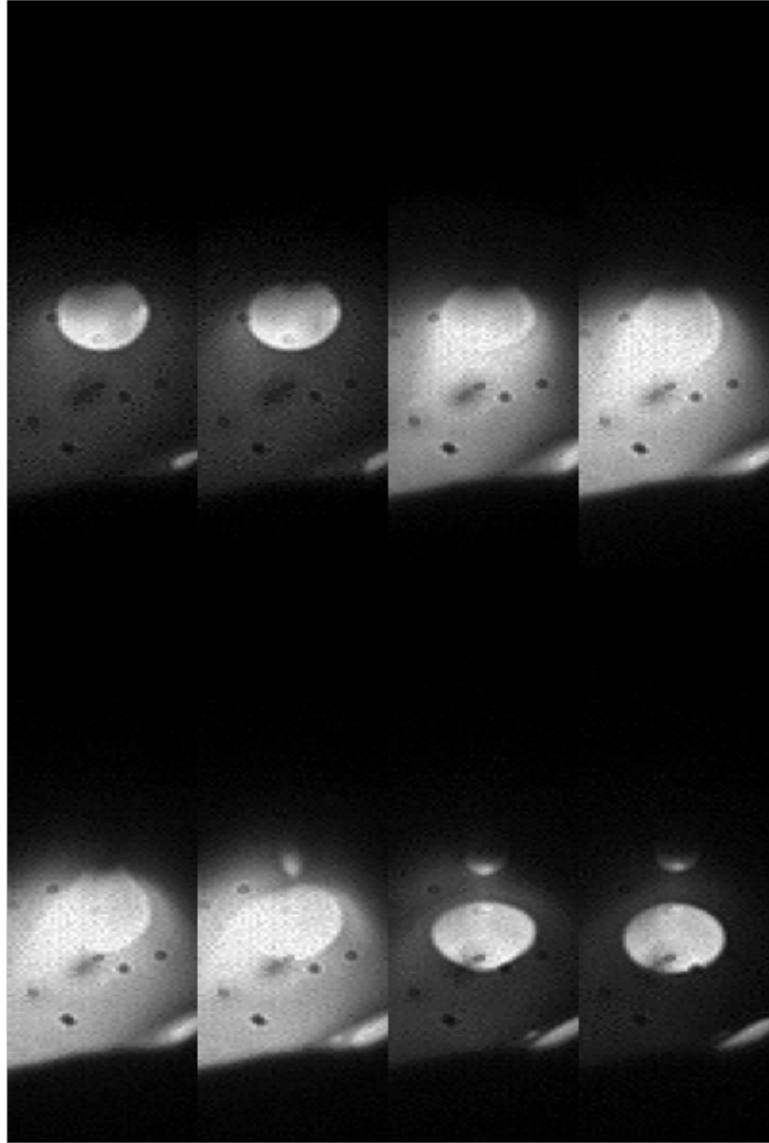


Fig. 8-1(b)

Fig. 8-1 Typical two consecutive cycles in experiment 1 with 150 amp peak current. (a) Cycle one; (b) Cycle two.

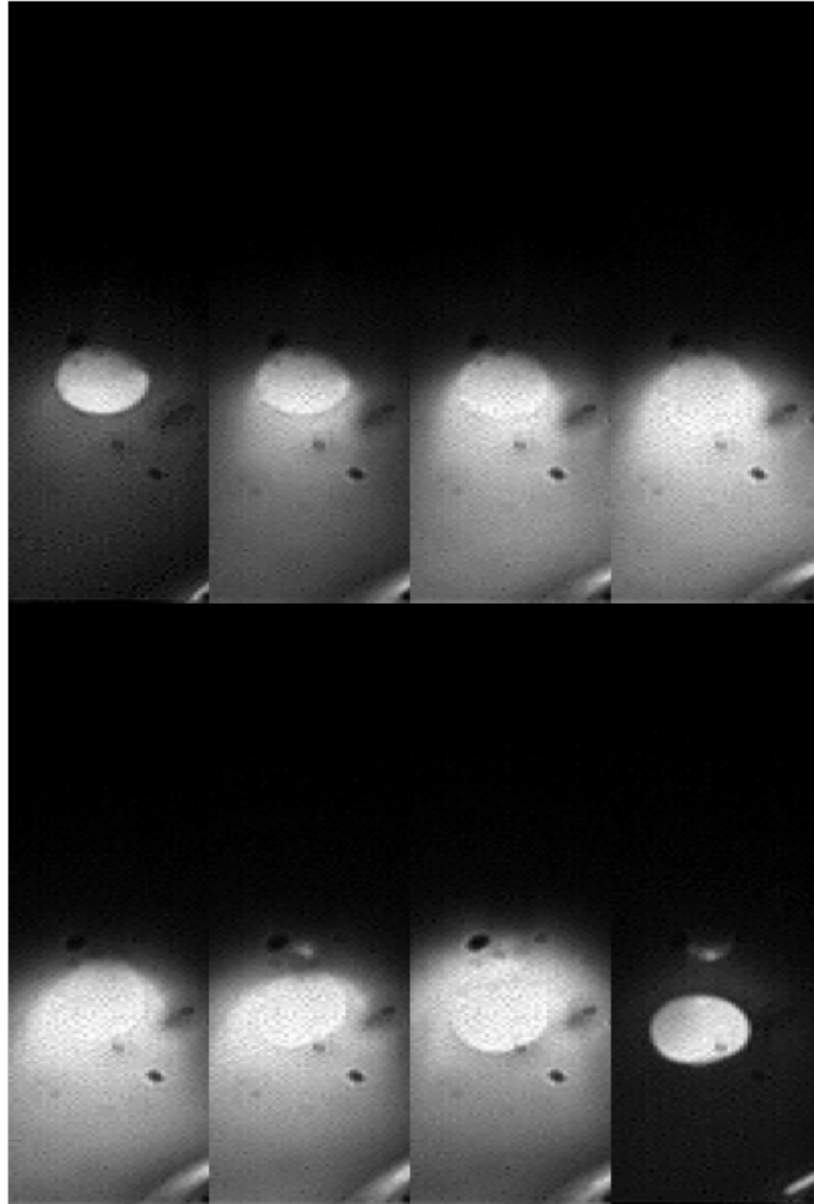


Fig. 8-2(a)

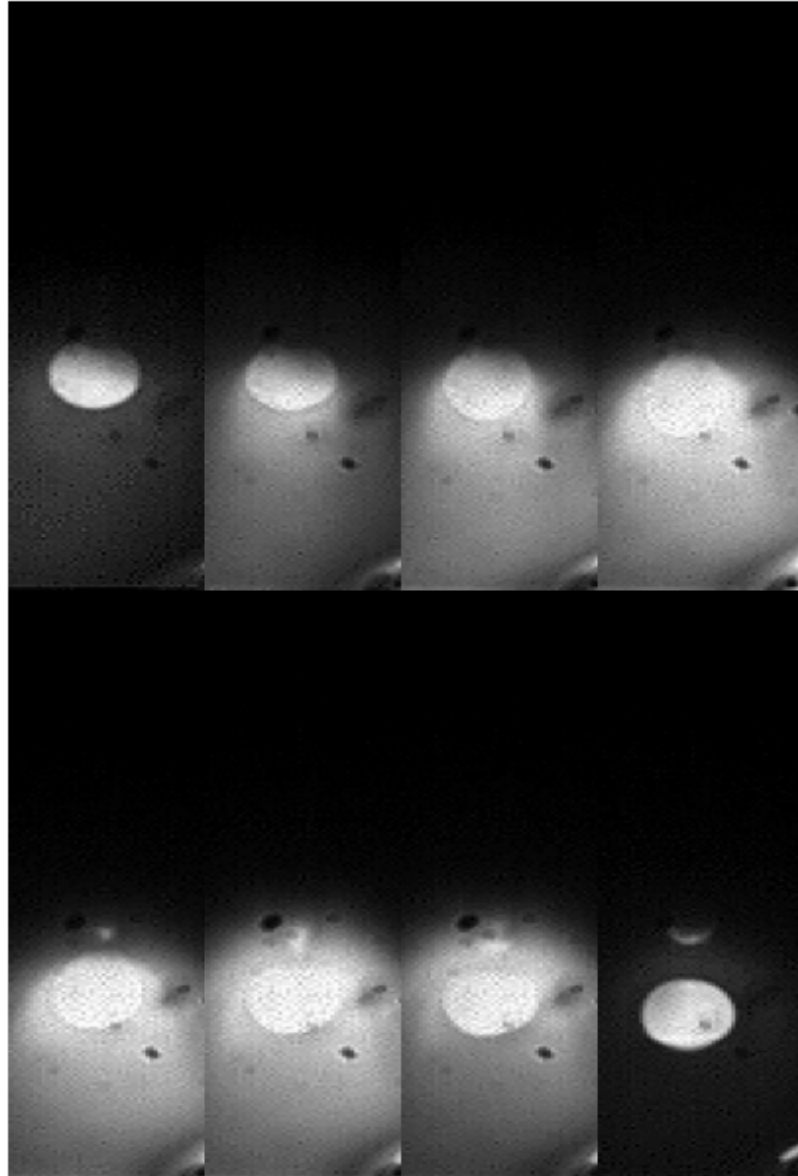


Fig. 8-2(b)

Fig. 8-2 Typical two consecutive cycles in experiment 2 with 145 amp peak current. (a)
Cycle one; (b) Cycle two.

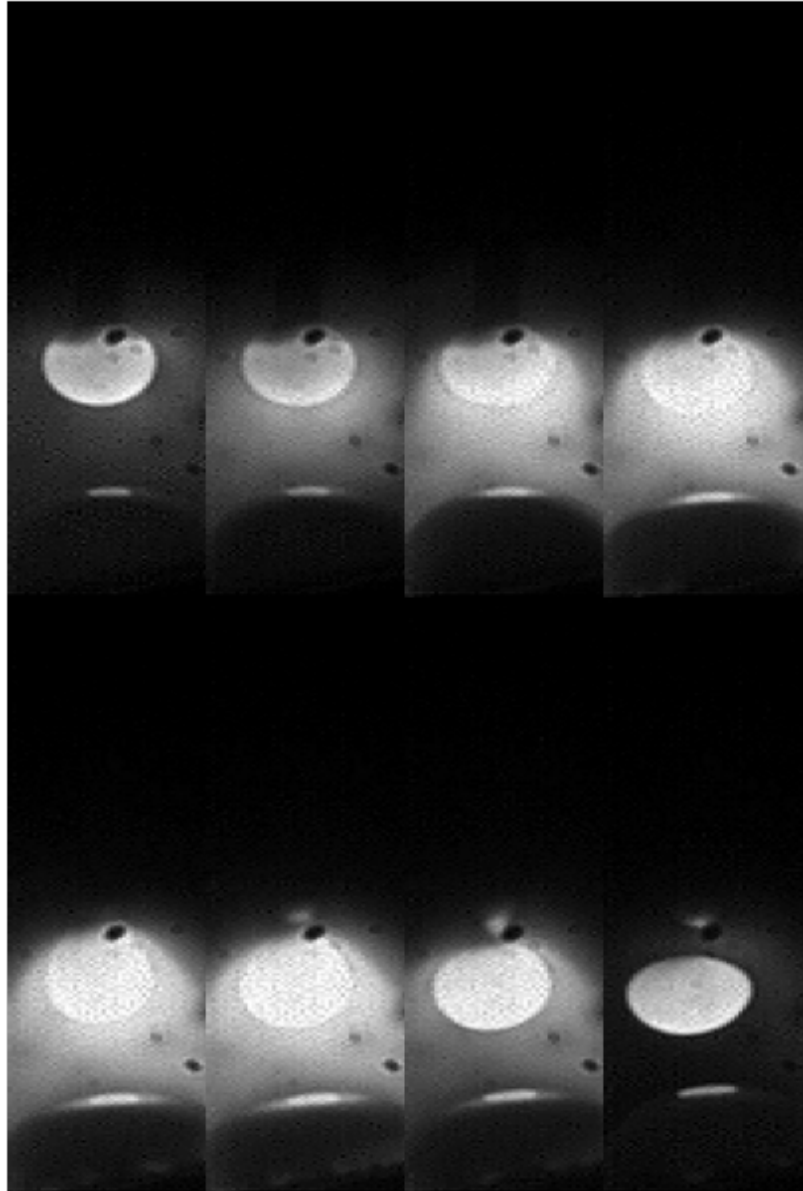


Fig. 8-3(a)

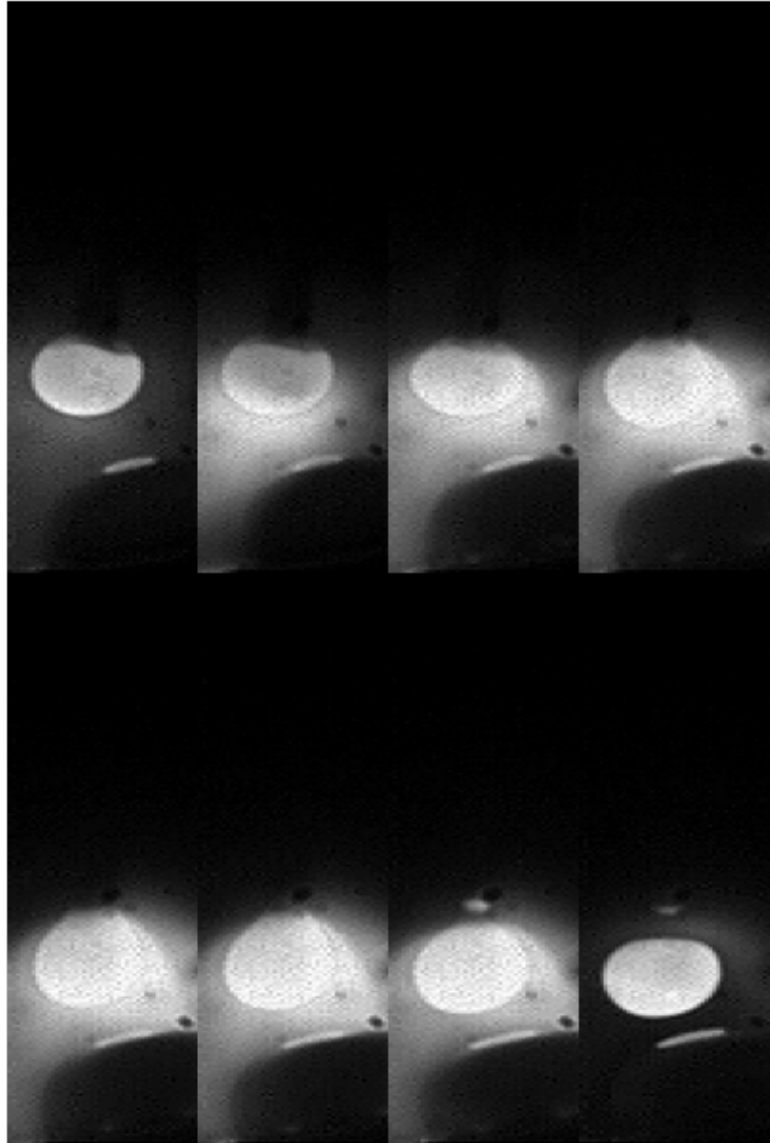


Fig. 8-3(b)

Fig. 8-3 Typical two consecutive cycles in experiment 3 with 140 amp peak current. (a) Cycle one; (b) Cycle two.

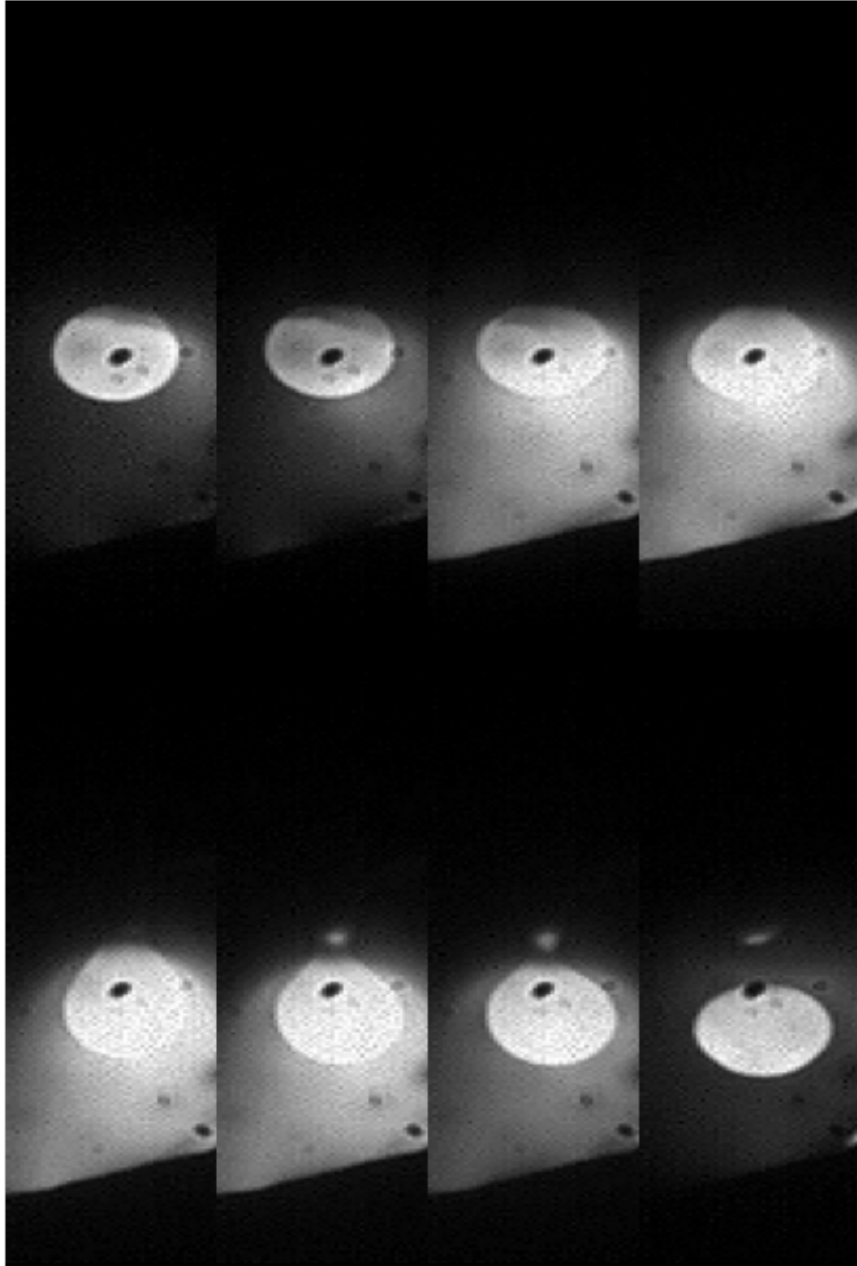


Fig. 8-4(a)

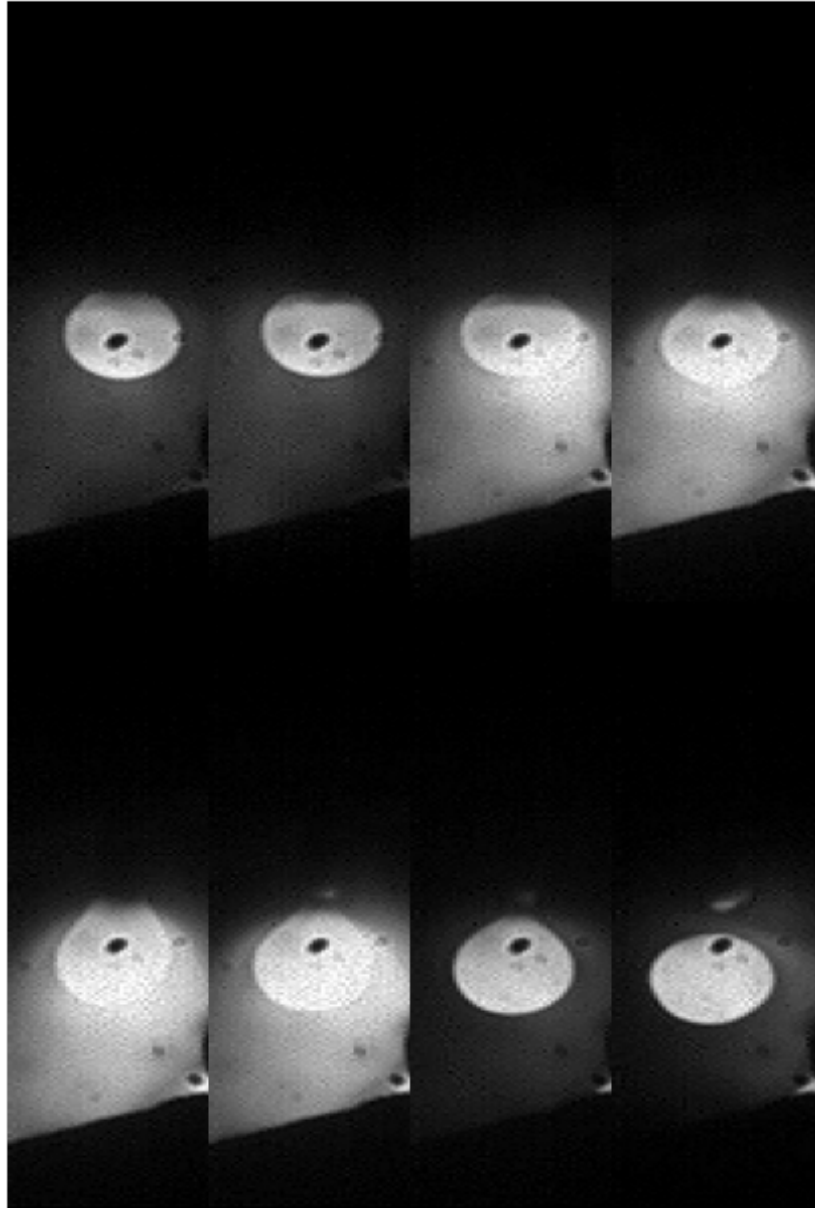


Fig. 8-4 (b)

Fig. 8-4 Typical two consecutive cycles in experiment 4 with 135 amp peak current. (a)
Cycle one; (b) Cycle two.

8.2 Discussion

As can be seen, the pulsed laser-enhanced GMAW successfully reduces the peak current from 160 amp to 135 amp. This reduction is achieved using the present system developed in this dissertation in which a 50 watt laser is used. This reduction is similar to that achieved in the previous effort by Huang [5-7] in his dissertation research as the first effort in laser-enhanced GMAW. He used the same wire (material and diameter). The laser he used is a continuous 1 kW laser but the effective laser power was approximately 850 watts and the length of the laser stripe was 14 mm. For the droplet detached, the length of the droplet along which the laser stripe is intercepted may be considered 1.0 mm approximately. The effective power projected on the droplet is thus approximately 60 watts, similar to that used in this dissertation. This dissertation thus verifies that the pulsed laser has approximately the same effect for the detachment enhancement. Continuous application of the laser is thus not necessary. Further, the continuous application produces unintentional adverse effects including over-heating the droplet, generating extra fume, and wasting energy.

The reduction for the peak current from 160 amp to 135 amp is determined by the laser power used. Based on the positive definite verification for the effectiveness of pulsed laser and real-time image processing based control, the University of Kentucky has recently ordered a pulsed laser with 200 W average but 1.5 kW peak power. The new laser may be directly integrated into the present system developed in this dissertation to see how much the peak current may be further reduced.

Previous efforts by Huang [5-7] have shown that the laser enhances the detachment by its recoil force when the laser vaporizes part of the metal. Arc also vaporizes the droplet metal due to its extremely high temperature at the anode. This vaporization increases with the anode power which increases linearly with the current. However, the recoil force due to arc caused evaporation is against the detachment. One may expect that the increase in

the evaporation due to the laser application should be smaller than the reduction in the arc caused evaporation due to the reduction in the current. As can be see, a 50 watt laser reduces the peak current by 25 amp. For the anode of a steel wire, its voltage is 10 volt [3]. The reduction in the anode power is thus 250 watts. The net vapors thus should be reduced.

The recoil force of the laser increases more than linearly with the laser power intensity intercepted by the droplet [5-8]. Hence, increasing the peak laser power is expected to reduce the peak current needed to detach the droplet. With 1.5 kW peak laser power, it is expected that the final goal for the project to detach the droplet at any (reasonable) size at any (reasonable) arc variables (welding current) may be realized. From this point of view, this dissertation research for pulsed laser-enhanced GMAW using a pulsed laser spot established the foundation to lead to the ideal laser-enhanced GMAW.

CHAPTER 9 Conclusions and future work

9.1 Conclusions

In the newly developed laser enhanced gas metal arc welding process, a laser is applied to provide an auxiliary detaching force to help detach the droplet such that welding may be made in gas tungsten arc welding high quality at GMAW high speeds. To this end, the state of the droplet development needs to be closely monitored in real-time. Since the metal transfer is an ultra-high speed process and the most reliable method to monitor should be based on visual feedback, a high imaging system has been proposed to monitor the real-time development of the droplet. A high-speed image processing system has been developed to real-time extract the developing droplet. A closed-loop control system has been established to use the real-time imaging processing result on the monitoring of the developing droplet to determine if the laser peak pulse needs to be applied. Experiments verified the effectiveness of the proposed methods and established system. A controlled novel process – controlled laser-enhanced GMAW - is thus established to produce high-quality welds at GMAW speeds.

The main conclusions and contributions of this thesis can be concluded:

1. The continuous laser used in the previously developed system has several disadvantages including unnecessary overheating, excessive fume, and waste of laser energy.
2. Although the laser line used in the previous system eases the alignment of the laser with the droplet, majority of the laser is projected onto the weld pool. Laser energy is wasted and produces unintentional adverse effects on the weld pool.
3. Pulsed laser enhanced GMAW process with a small laser spot eliminates most of the problems with the previous system including overheating, excessive fume, energy waste, and side effects on the weld pool. The pulsed laser-enhanced GMAW with a small laser spot should be the ideal choice for the laser enhanced GMAW.

4. Pulsed laser enhanced GMAW is a controlled process that relies on accurate real-time machine vision feedback and corresponding synergistical controls to function.
5. This research established the foundation to operate the ideal laser enhanced GMAW process.
6. It is found that pulsing is the same effective as the application of a continuous laser. In addition, pulsed laser increases the control accuracy for the droplet detachment and droplet size.
7. For the used small spot laser of 50 watt power, the peak current needed to detach the droplet is reduced from 160A to 135A, i.e., by 16%.

9.2 Future work

1. A pulsed laser with a greater power is needed to further reduce the peak current needed for the detachment.
2. When microprocessor's computation power significantly improves, the advanced control proposed including droplet size/mass control should be implemented.
3. The pulsed laser enhanced GMAW with advanced controls and greater laser power should be compared with GTAW for quality and productivity.
4. A more advanced torch with two laser heads attached and be applied from inside of the torch is needed to precisely control the size/mass and trajectory of the droplets.

References

- [1] Pan Jiluan. Arc Welding Control. Woodhead Publishing Limited, Cambridge, United Kingdom, 2005
- [2] Jesper Sandberg Thomsen. Control of pulsed gas metal arc welding. International Journal of Modeling, Identification and Control, 1(2):115-125, 2006
- [3] Welding Handbook, 1991. 8th Edition Vol. 2: Welding Processes, AWS
- [4] Yi Huang, Y. M. Zhang, "Laser-enhanced GMAW", Welding Journal, 89(9): 181s-188s, 2010
- [5] Yi Huang, Yan Shao, YuMing Zhang, "Nonlinear modeling of dynamic metal transfer in laser enhanced GMAW," Welding Journal, vol. 91, no. 5, 140s-148s, 2012.
- [6] Y. Huang, Y.M Zhang, "Laser-enhanced metal transfer: Part I: System and observations," Welding Journal, 90(10): 183s-190s, 2011.
- [7] Y. Huang, Y.M Zhang, "Laser-enhanced metal transfer: Part II: Analysis and influence factors," Welding Journal, 90(11): 205s-210s, 2011.
- [8] O'Brien, R.L. 1991. Welding Handbook Vol. 2: Welding Processes. 8th edition, Miami, FL. American Welding Society.
- [9] Song, T. H.. 2001. Welding handbook: Welding methods and equipments.1 [M], Second Edition. Beijing, P R China, Chinese Welding Society.
- [10] Lincoln Electric. 1994. The Procedure Handbook of Arc Welding. Cleveland: Lincoln Electric. ISBN 99949-25-82-2.
- [11] Thomsen, J.S., 2006. Control of pulsed gas metal arc welding. International Journal of Modelling, Identification, and Control, 1(2): 115-125.
- [12] Casalino G.. 2007. Statistical analysis of MIG-laser CO2 hybrid welding of Al-Mg alloy. Journal of Materials Processing Technology. 191 (1): 106-110.
- [13] Cary, Howard B. and Scott C. Helzer. 2005. Modern Welding Technology. Upper Saddle River, New Jersey: Pearson Education. ISBN 0-13-113029-3.
- [14] Kalpakjian, Serope and Steven R. Schmid. 2001. Manufacturing Engineering and Technology. Prentice Hall. ISBN 0-201-36131-0.

- [15] Althouse, A. D., Turnquist, C. H., Bowditch, W. A. and Bowditch, K. E. 1984. Modern Welding [M], South Holland, ILL: The Goodheart – Willcox Company, Inc..
- [16] Kim Y. S., Eagar T. W. 1993. Analysis of metal transfer in gas metal arc-welding, *Welding Journal*. 72(6): 269s to 278s.
- [17] Kim Y. S. 1989. Metal transfer in gas metal arc welding. PhD dissertation, Massachusetts Institute of Technology
- [18] Kim Y. S., Eagar T. W. 1993. Metal transfer in pulsed current gas metal arc-welding, *Welding Journal*. 72(7): 279s to 287s
- [19] Lesnewich A. 1958. Control of melting rate and metal transfer in gas-shielded metal arc welding: Part II control of metal transfer. *Welding Journal*. 37(9): 418s-425s
- [20] Lesnewich A. 1997. Letters to the Editor: Metal Transfer Modes Made Correct. *Welding Journal*. 76(7): 21-22.
- [21] Lancaster, J. F. 1984. *The Physics of Welding*. Pergamon Press, Oxford, England.
- [22] Zhang Y. M., Liguó E. 1999. Method and system for gas metal arc welding. U.S. Patent, #6,008,470.
- [23] Zhang Y. M., Liguó E, Kovacevic R. 1998. Active metal transfer control by monitoring excited droplet oscillation, *Welding Journal*. 77(9): 388s-395s.
- [24] Zhang Y. M., Li P. J. 2001. Modified active control of metal transfer and pulsed GMAW of titanium, *Welding Journal*. 80(2): 54s-61s.
- [25] Lin Q., Li, X. S., Simpson W. 2001. Metal transfer measurements in gas metal arc welding, *J. Phys. D: Appl. Phys.* 34: 347-353.
- [26] Ponomarev, V., Scotti, A., Silvinskiy, A., Al-Erhayem, O. 2003. Atlas of MIG/MAG welding metal transfer modes. IIW Doc. XII-1771 to 1775-03. Bucharest.
- [27] Iordachescua D., Quintinob L. 2008. Steps toward a new classification of metal transfer in gas metal arc welding. *Journal of materials processing technology*. 202: 391-397.
- [28] Klas, W.. 2003. *Welding processes handbook*. [M], New York: CRC Press LLC.
- [29] Ed, C.. 1991. “Gas Metal Arc & Flux Cored Welding Parameters”. [M], Chicago: Weldtrain.

- [30] Heald, P. R., Madigan, R B., Siewert, T. A and Liu, S.. 1994. Mapping the droplet transfer modes for an ER100S-1 GMAW electrode, *Welding Journal*, 73(2): 38s-44s.
- [31] Fan, H. G. and Kovacevic, R. 1999. Droplet formation, Detachment, and Impingement on the molten pool in Gas Metal Arc Welding, *Metallurgical and Materials Transactions B*, 30 (4): 791-801.
- [32] CAana G., Fortunato A., Ascari A., Tani G., Tomesani L. 2007. The influence of arc transfer mode in hybrid laser-mig welding, *Journal of Materials Processing Technology*, 191(1): 111-113.
- [33] Norman P., Karlsson J., Kaplan A. 2011. Mechanisms forming undercuts during laser hybrid arc welding, *Physics Procedia*, 12: 201-207.
- [34] Fennander, H., Kyrki, V., Fellman, A., Saleminen, A. and Kälviäinen, H. 2007. Visual measurement and tracking in laser hybrid welding, *Machine Vision and Applications*, s00138-007-0111-1.
- [35] Schubert, E. 2004. *Process Stability of Automated Gas Metal Arc Welding of Aluminum [M]*. Springer Berlin/Heidelberg, Vol299.
- [36] Kaierle, S., Bongard, K., Dahmen, M., Poprawe, R., 2000. Innovative hybrid welding process in an industrial application. *Proceedings of International Conference on the Applications of Lasers and Electro-Optics ICALEO 2000*, Dearborn, MI, USA, 2–5 October: 91–98.
- [37] Process of Surface Tension Transfer, <http://content.lincolnelectric.com/pdfs/products/literature/nx220.pdf>
- [38] Application of Surface Tension Transfer, <http://content.lincolnelectric.com/pdfs/products/literature/nx310.pdf>
- [39] Parks J.M., Stava E.K.. 1991. Apparatus and method of short circuiting arc welding. U.S. Patent, #5,003,154.
- [40] Stava E.K.. 1992. System and method of short circuiting arc welding. U.S. Patent, #5,148,001.
- [41] Stava E.K.. 2006. Short circuit arc welder and method of controlling same. US Patent, #7,109,439.
- [42] Hsu C.. 2006. Two stage welder and method of operating same. US Patent, #7,067,767.

- [43] Stava E.K.. 1993. A new, low-spatter arc welding machine. *Welding Journal*, 72(1): 25-29.
- [44] Stava E.K.. 2002. Short circuit arc welder and method of controlling same. US Patent, #6,501,049.
- [45] Stava E.K.. 2001. Short circuit welder. US Patent, # 6,215,100.
- [46] Li K.H., Chen J., Zhang Y.M.. 2007. Double-electrode GMAW process and control. *Welding Journal*, 86(8): 231s-237s.
- [47] Wu C.S., Zhang M.X., Li K.H., Zhang Y.M.. 2007. Numerical analysis of double-electrode gas metal arc welding Process. *Computational Materials Science*, 39: 416-423.
- [48] Li K.H.. Double-Electrode Gas Metal Arc Welding: Process, Modeling and Control. PhD Dissertation, University of Kentucky, Sept. 21, 2007.
- [49] Li K.H., Zhang Y.M.. 2008. Consumable Double-Electrode GMAW Part I: The Process. *Welding Journal*, 87(1): 11s-17s.
- [50] Li K.H., Zhang Y.M.. 2008. Consumable Double-Electrode GMAW Part II: Monitoring, Modeling, and Control. *Welding Journal*, 87(2): 44s-50s.
- [51] Li K.H., Zhang Y.M.. 2007. Metal transfer in double-electrode gas metal arc welding, *Journal of Manufacturing Science and Engineering-Transactions of the ASME*, 129(6): 991-999.
- [52] Li K.H., Zhang Y.M.. Xu P., Yang F.Q.. 2008. High strength steel welding with consumable DE-GMAW, *Welding Journal*, 88(3): 57s-64s.
- [53] Liu, X. P., Li, K. H., Zhang, Y. M., Johnson, Q. M.. 2007. Dual Bypass GMAW of Aluminum, *Transactions of NAMRI/SME*, 35: 335-341.
- [54] Shi, Y., Liu, X., Zhang, Y.M., Johnson, M. 2008. Analysis of Metal Transfer and Correlated Influences in Dual Bypass GMAW of Aluminum, *Welding Journal*, 87: 229s-236s.
- [55] Liu, X., Shi, Y., Johnson, M., Zhang, Y.M. 2007. Dual Bypass GMAW of Aluminum Rings. *Transaction of FABTECH International & AWS Welding Show, Chicago*: 157-158.
- [56] Zhang Y. M., Liguó E.. 1999. Method and system for gas metal arc welding. U.S. Patent, #6,008,470.

- [57] Wu Y., Kovacevic R.. 2002. Mechanically assisted droplet transfer process in gas metal arc welding. *Journal of engineering manufacturing*, 216: 555-564.
- [58] Yang, S. Y. Projected droplet transfer control with additional mechanical forces (AMF) in MIG/MAG welding process. PhD dissertation, Harbin Institute of Technology, 1998.
- [59] Mahrle, A. and Beyer, E., 2006. Hybrid laser beam welding-classification, characteristics, and applications. *Journal of Laser Applications*. 18 (3): 169-180.
- [60] Liu, L., Hao, X. and Song, G., 2006. A new laser-arc hybrid welding technique based on energy conservation. *Materials Transactions*. 47 (6): 1611-1614.
- [61] Bagger, C. and Olsen, F.O., 2005. Review of laser hybrid welding. *Journal of Laser Applications*. 17 (1): 2-14.
- [62] Weisheit, A., Galun, R., and Mordike, B.L., 1998. CO2 laser beam welding of magnesium-based alloys. *Welding Journal*. 77 (4): 149s-154s.
- [63] CAana G., Fortunato A., Ascari A., Tani G., Tomesani L. 2002. The influence of arc transfer mode in hybrid laser-mig welding. *Journal of Materials Processing Technology*. 191 (1): 111-113.
- [64] Liu L.M., Zhao X. 2008. Study on the weld joint of Mg alloy and steel by laser-GTA hybrid welding. *Materials Characterization*. 59(9): 1279-1284.
- Zhou J., Thai H.L. 2008. Modeling of transport phenomena in hybrid laser-MIG keyhole welding. *International Journal of Heat and Mass Transfer*. 51(17): 125-134.
- [65] Zhou J., Thai H.L. 2008. Modeling of transport phenomena in hybrid laser-MIG keyhole welding. *International Journal of Heat and Mass Transfer*. 51(17): 125-134.
- [66] R. C. Gonzalez, R. E. Woods, 2002. *Digital Image Processing, Second Edition*, Prentice-Hall.
- [67] Z. Z. Wang and Y. M. Zhang, 2009. "Brightness based selection and edge detection based enhancement separation algorithm for low resolution metal transfer images," *IEEE Transactions on Automation Science and Engineering*, 6(1): 181-187.
- [68] Z. Z. Wang and G. L. Li, 2003. "A new cross based gradient descent search algorithm for block matching in MPEG-4 encoder," *Chinese Journal of Electronics*, 12(4): 648-651.

- [69] J. A. Hartigan and M. A. Wong, 1979. "Algorithm as 136, a K-means clustering algorithm," *Journal of RSS*, 28 (1): 100-108.

VITA

Yan Shao was born in Harbin, Heilongjiang, China.

Education:

M.S. in Electrical Engineering, University of Bradford, Bradford, UK	Dec. 2005
B.S. in Electrical Engineering, Heilongjiang University, Harbin, China	Jul. 2003

Journal Publications:

Yan Shao, YuMing Zhang. Monitoring of liquid droplets in laser-enhanced GMAW. International Journal of Advanced Manufacturing Technology, 2011. 57:203-214.

Yan Shao

03/25/2013